magnetic resonance imaging (MRI)

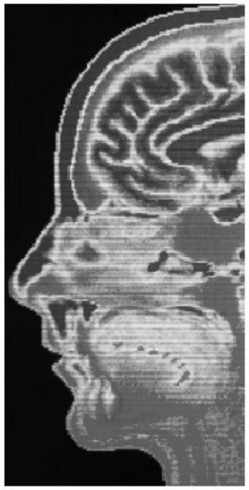

Magnetic resonance image of a mid-saggital section through the head of a 42-year-old woman.

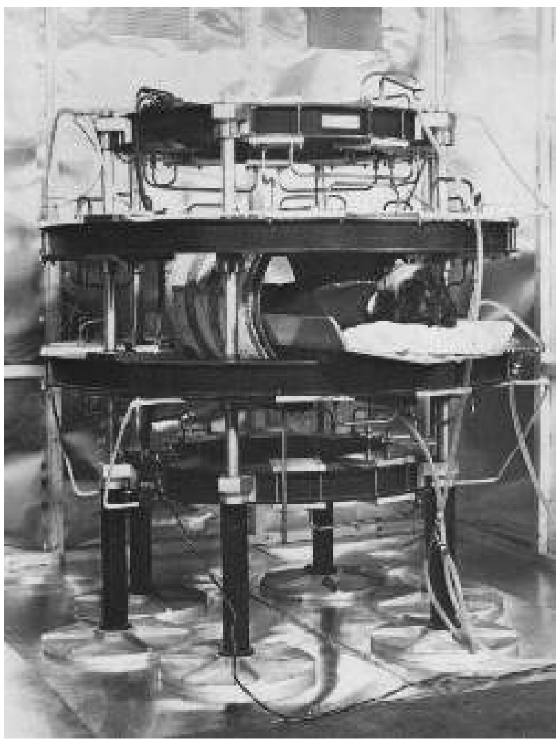

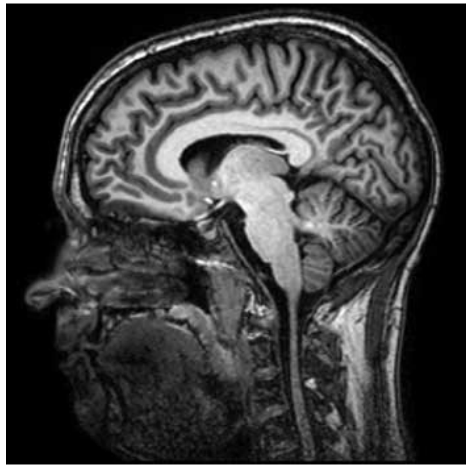

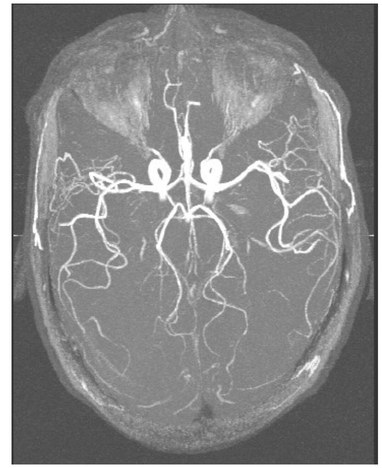

magnetic resonance imaging (MRI)

principle

- ***active*** imaging through exposure of energy
  (strong constant magnetic field + electromagnetic pulses)

  and

- ***passive*** imaging through recording of “endogenous” signals (spin ensembles as radio wave emitter)

- characterize **distribution of magnetization** in body tissue depending on structure, function, and metabolism

magnetic resonance imaging (MRI)

- **tomographic imaging technique (cf. CT, SPECT, and PET)**

  (*gr*. tomos (τομοσ) - slice)

- **MRI scanner provides multi-dimensional data (image) of spatial distribution of physical observables**

  - 2D slice with arbitrary orientation
  - 3D volume data
  - 4D images (spatial + spectral distributions)

- **MRI signals emitted from the body**

  "emission" tomography; (cf. PET, SPECT)
  but does not require radioactive substances!

magnetic resonance imaging (MRI)

- **MRI operates in radio frequency range**

  no ionizing radiation

- **MRI images provide multiple information**

  grey level of pixel (signal intensity) depends on:
    - density of nuclear spins ρ
    - spin-lattice relaxation time T_1
    - spin-spin relaxation time T_2
    - molecular movements (transport, diffusion, perfusion)
    - susceptibility
    - chemical shift

magnetic resonance imaging (MRI)

frequency [Hz]	wave length [m]	photon energy [eV]	type of radiation	effects on molecular level
10^{26}	10^{-18}	10^{12}		
10^{24}	10^{-16}	10^{10}		
10^{22}	10^{-14}	10^{8}	x-rays and gamma-rays	dissociation
10^{20}	10^{-12}	10^{6}		
10^{18}	10^{-10}	10^{4}		
10^{16}	10^{-8}	10^{2}	UV radiation	e^- excitation (shell)
10^{14}	10^{-6}	10^{0}	visible light	oscillation
10^{12}	10^{-4}	10^{-2}	IR radiation	rotation
10^{10}	10^{-2}	10^{-4}		
10^{8}	10^{0}	10^{-6}	UKW	MRI ??
10^{6}	10^{2}	10^{-8}	KW	
10^{4}	10^{4}	10^{-10}	MW	
10^{2}	10^{6}	10^{-12}	LW	
10^{0}		10^{-14}		

magnetic resonance imaging (MRI)

wave length > 0.3 m

↓

insufficient spatial resolution

↓

ansatz:

superimpose RF-fields onto spatially variable but otherwise constant magnetic field

+

exploit resonance absorption of specific nuclei (spin ½) in biological tissue (^{1}H, ^{13}C, ^{19}F, ^{23}Na, ^{31}P)

↓

spatial mapping of nuclear magnetization

magnetic resonance imaging (MRI)

contents:

- historical overview
- physical basics
  - classical, quantum-mechanical description
- basics of MRI
  - from signal to image, recording techniques
  - contrast, resolution, signal-noise ratio
- applications

(images: Dössel, 2000; Morneburg, 1995; Siemens, Philips, internet)

magnetic resonance imaging (MRI)

PHYSICAL REVIEW VOLUME 70, NUMBERS 7 AND 8 OCTOBER 1 AND 15, 1946

Nuclear Induction

F. BLOCH
Stanford University, California

(Received July 19, 1946)

The magnetic moments of nuclei in normal matter will result in a nuclear paramagnetic polarization upon establishment of equilibrium in a constant magnetic field. It is shown that a radiofrequency field at right angles to the constant field causes a forced precession of the total polarization around the constant field with decreasing latitude as the Larmor frequency approaches adiabatically the frequency of the r-f field. Thus there results a component of the nuclear polarization at right angles to both the constant and the r-f field and it is shown that under normal laboratory conditions this component can induce observable voltages. In Section 3 we discuss this nuclear induction, considering the effect of external fields only, while in Section 4 those modifications are described which originate from internal fields and finite relaxation times. !

magnetic resonance imaging (MRI)

PHYSICAL REVIEW VOLUME 80, NUMBER 4 NOVEMBER 15, 1950

Spin Echoes*†

E. L. HAHN‡
Physics Department, University of Illinois, Urbana, Illinois
(Received May 22, 1950)

Intense radiofrequency power in the form of pulses is applied to an ensemble of spins in a liquid placed in a large static magnetic field H_0. The frequency of the pulsed r-f power satisfies the condition for nuclear magnetic resonance, and the pulses last for times which are short compared with the time in which the nutating macroscopic magnetic moment of the entire spin ensemble can decay. After removal of the pulses a non-equilibrium configuration of isochromatic macroscopic moments remains in which the moment vectors precess freely. Each moment vector has a magnitude at a given precession frequency which is determined by the distribution of Larmor frequencies imposed upon the ensemble by inhomogeneities in H_0. At times determined by pulse sequences applied in the past the constructive interference of these moment vectors gives rise to observable spontaneous nuclear induction signals. The properties and underlying principles of these spin echo signals are discussed with use of the Bloch theory. Relaxation times are measured directly and accurately from the measurement of echo amplitudes. An analysis includes the effect on relaxation measurements of the self-diffusion of liquid molecules which contain resonant nuclei. Preliminary studies are made of several effects associated with spin echoes, including the observed shifts in magnetic resonance frequency of spins due to magnetic shielding of nuclei contained in molecules. !
!

magnetic resonance imaging (MRI)

Reprinted from
19 March 1971, Volume 171, pp. 1151-1153

SCIENCE

Tumor Detection by Nuclear Magnetic Resonance

Raymond Damadian

Abstract. *Spin echo nuclear magnetic resonance measurements may be used as a method for discriminating between malignant tumors and normal tissue. Measurements of spin-lattice (T_1) and spin-spin (T_2) magnetic relaxation times were made in six normal tissues in the rat (muscle, kidney, stomach, intestine, brain, and liver) and in two malignant solid tumors, Walker sarcoma and Novikoff hepatoma. Relaxation times for the two malignant tumors were distinctly outside the range of values for the normal tissues studied, an indication that the malignant tissues were characterized by an increase in the motional freedom of tissue water molecules. The possibility of using magnetic relaxation methods for rapid discrimination between benign and malignant surgical specimens has also been considered. Spin-lattice relaxation times for two benign fibroadenomas were distinct from those for both malignant tissues and were the same as those of muscle.*

magnetic resonance imaging (MRI)

history

1946 nuclear magnetic resonance (NMR)

F. Bloch, W.W. Hansen, M. Packard. Phys Rev 69, 127, 1946
E.M. Purcell, H.C. Torrey, R.V. Pound. Phys Rev 69, 37, 1946

1950 E.L. Hahn: Spin echoes. (Phys Rev 80, 580, 1950)

1950 – 1970 applications of NMR in physics and chemstry (structural analyses)

1952 Nobel price awarded to Bloch and Purcell

1970 first MRI of brain (recording: 8 h, image proc.: 72 h)

1971 R. Damadian: tumor and normal tissue have different NMR relaxation times (MRI as diagnostic method)

magnetic resonance imaging (MRI)

history

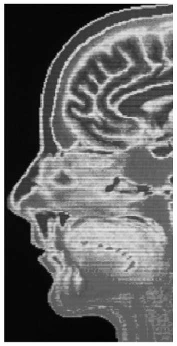

1973 P. Lauterbur: MRI imaging with gradient fields
(Nature, 242, 190)

1975 R. Ernst: MRI with phase- and frequency encoding and use of Fourier transform

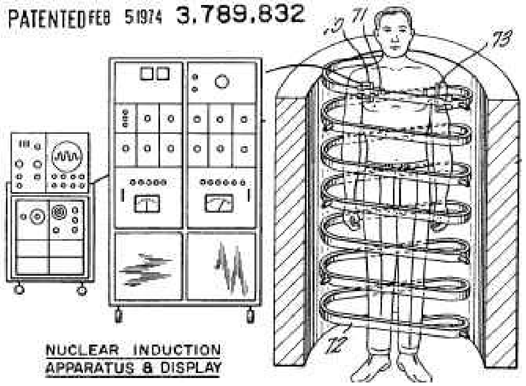

1977 R. Damadian: first whole-body scan
(recording: 4 -5 h)

1977 P. Mansfield: Echo-Planar-Imaging (EPI)

1980 Edelstein et al.: whole-body scan with Ernst technique
(data acquisition: 5 min/slice; 1986: 5 s/slice)

since 1980: first commercial MRI systems

magnetic resonance imaging (MRI)

history

1986 – 1989: Gradient Echo Imaging, NMR microscope

1990 Ogawa et al.: BOLD effect

fMRI

1991 Nobel price awarded to R. Ernst

1992 Kwong et al.: BOLD + neuronal activity

2003 Nobel price awarded to
P. Lauterbur and P. Mansfield

standard technique for clinical diagnosis
ca. 60 Mio. examinations worldwide
> 30.000 installations worldwide

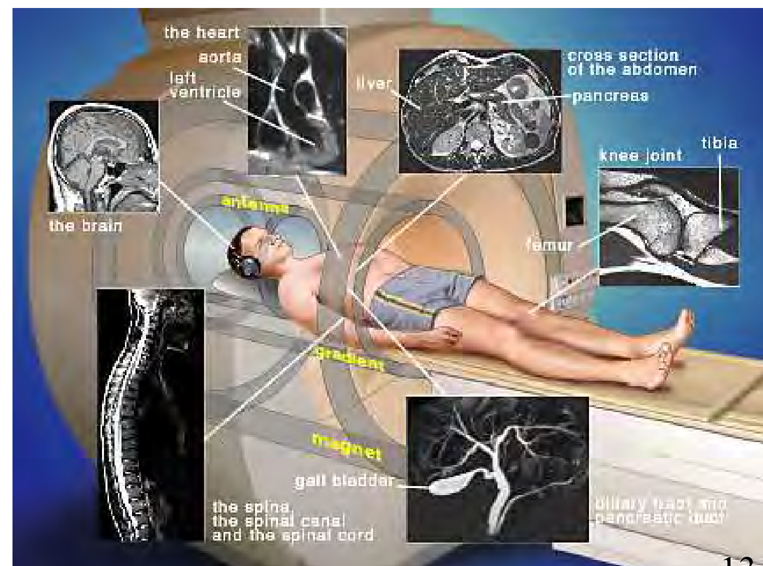

magnetic resonance imaging (MRI) *magnetic gyroscope (class.)*

compass needle in magnetic field

the magnetic dipole moment can be assessed through measuring the torque in a homogeneous magnetic field

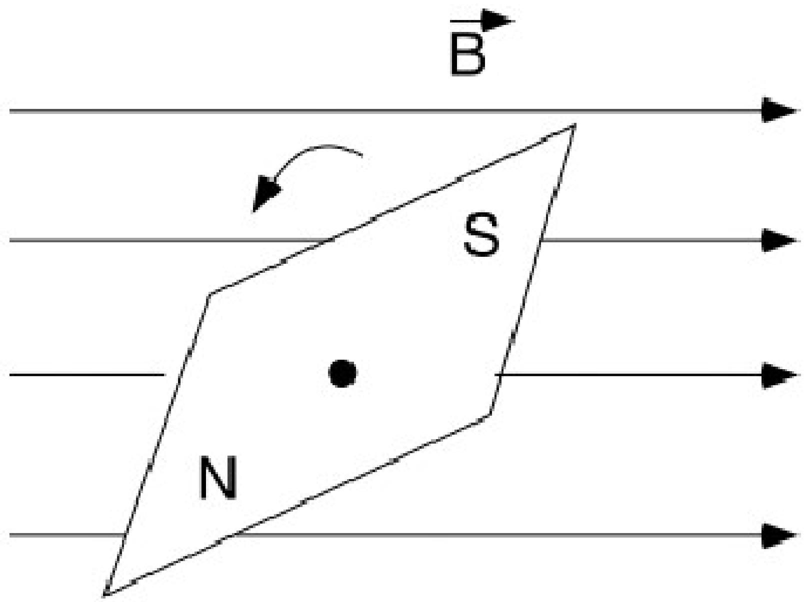

$$\vec{T} = \vec{m} \times \vec{B}$$

$\vec{T}$ = torque

$\vec{m}$ =magnetic dipole moment

$\vec{B}$ = magnetic flux density

symbol B **= magnetic induction or flux density**

symbol H **= magnetic field !**

symbol B **= magnetic field typically used in MRI literature**

magnetic resonance imaging (MRI) *magnetic gyroscope (class.)*

magnetization of paramagnetic and diamagnetic materials

diamagnetic materials:
e^- induce shielding current $\rightarrow$ reduced $\vec{B}$ field inside material

paramagnetic materials :
alignment of elementary magnets (e^- spin) to external $\vec{B}$ field
$\rightarrow$ increased $\vec{B}$ field inside material

the vectorial sum of all magnetic moments in some volume element wrt the size of the volume element is called magnetization:

$$\vec{\mathrm{M}} = \frac{\mathrm{d}\vec{\mathrm{m}}}{\mathrm{dV}}$$

for a probe composed of different materials, we have:
$M = M(x,y,z)$

magnetic gyroscope in constant magnetic field

magnetic gyroscope: rotating object with magn. dipole moment $\vec{m}$

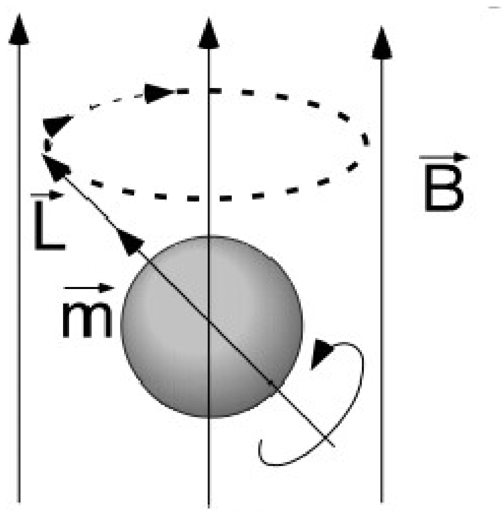

$$\vec{T} = \frac{d\vec{L}}{dt} = \vec{m} \times \vec{B}$$

$$T = -L \cdot \omega_0 \cdot \sin\alpha = m \cdot B \cdot \sin\alpha$$

$$\boxed{\omega_0 = -\frac{m \cdot B}{L} = -\gamma \cdot B}$$ angular velocity of precession

$L =$ angular momentum

$\gamma = \frac{m}{L} =$ gyromagnetic ratio

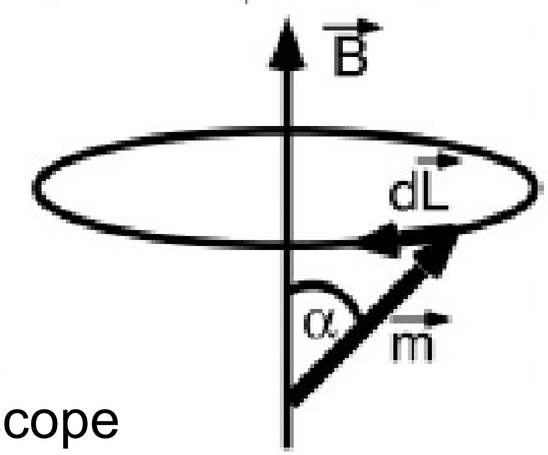

precession of a magnetic gyroscope in $\vec{B}$ field

magnetic gyroscope in constant magnetic field

laboratory system

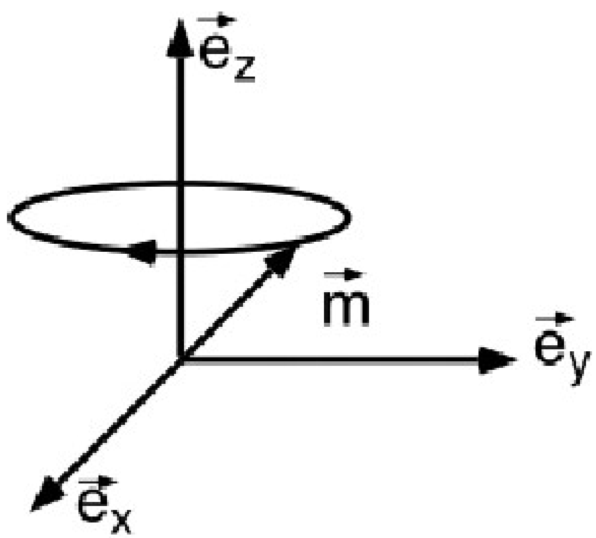

coordinate system that rotates around z-axis

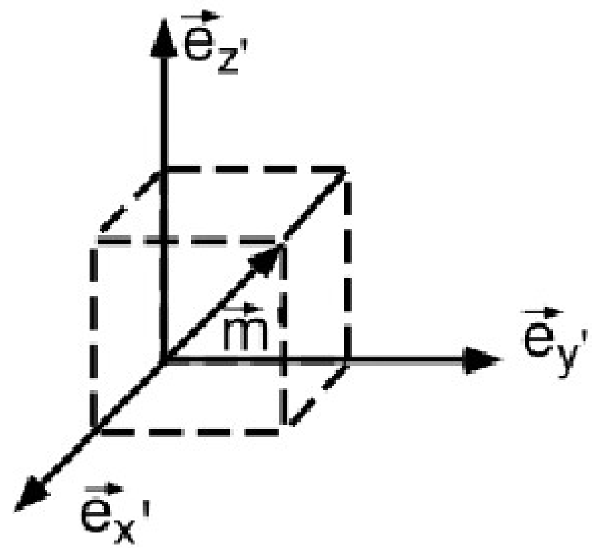

gradient fields (1)

special case of an inhomogeneous field B_{G}, whose z-component varies linearly along some predefined direction (x,y,z) (direction of gradient)

z-gradient field	*y*-gradient field	*x*-gradient field
$B_{\mathrm{G,z}} = G_z z$	$B_{\mathrm{G,z}} = G_y y$	$B_{\mathrm{G,z}} = G_x x$

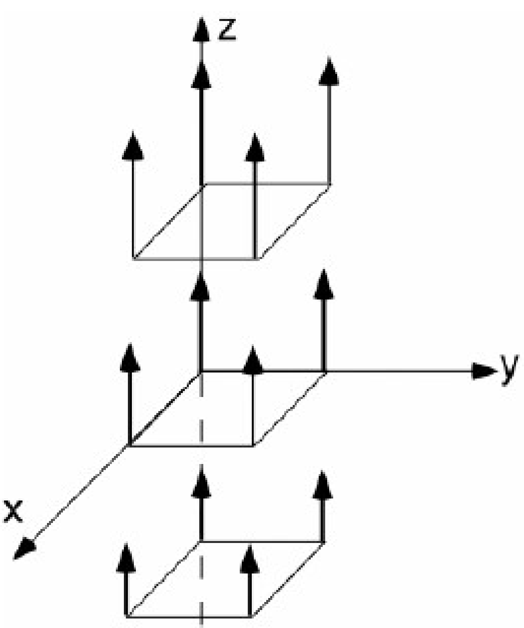

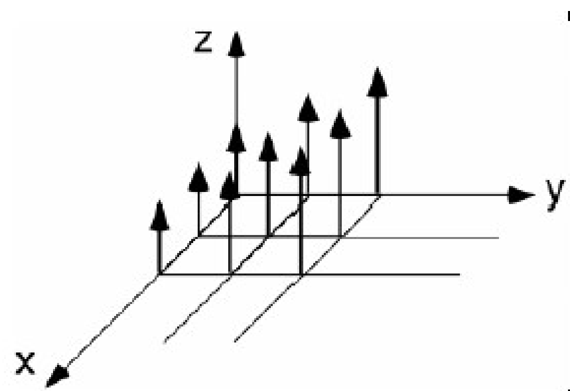

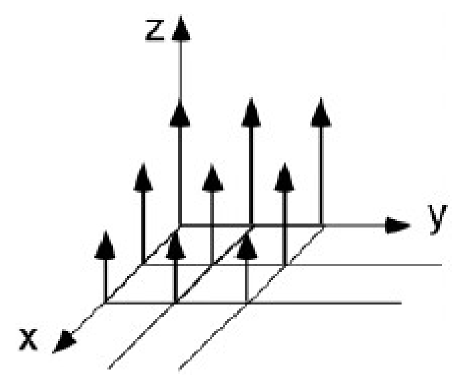

gradient fields (2)

let $B_z = B_{00} + G_z z$; let $B = (0, 0, B_z)$ denote field gradient in z-direction

with: $\omega_0 = \gamma B = \gamma B_{00} + \gamma G_z z = \omega_{00} + \gamma G_z z$

(where ω_0 = local precession frequency and
ω_{00} = precession frequency at $z = 0$ = center of MRI system)

we have: angular velocity of precession ω_0 depends linearly on z

- all gyroscopes in x-y-plane precess with identical angular velocity

- in a coordinate system that rotates with ω_{00}, one observes gyroscopes with $z > 0$ to advance and those with $z < 0$ to retard

gradient fields (3)
precession in a gradient field

stationary laboratory system **rotating frame**

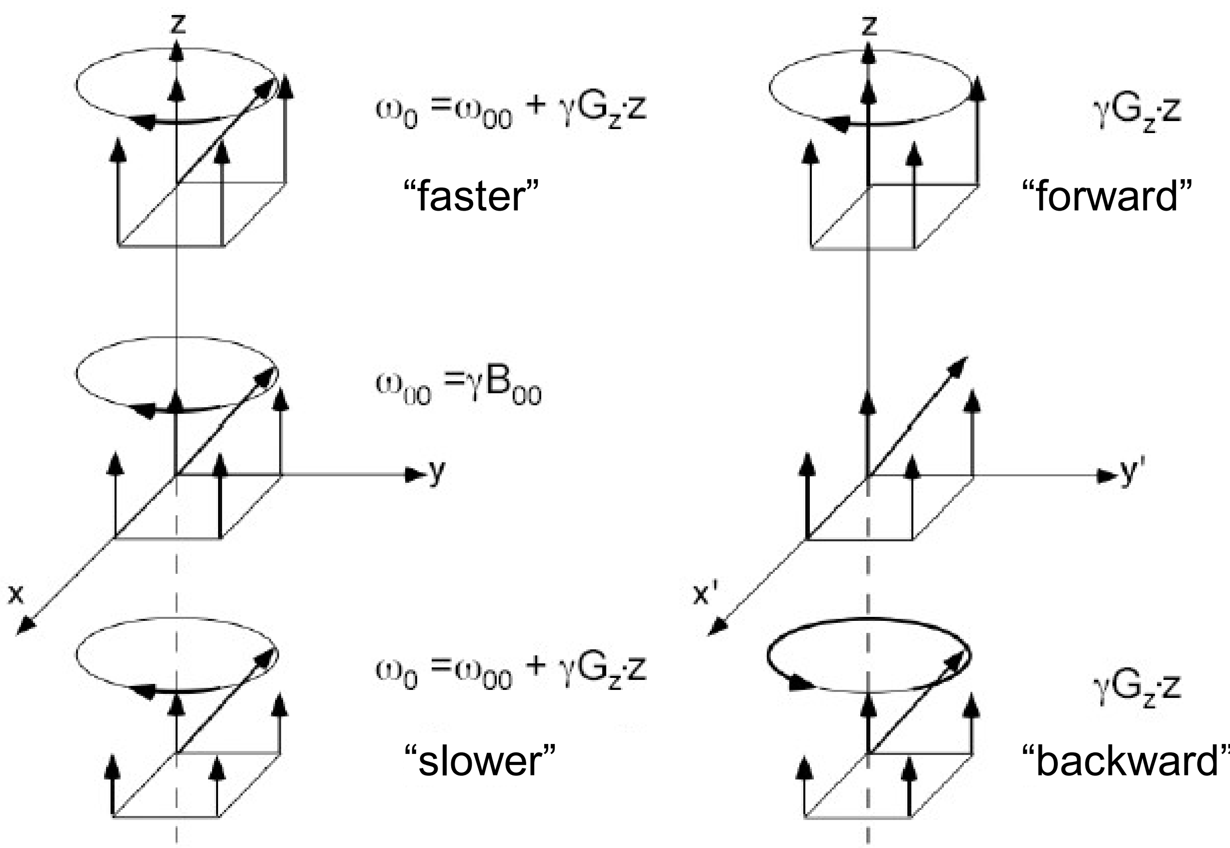

magnetic gyroscope in a constant magnetic field with a superimposed transversal alternating magnetic field (1)

stationary field B_z in z-direction and an alternating magnetic field B_T that rotates with frequency ω_T in the x-y-plane

alternating magnetic field:

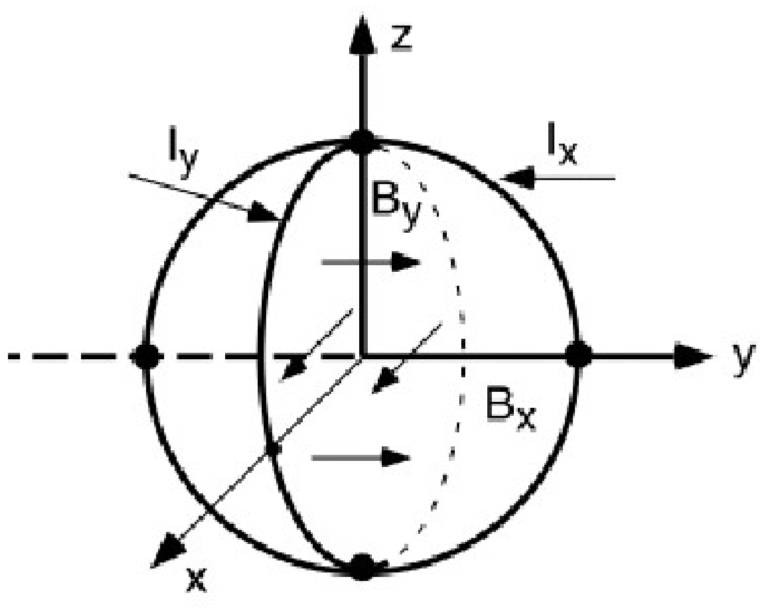

$$B_x = B_T \cdot \cos\omega_T t = \mathrm{Re}\left\{B_T \cdot e^{j\omega_T t}\right\}$$

$$B_y = B_T \cdot \sin\omega_T t = \mathrm{Im}\left\{B_T \cdot e^{j\omega_T t}\right\}$$

magnetic gyroscope in a constant magnetic field with a superimposed transversal alternating magnetic field (2)

additive superposition of B_z and B_T:

lateral view

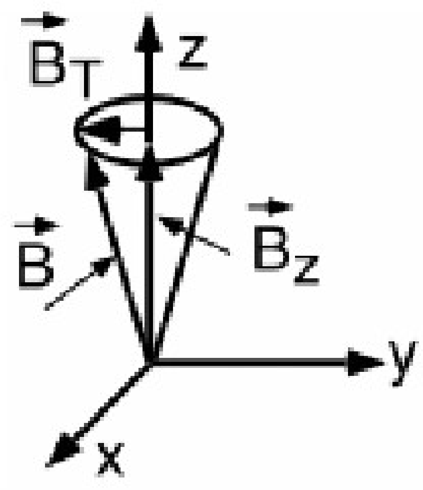

top view

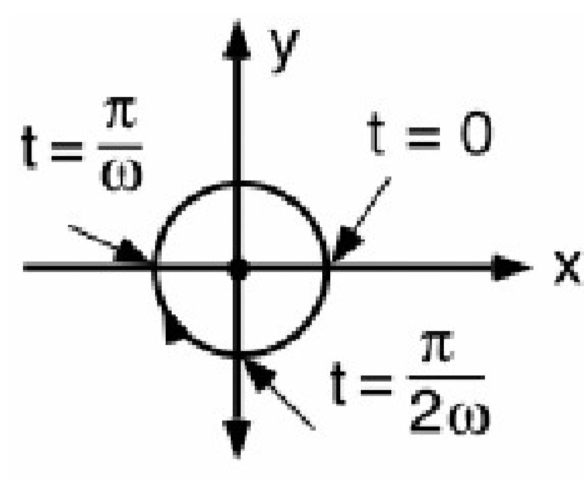

stationary laboratory system

magnetic gyroscope in a constant magnetic field with a superimposed transversal alternating magnetic field (3)

consider the case $\omega_T = \omega_0 = \gamma B_z$
(transversal field rotates with angular velocity of precession)

$\rightarrow$ direction of magnetic dipole moment is tilted from its resting position (z-direction) due to the alternating field

lateral view

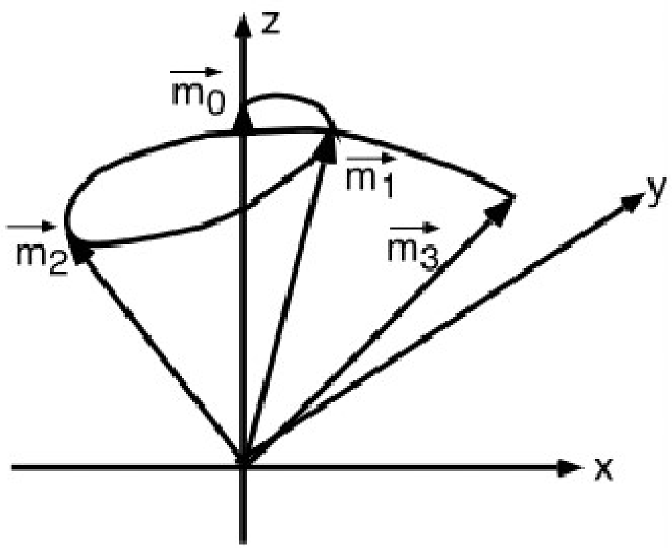

top view

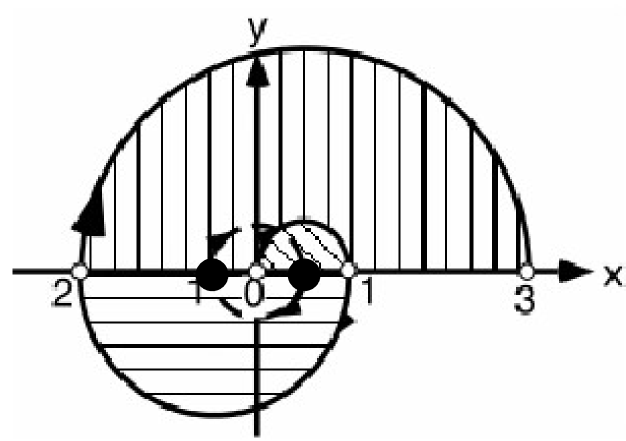

● magn. dipole moment

○ $B = B_z + B_T$

magnetic gyroscope in a constant magnetic field with a superimposed transversal alternating magnetic field (4)

direction of magnetic dipole moment is tilted from its resting position (z-direction) due to the alternating field

stationary laboratory system

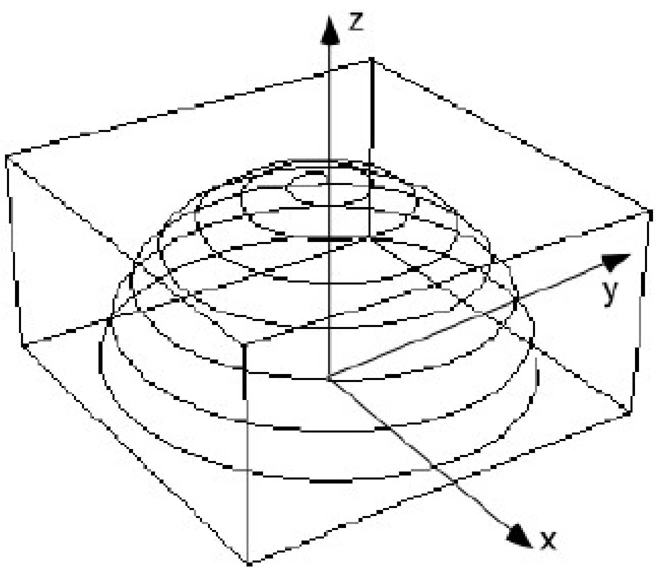

rotating frame

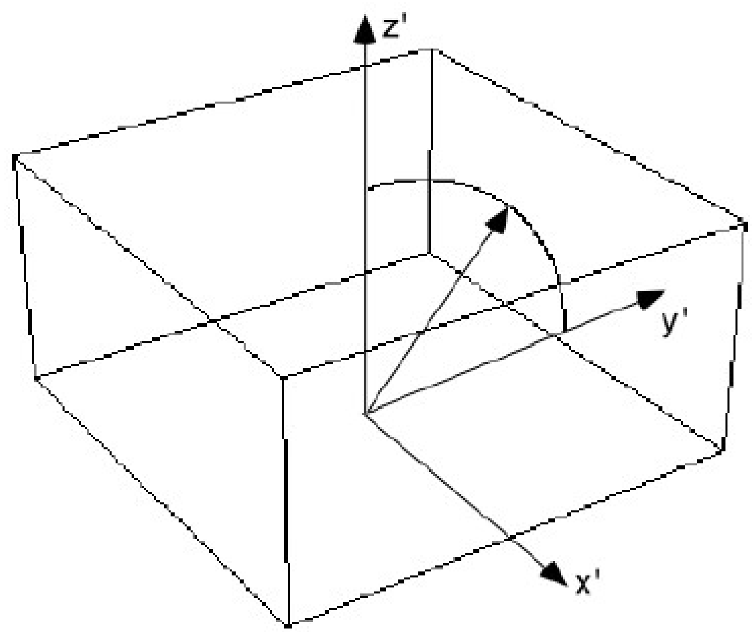

magnetic gyroscope in a constant magnetic field with a superimposed transversal alternating magnetic field (5a)

- magnetic dipole moment precesses around $\vec{B} = \vec{B}_z + \vec{B}_T$

- for $\omega_T = \omega_0$:
  amplification of phenomena "precession" and "wobbling due to $\vec{B}_T$"

- precession also starts with $\vec{m}_0 \parallel \vec{e}_z$

- length of $\vec{m}_0$ remains constant

- after some time T_{90}, $\vec{m}$ is in x-y-plane (even if $\vec{B}_T \ll \vec{B}_z$)

- $\vec{m}$ points to negative z-direction after $2 \cdot T_{90}$

magnetic gyroscope in a constant magnetic field with a superimposed transversal alternating magnetic field (5b)

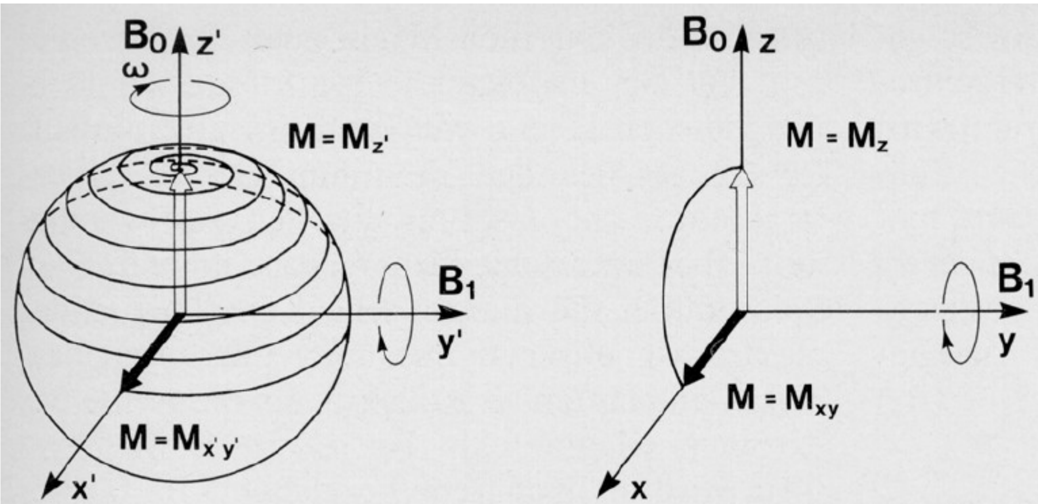

90°-HF-pulse in stationary and in rotating frame

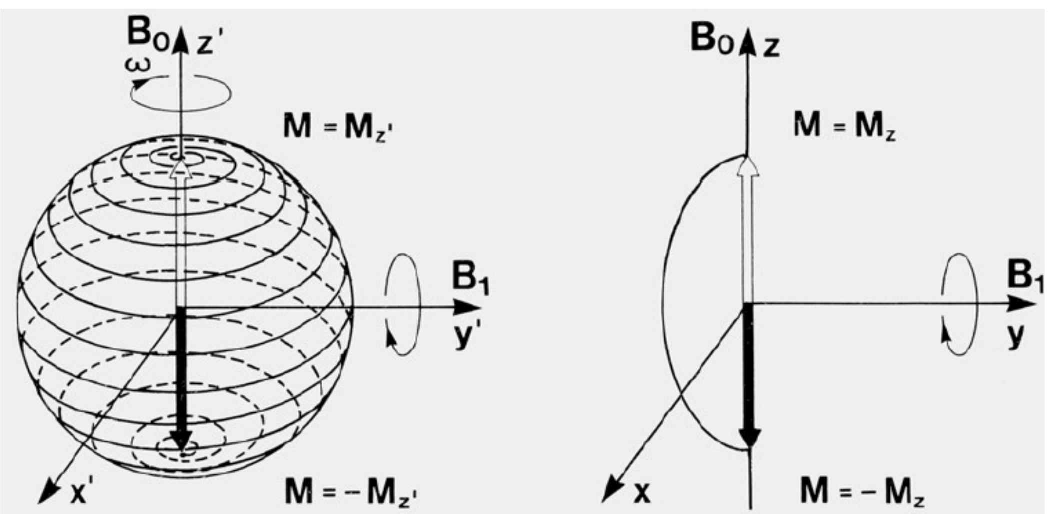

180°-HF-pulse in stationary and in rotating frame

magnetic gyroscope in a constant magnetic field with a superimposed transversal alternating magnetic field (6)

equation of motion of magnetic dipole:

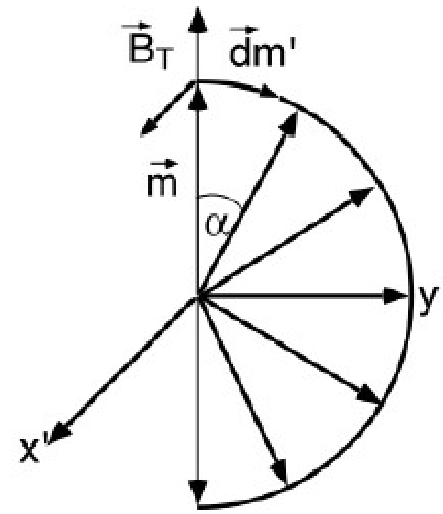

$$\frac{d\vec{m}'(t)}{dt} = \gamma \vec{m}'(t) \times \vec{B}_T$$

angular velocity of increasing α:

$$\omega_F = \frac{d\alpha}{dt} = -\frac{T}{L\sin\alpha} = -\frac{mB_T \sin\alpha}{L\sin\alpha} = -\frac{m}{L} B_T = -\gamma B_T$$

$\Rightarrow$

$\omega_F = \gamma B_T$ (convention)

$\alpha = \gamma B_T \tau$

α = flip angle
τ = pulse duration
B_T = amplitude of alternating field in x-direction

magnetic gyroscope in a constant magnetic field with a superimposed transversal alternating magnetic field (7a)

data acquisition (1):

assumptions:

- transversal field $\vec{B}_\mathrm{T}$ moves magnetic moment (from z-direction) into x-y-plane and is the turned off (pulse with duration τ)
- magnetic moment rotates in x-y plane without external influences

direction of normal of antenna coil is perpendicular to z-axis
flux proportional to transversal component of $\vec{m}$: m_T

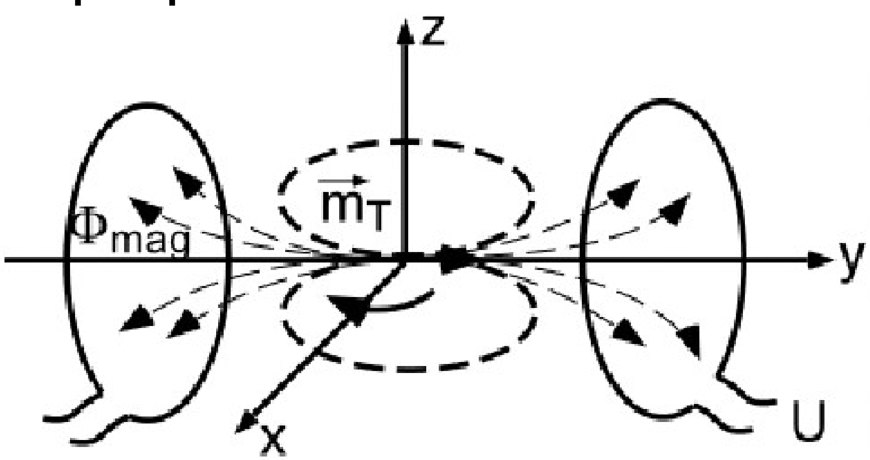

with $\vec{M} = \dfrac{d\vec{m}}{dV}$

$\Rightarrow$

$$\boxed{\begin{aligned}\Phi_\mathrm{mag} &\sim M_T \cos(\omega_0 t)\\ U &\sim M_T \omega_0 \sin(\omega_0 t)\end{aligned}}$$

magnetic gyroscope in a constant magnetic field with a superimposed transversal alternating magnetic field (7b)

data acquisition (2):

induced voltage in antenna is HF-signal with frequency ω_{00} (or near ω_{00}, if probe is placed in gradient field)

measurement technique (**quadrature detector**):

down-mixing of signal of antenna with HF-signal with frequency ω_{00} (precession frequency at z=0)

corresponds to multiplication with reference signal

magnetic gyroscope in a constant magnetic field with a superimposed transversal alternating magnetic field (7c)

data acquisition (3):

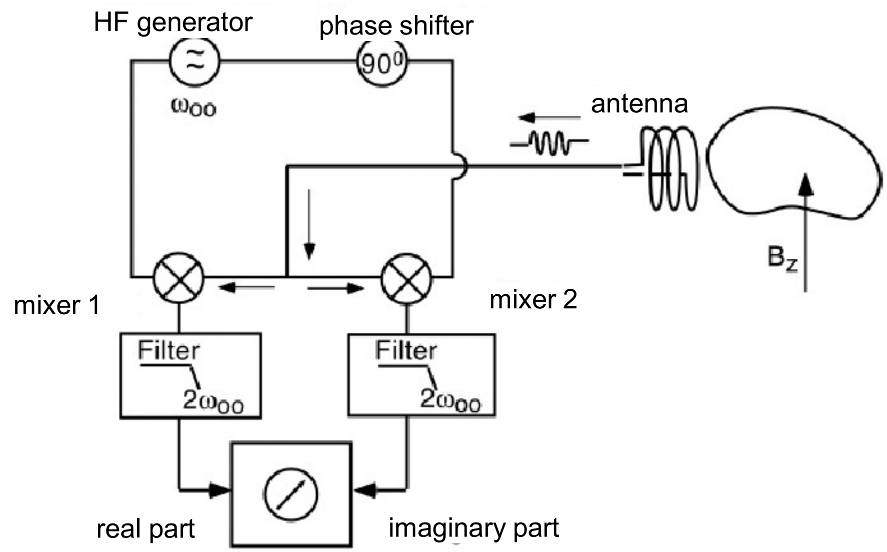

real part:

$$U_R = U_1 \sin(\omega_{00} t) U_2 \sin\big((\omega_{00} + \Delta\omega)t\big)$$

$$= U_1 U_2 \frac{1}{2} \left\{ \cos(\Delta\omega t) - \cos\big((2\omega_{00} + \Delta\omega)t\big) \right\}$$

$\Delta\omega$ via low-pass filtering

imaginary part

(phase shifter required, since cos-term symmetric $\rightarrow$ you loose the sign of $\Delta\omega$!)

$$U_I = U_1 \cos(\omega_{00} t) U_2 \sin\big((\omega_{00} + \Delta\omega)t\big)$$

$$= U_1 U_2 \frac{1}{2} \left\{ \sin(\Delta\omega t) + \sin\big((2\omega_{00} + \Delta\omega)t\big) \right\}$$

$$U^* = U_R + \mathrm{i} U_i \sim m_T$$

- U^* rotates in in the complex plane with $\Delta\omega$
- measures m_T in a rotating (with ω_{00}) frame

magnetic gyroscope in a constant magnetic field with a superimposed transversal alternating magnetic field (7d)

data acquisition (4):

$\Delta\omega < 0$

reference oscillator

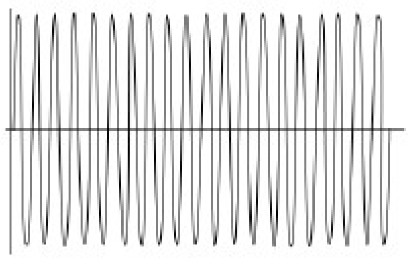

Y0 : f = 40.000 kHz

signal@antenna

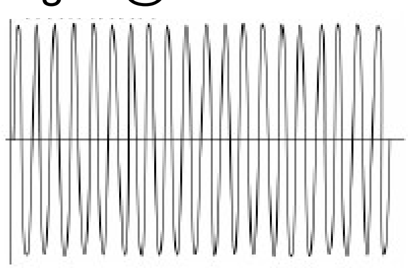

Y1 : f = (40.000+2000) kHz

signal after mixer 1

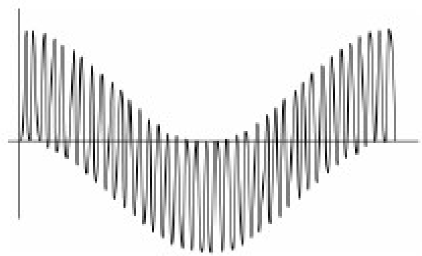

Y0 · Y1

signal after lowpass

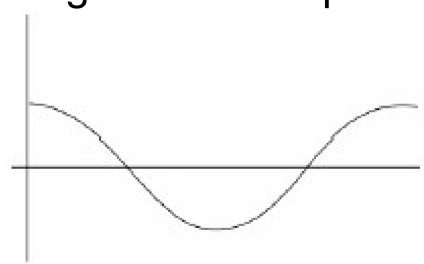

Y0 · Y1 nach Tiefpass → Realteil

signal after mixer 2

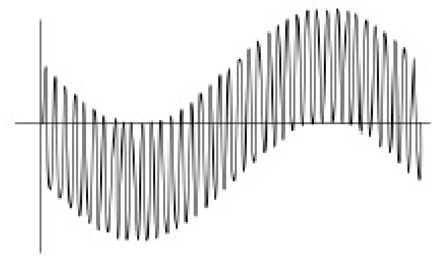

(Y0 + 90°) · Y1

signal after lowpass 2
pointer in complex plane

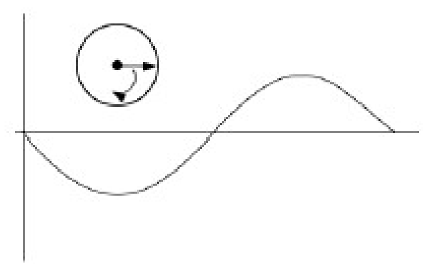

(Y0 + 90°) · Y1 nach Tiefpass → Imaginärteil

magnetic resonance imaging (MRI) *magnetic gyroscope (class.)*

magnetic gyroscope in a constant magnetic field with a superimposed transversal alternating magnetic field (7e)

data acquisition (5):

$\Delta\omega > 0$

reference oscillator

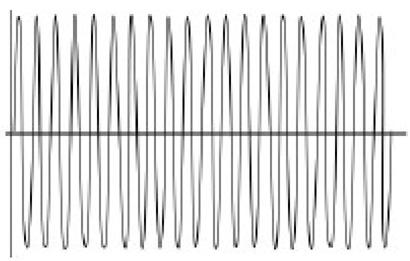

Y0 : f = 40.000 kHz

signal@antenna

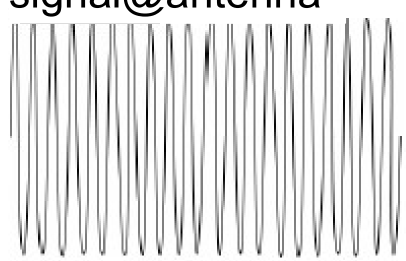

Y2 : f = (40.000-2000) kHz

signal after mixer 1

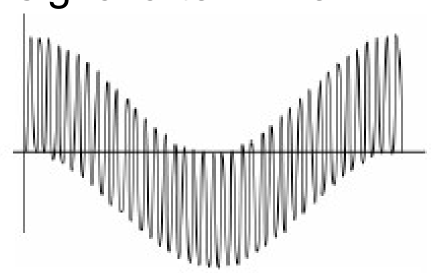

Y0 · Y2

signal after lowpass

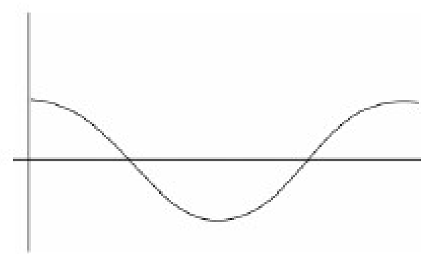

Y0 · Y2 nach Tiefpass Realteil

signal after mixer 2

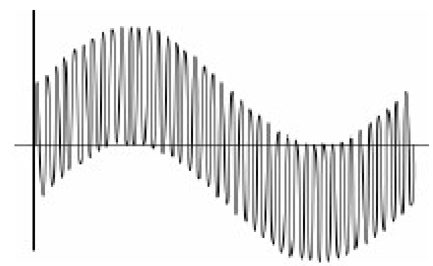

(Y0 + 90°) · Y2

signal after lowpass 2
pointer in complex plane

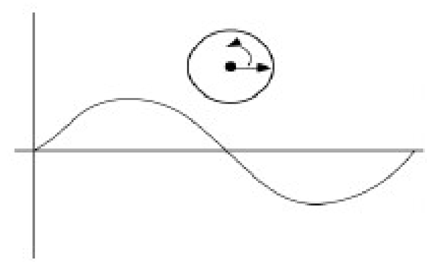

(Y0 + 90°) · Y2 nach Tiefpass ⟶ Imaginärteil

protons, neutrons, electrons as (quantum mechanical) magnetic gyroscopes

gyromagnetic ratio of a rotating charged particle:

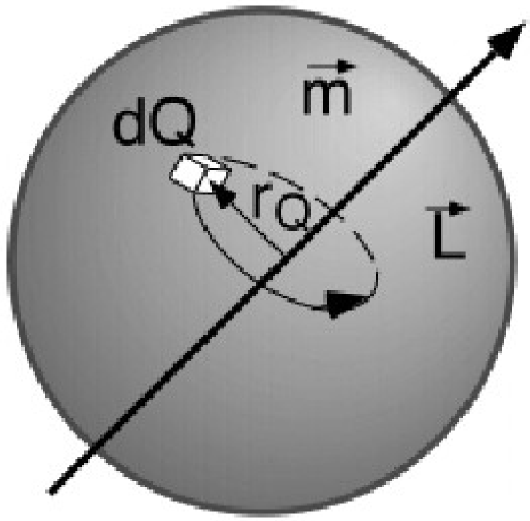

$$\vec{\mu} = \vec{\gamma} \cdot \vec{L}$$

$\vec{\mu}$, $\vec{m}$ = magnetic dipole moment

$\vec{L}$ = angular momentum

γ = gyromagnetic ratio

precession of nuclear spins in a constant magnetic field:
if μ is aligned in direction of $B \rightarrow$ precession with Larmor frequency

$$\omega_0 = \gamma\, B = g_L \frac{q}{2m} B$$

g_L = Landé factor

gyromagnetic ratio of some nuclei

nucleus	^{1}H	^{31}P	^{19}F	^{13}C
γ^*[MHz/T]	42,6	17,2	40,0	10,8

$$\gamma^* = \frac{\gamma}{2\pi}$$

precession frequency of protons

$$\boxed{f_0 = \gamma^* \left[\frac{MHz}{T}\right] \cdot B[T] \qquad \omega_0 = 2\pi f_0}$$

B	50 μT	0,5 T	1 T	4 T
f_0	2,13 kHz	21,3 MHz	42,6 MHz	170,4 MHz

nucleus	spin quantum number I	gyro magnetic ratio γ [10^8 rad s^{-1} T^{-1}]	natural abundance of isotopes [%]	sensitivity for B_0=const [%] wrt ^1H
^{1}H	1/2	2,675	99,98	100,00
^{31}P	1/2	1,084	100,00	6,65
^{23}Na	3/2	0,708	100,00	9,27
^{13}C	1/2	0,673	1,11	$1{,}75 \times 10^{-2}$
^{14}N	1	0,193	99,63	$1{,}0 \times 10^{-1}$
^{17}O	5/2	-0,363	0,038	$1{,}11 \times 10^{-3}$
^{19}F	1/2	2,518	100,00	83,4
^{35}Cl	3/2	0,262	75,77	$3{,}58 \times 10^{-1}$
^{39}K	3/2	0,125	93,26	$4{,}76 \times 10^{-2}$
^{25}Mg	5/2	-0,164	10,00	$2{,}68 \times 10^{-2}$
^{43}Ca	7/2	-0,180	0,135	$8{,}68 \times 10^{-4}$
^{33}S	3/2	0,205	0,75	$1{,}70 \times 10^{-3}$

example:

- proton (^{1}H) measurement
- constant B-field (1T) in z-direction
- gradient field (3mT/m) in z-direction
- at z = 0: f_{00} = 42,6 MHz

how much is the frequency shift Δf of the spins at z = 10 mm?

$$\Delta f_{(10\,\mathrm{mm})} = \gamma^* \left[\frac{\mathrm{MHz}}{\mathrm{T}}\right] G_z \left[\frac{\mathrm{T}}{\mathrm{m}}\right] z[\mathrm{m}]$$

$$= 42.6 \times 3 \cdot 10^{-3} \times 10 \cdot 10^{-3} [\mathrm{MHz}]$$

$$= 1.28 [\mathrm{kHz}]$$

(cf. quadrature detector)

frequency shift does not depend on the strength of the constant field !

directional quantization of angular momentum

$\left|\vec{L}\right| = \sqrt{l(l+1)}\hbar$ $\vec{L} = \text{angular momentum}, l = \text{secondary quantum number}$

$L_z = m_l \hbar$ $m_l = \text{magnetic quantum number}$

$m_l \in \{-l, -l+1, \ldots, +l\}$

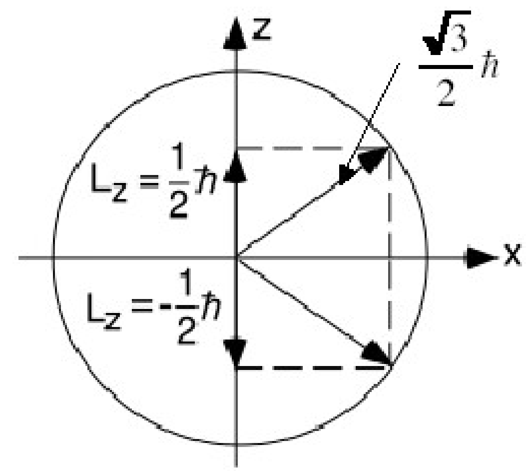

for spin-1/2-particles (protons!), we have:

$$\left|\vec{L}\right| = \sqrt{\frac{1}{2}\left(\frac{1}{2}+1\right)}\hbar = \frac{\sqrt{3}}{2}\hbar$$

$$L_z = \pm\frac{1}{2}\hbar$$

with uncertainty principle: is L_z defined, then L_x, L_y undefined

magnetic dipole moment: $\boxed{\langle \mu_z \rangle = \pm\gamma\frac{1}{2}\hbar}$

energy levels (spin-1/2 particles)

class. magn. dipole in $\vec{B}$ - field:

$$E = -\vec{m} \cdot \vec{B}$$

spin-1/2 particles in $\vec{B} = (0,0,B_z)$ - field:

$$E = -\mu_z B_z = \mp \gamma \frac{1}{2} \hbar B_z$$

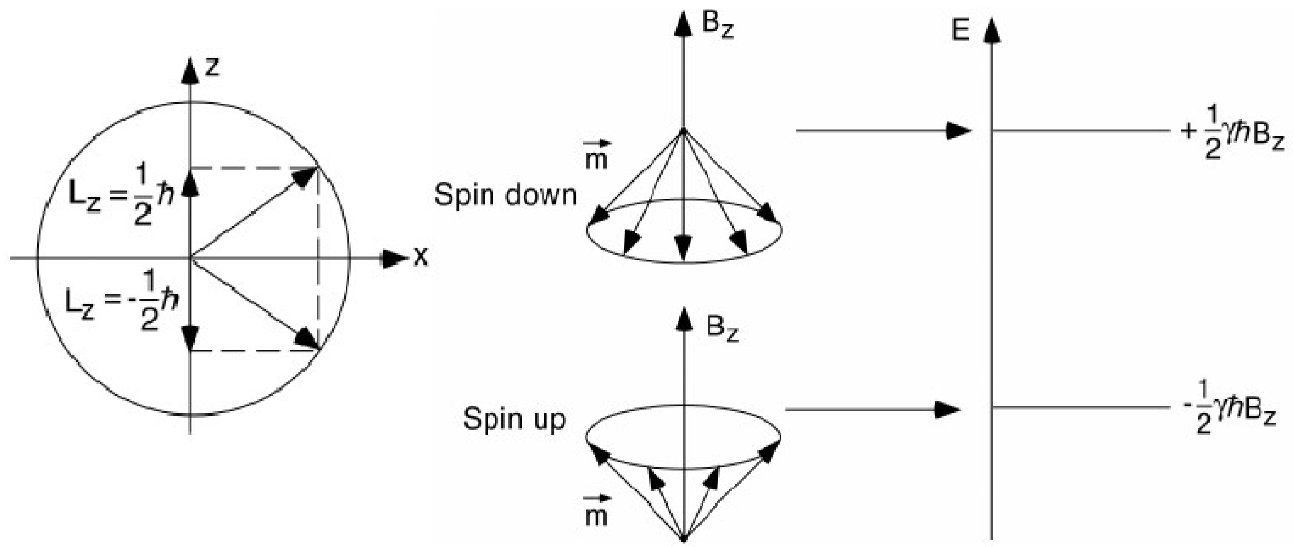

Zeeman effect (weak field)
Paschen-Back effect (strong field)

energy levels and resonance

- photons, that can induce a spin flip, have energy of:

$$\hbar\omega_0 = \gamma\hbar B_z$$

- the related electromagnetic wave has angular velocity:

$$\omega_0 = \gamma B_z$$

- since ω_0 = Larmor frequency $\rightarrow$ **resonance phenomenon**

- absorption line is Lorentzian with life time T_2:

$$\sim \frac{T_2}{1+(\omega-\omega_0)^2 T_2^2}$$

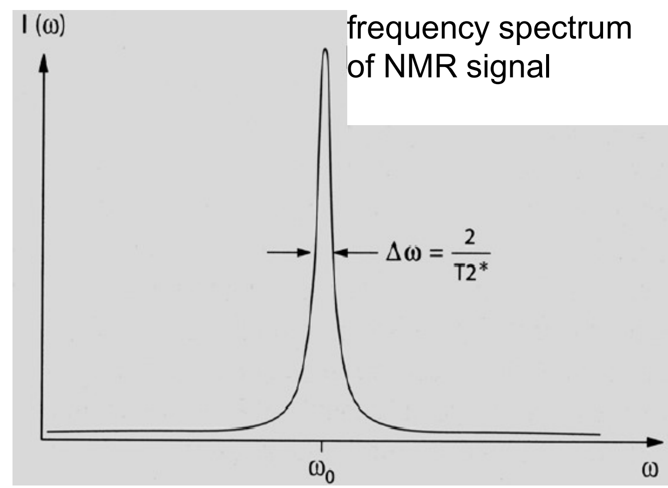

frequency spectrum of NMR signal

population of energy levels

N^+ = number of spin-ups (upper energy level)
N^- = number of spin-downs (lower energy level)
with Boltzmann statistics, we have:

$$\frac{N^-}{N^+} = e^{(\Delta E/kT)} = e^{(+\gamma\hbar B_0/kT)}$$

with small values of argument of exponential: $\boxed{\frac{N^-}{N^+} = 1 + \gamma\hbar B_0/kT}$

example:
proton measurement with 1T B_0-field at 37°C (310K):

$$\boxed{\frac{N^-}{N^+} = 1.0000066 \;\propto\; 6.6\,\text{ppm}}$$

macroscopic magnetization

$$M_z = (N^- - N^+)\langle \mu_z \rangle / V$$

$$N^- = N^+ + N^+ \gamma \hbar B_0 / kT$$

$$N^- - N^+ \approx \frac{N}{2} \gamma \hbar B_0 / kT$$

$$M_z = \frac{N}{2} \gamma \hbar B_0 \langle \mu_z \rangle / kTV$$

$$= \frac{N}{2} \gamma \hbar B_0 \frac{1}{2} \gamma \hbar / kTV = \boxed{\left(\frac{N}{V}\right)\left(\gamma^2 \hbar^2 / 4kT\right) B_0}$$

1 mm^3 water contains $6.7 \cdot 10^{19}$ protons

with B_0=1T and T=37 °C, we have: $\boxed{M_z \sim 3 \cdot 10^{-3}\text{ A/m}}$

magnetization has z-component only (x,y-components “undefined”)

q.m. gyroscope in constant magnetic field with superimposed transversal alternating magnetic field

an ensemble of quantum-mechanic spins can be viewed as a classical magnetic gyroscope

- constant field: ground state = longitudinal magnetization
- magnetic moment m in alternating field B_T is tilted from its resting position in a spiral-like manner (precession)
- length of m remains constant: $|\vec{m}| = 1/2\,\gamma\hbar$
- if $\omega_T = \omega_0$ (resonance condition): magnetic moment m of spin ensembles is turned away from z-axis (resonance phenomenon)
- after time T_{90}, m is in x-y-plane, measurable mean magnetic moment, precession with $\omega_0 = \gamma\, B$
- after time $2 \cdot T_{90}$, m points to negative z-direction
- $\alpha = \gamma \cdot B_T \cdot \tau$ (flip angle) is achieved with irradiating a transversal wave with amplitude B_T lasting time τ

relaxation to thermic equilibrium

without external forcing: magnetic gyroscope continues to precesses with angle α between B and m (α = m_z = const.)

in human body: interactions with environment:

$\Rightarrow$

spin-lattice relaxation or longitudinal relaxation (T_1 time)
(interactions with surrounding atoms)

spin-spin relaxation or transversal relaxation (T_2 time)
("collisions" with other magnetic gyroscopes)

cf. Bloch equations

spin-lattice relaxation

following an excitation, the system returns to its equilibrium state due to interactions with the lattice (T1 time)

longitudinal relaxation: $$\frac{dM_z}{dt} = -(M_z - M_0)/T_1$$

M_z: longitudinal magnetization
M_0: longitudinal magnetization in thermal equilibrium
T_1: time constant for relaxation

$$M_z(t) = M_0(1 - e^{-t/T_1})$$

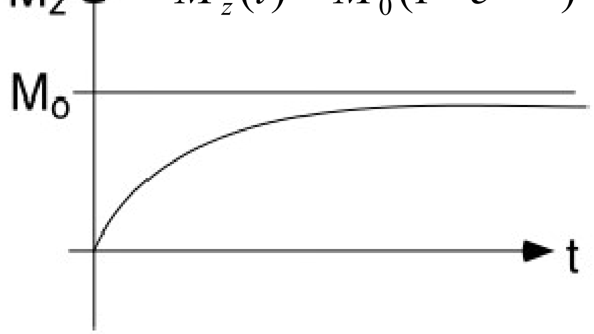

free induction decay (FID)

$$M_z(t) = M_0(1 - 2e^{-t/T_1})$$

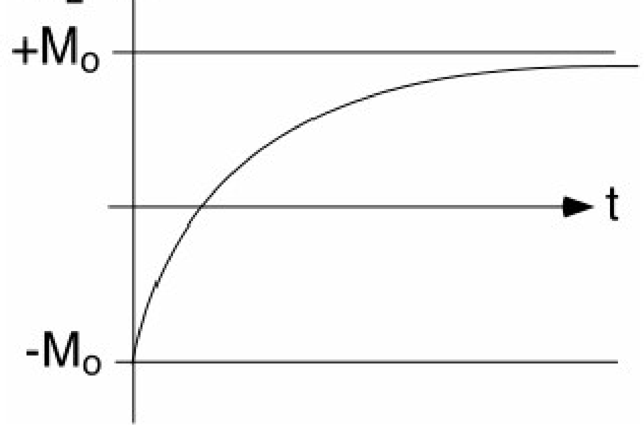

inversion recovery (IR)

spin-lattice relaxation (T_1 time)

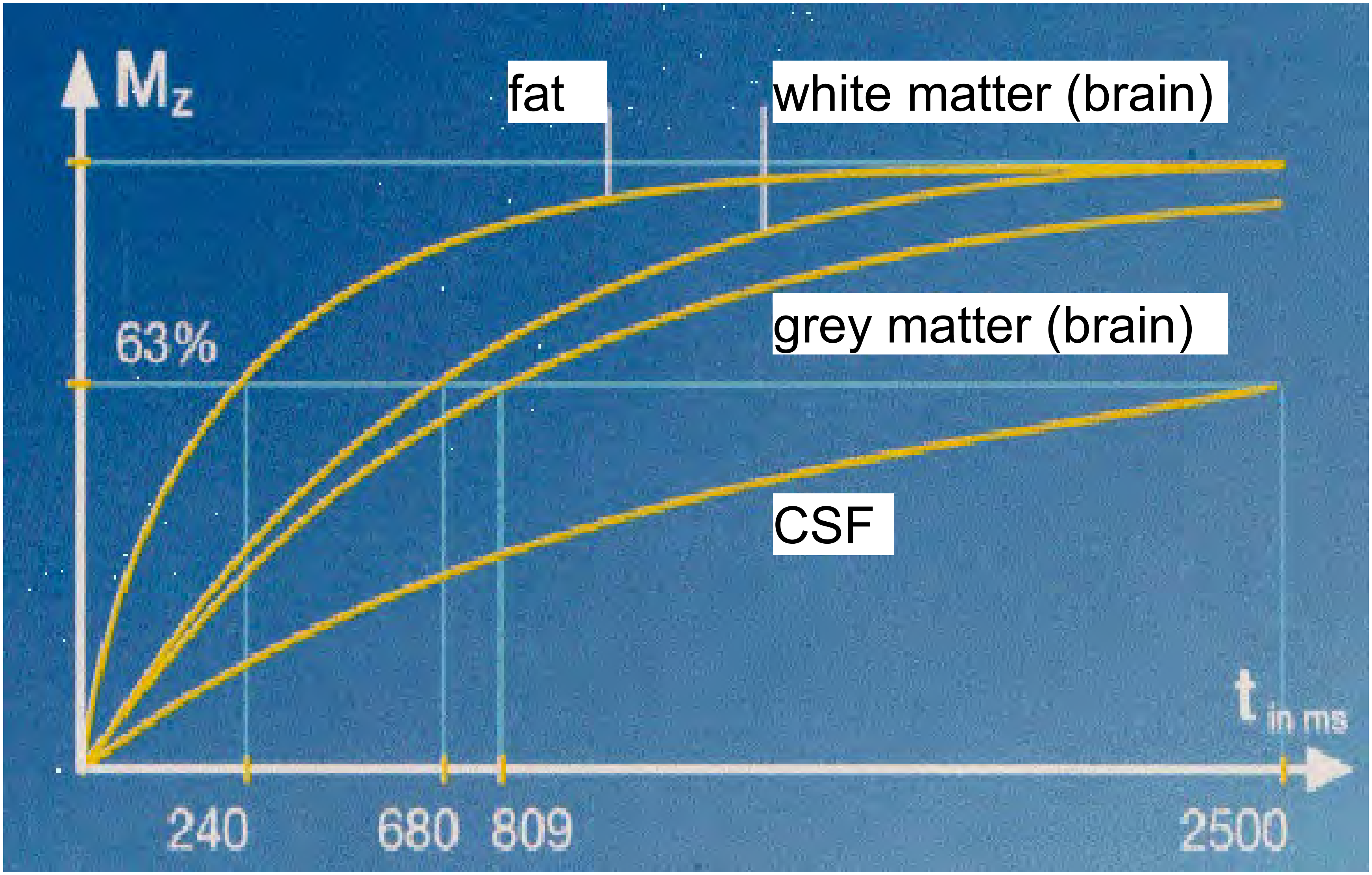

spin-spin relaxation

transversal magnetization M_{T} "dephases" due to spin-spin interaction (T_2 time)

transversal magnetization M_{T} "dephases" due to different precession frequencies of spin-ensembles (T_2^* time)

$$M_T(t) = M_{T0} e^{-t/T_2^*}$$

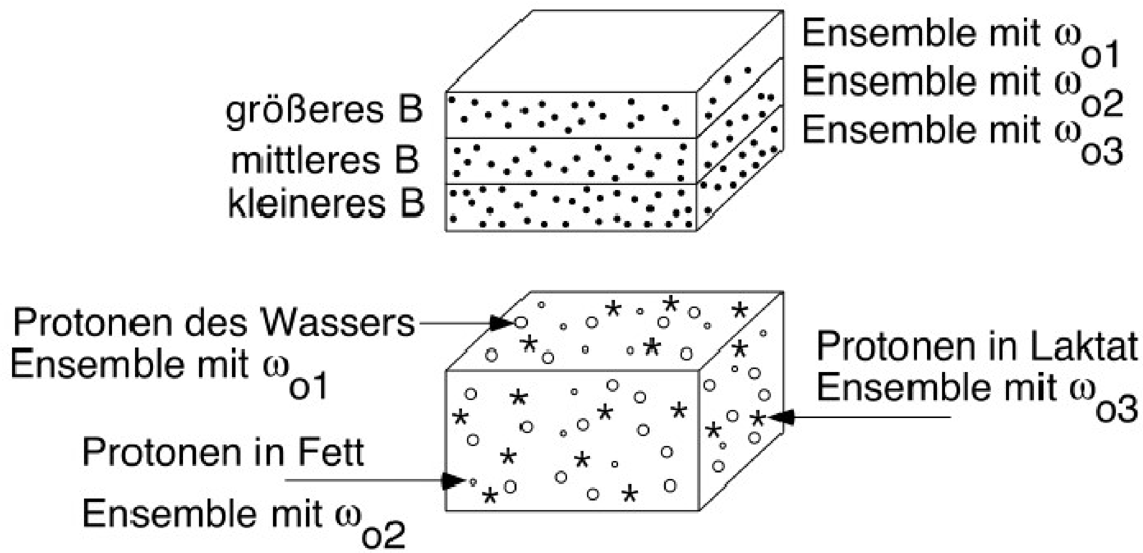

$$\frac{1}{T_2^*} = \frac{1}{T_1} + \frac{1}{T_2}$$

we always have: $T_2^* \leq T_1$

spin-spin relaxation (dephasing)

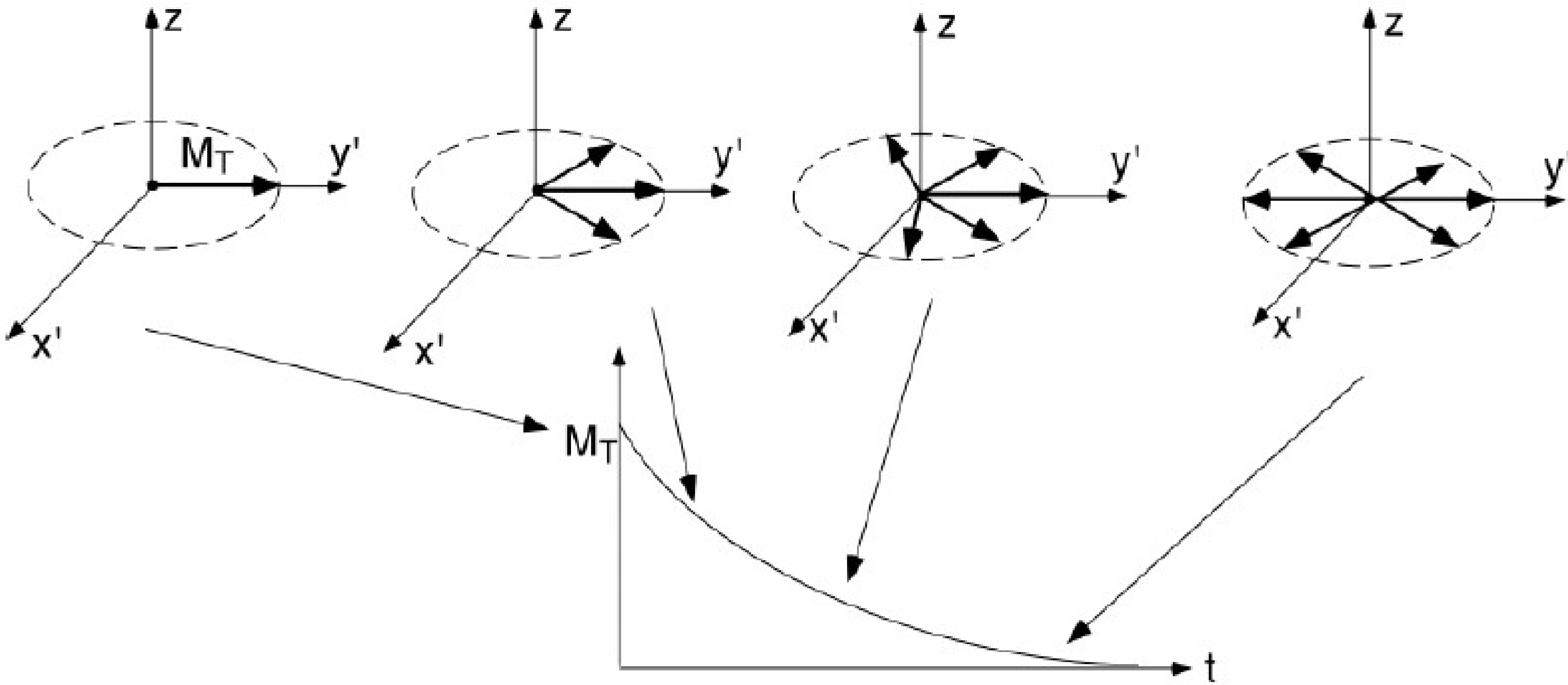

spin-spin relaxation (T_2 time)

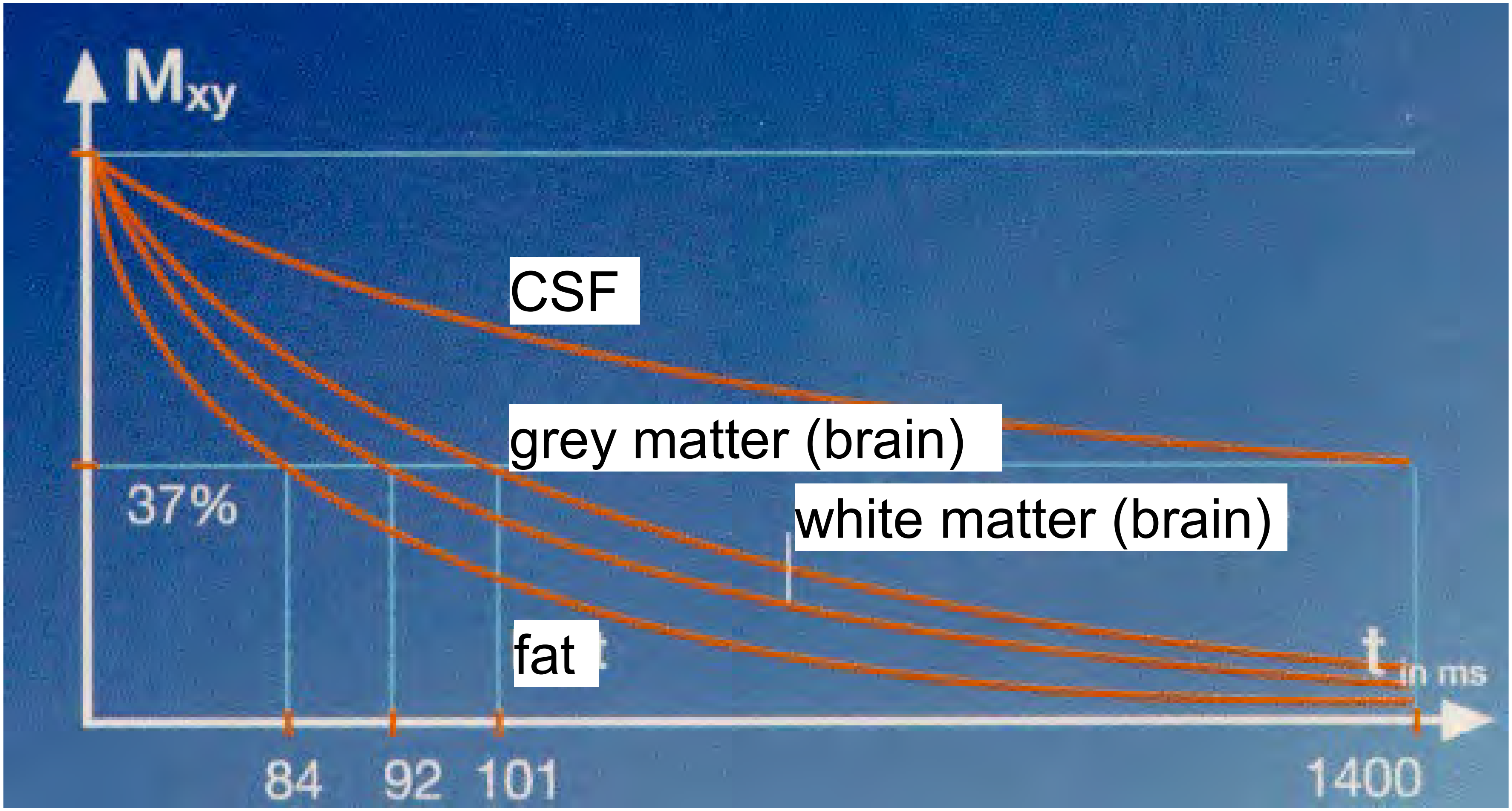

T_1- and T_2 times for different tissues

tissue	T_1 in ms	T_2 in ms
muscle	730 ± 130	47 ± 13
heart	750 ± 120	57 ± 16
liver	420 ± 90	43 ± 14
kidneys	590 ± 160	58 ± 24
spleen	680 ± 190	62 ± 27
fat	240 ± 70	84 ± 36
grey matter	810 ± 140	102 ± 13
white matter	680 ± 120	92 ± 22

Free-Induction Decay (FID) after 90° pulse

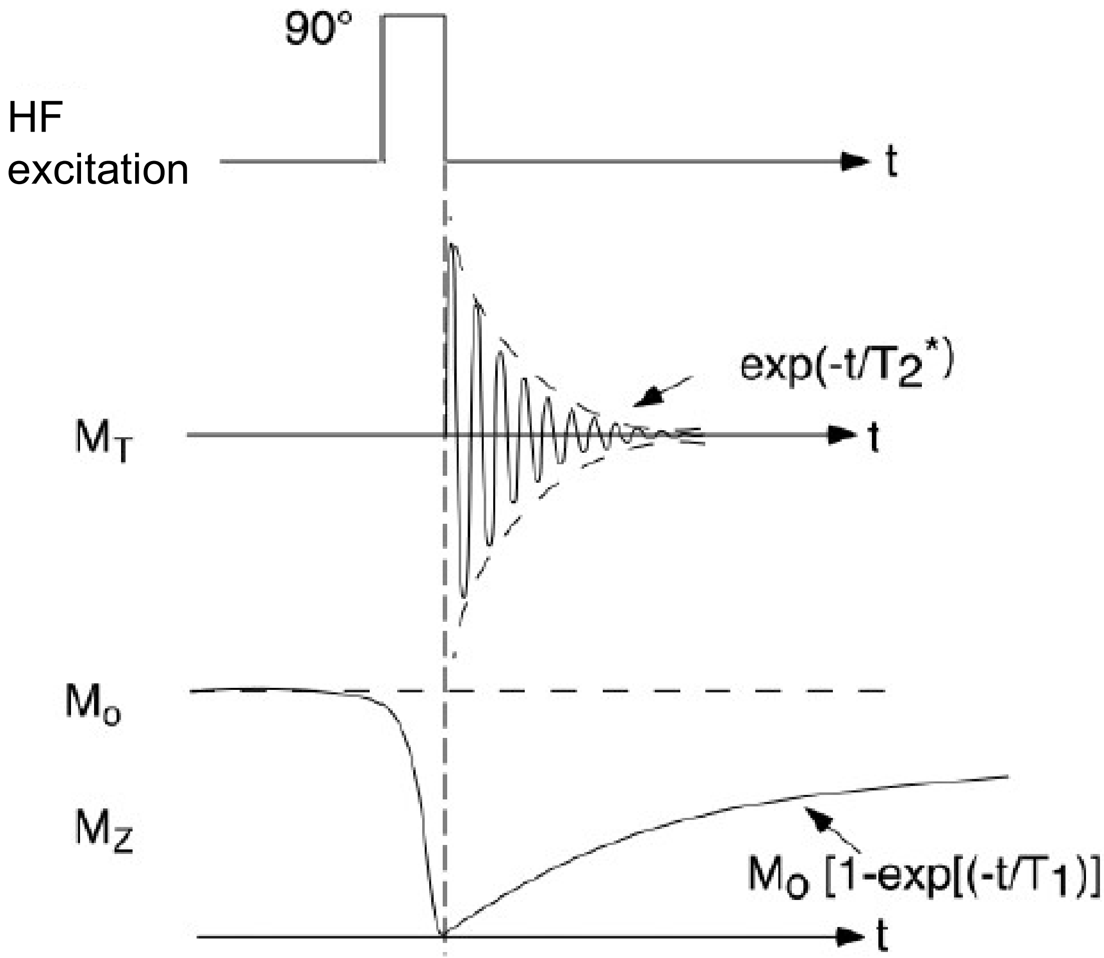

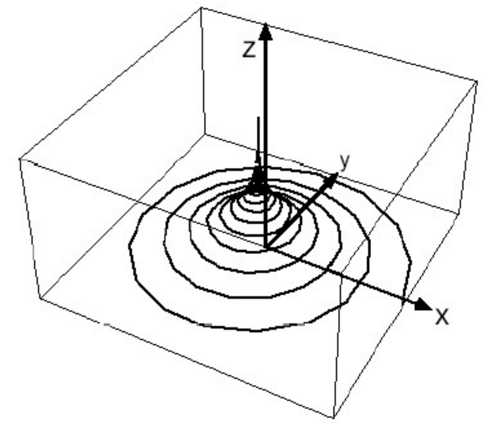

rotating transversal magnetization M_T induces AC-voltage in antenna with frequency ω_0 und decaying amplitude ~ $\exp(-t/T_2^*)$:

$$M_x = M_{z0} e^{-t/T_2^*} \cos\omega_0 t$$

after mixing in quadrature detector, we find:

$$M_x^{'} = M_{z0}\, e^{-t/T_2^*}$$

however: M_z not yet in thermal equilibrium due to $T_2^* \leq T_1$

Saturation-Recovery **pulse sequence**

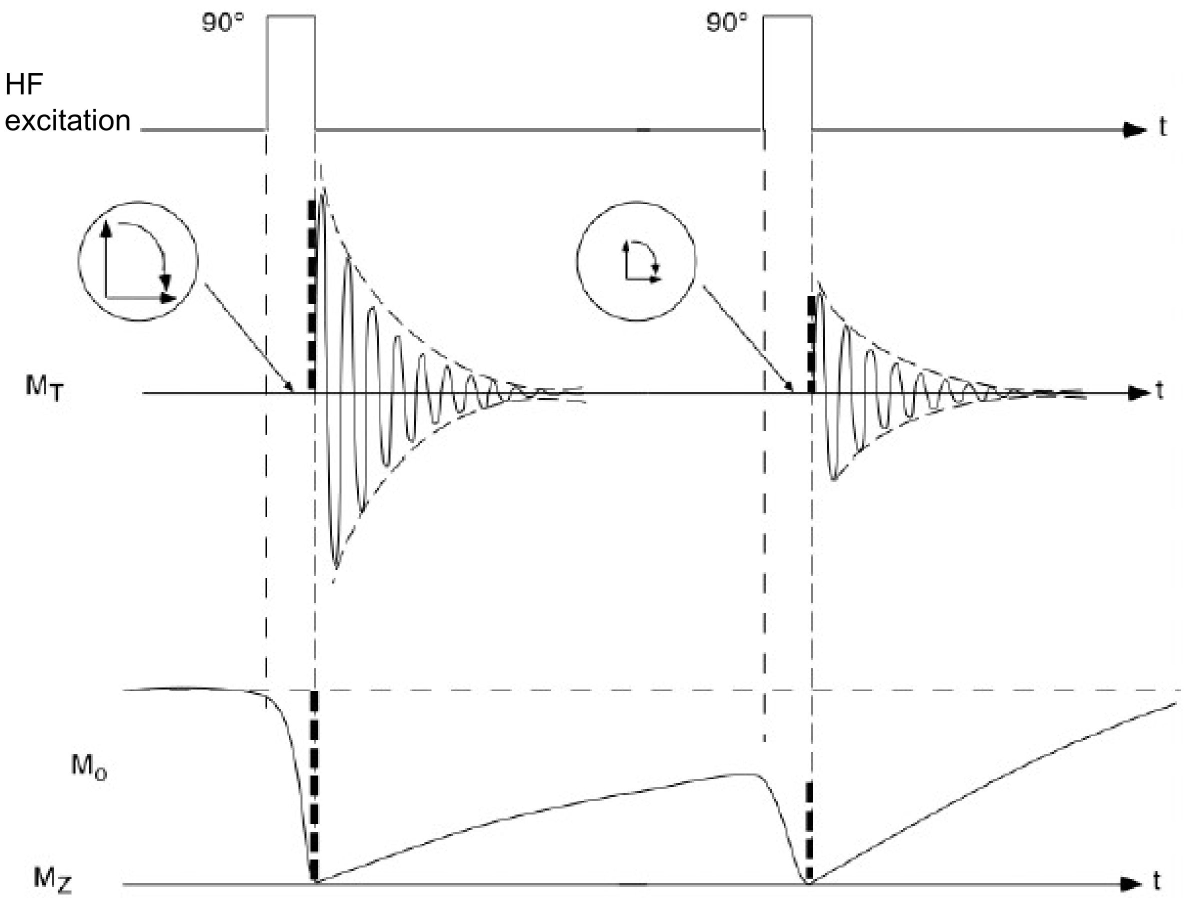

1. pulse:
regular FID signal

2. pulse:
FID signal with smaller amplitude since M_z not yet in thermal equilibrium due to $T_2^* \leq T_1$

amplitude of following FID signal can be increased by choosing longer time (T_R time) between pulses

However:

allows for contrast selection !
(T_1/T_2 weighting)

Inversion-Recovery **pulse sequence**

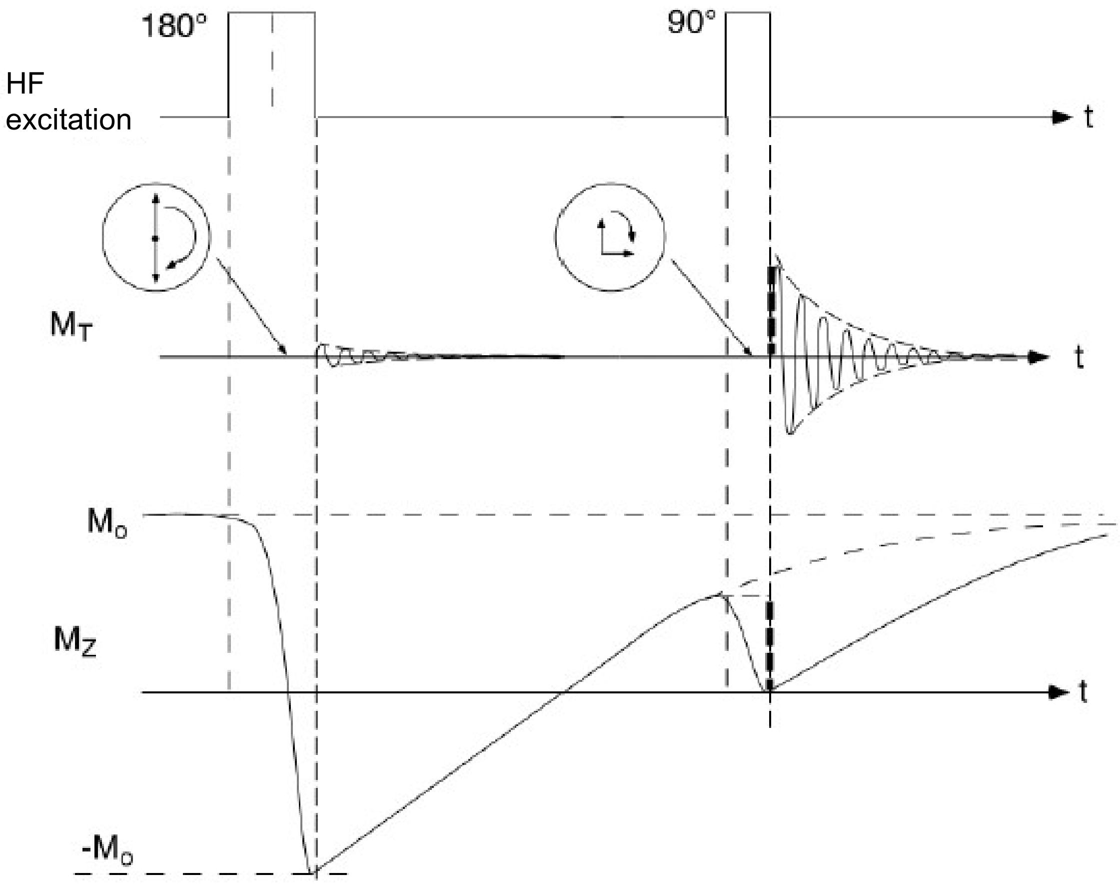

1. pulse:
no transversal magnetization ⇒
no signal in antenna, but

$$M_z = M_{z0}\left(1-2e^{-t/T_1}\right)$$

2. pulse:
induces transversal magnetization ⇒
FID signal with amplitude that depends on remaining longitudinal magnetization

if time between pulses ($t_{1/2}$)

$$e^{(-t_{1/2}/T_1)} = 1/2$$

$$\Rightarrow$$

$$-t_{1/2} = T_1 \ln(1/2)$$

$$t_{1/2} = T_1 \ln(2)$$

⇒ if $t_{1/2}$ chosen optimally, determine T_1 !

magnetic resonance imaging (MRI) *nuclear spin*

PHYSICAL REVIEW VOLUME 80, NUMBER 4 NOVEMBER 15, 1950

Spin Echoes*†

E. L. HAHN‡
Physics Department, University of Illinois, Urbana, Illinois
(Received May 22, 1950)

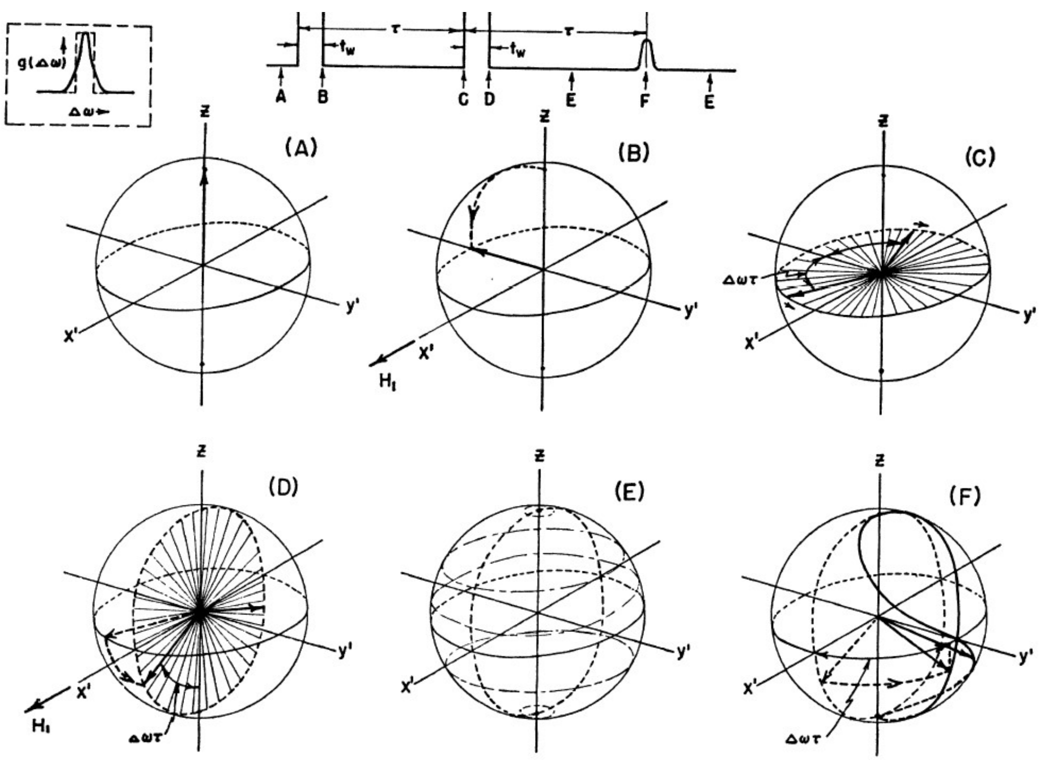

$\omega_1 >> (\Delta\omega)_{1/2}$, $t_w << \tau < T_1, T_2$, $\omega_1 t_w = \frac{\pi}{2}$

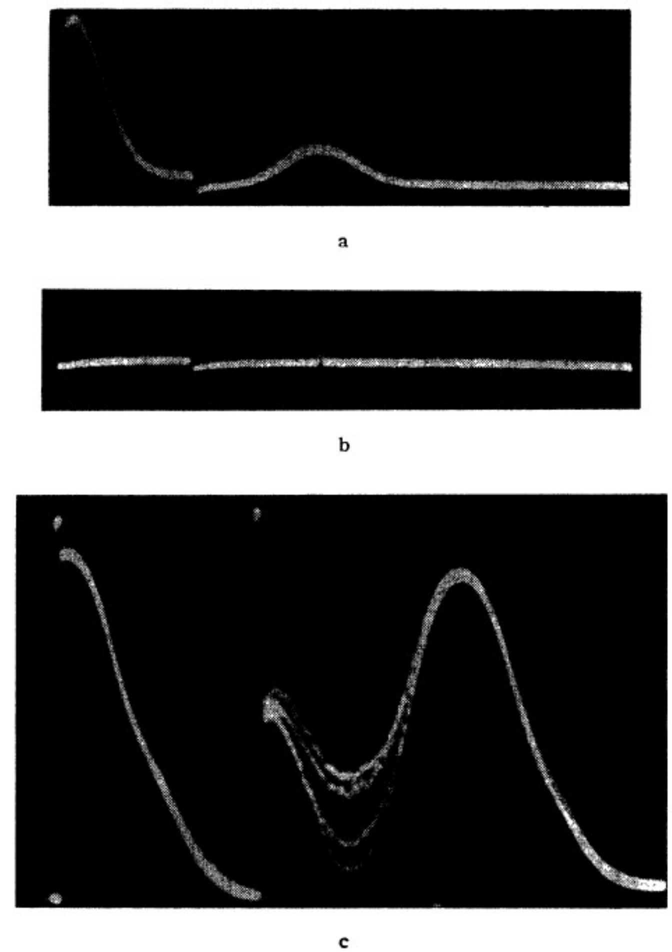

FIG. 2. Oscillographic traces for proton echoes in glycerine. The two upper photographs indicate broad and narrow signals corresponding to H_0 fields of good and poor homogeneity. The pulses, scarcely visible, are separated by 0.0005 sec. The induction decay following the first pulse in the top trace has an initial dip due to receiver saturation. The bottom photograph shows random interference of the induction decay with the echo for several exposures. The two r-f pulses are phase incoherent relative to one another.

spin echoes (1)

given:
constant B_0 field in z-direction and a rotating transversal field B_T with frequency ω_T :

$$B_x = B_T \cos(\omega_T t + \Psi)$$
$$B_y = B_T \sin(\omega_T t + \Psi)$$
$$B_z = B_0$$

observation:
after 90° HF excitation: FID signal (transversal magnetization, T_2* time) decays faster than longitudinal magnetization (T_1 time)

reason:
every spin ensemble is subjected to slightly different magnetic field strengths (inhomogeneities) $\Rightarrow$ dephasing of spin ensembles

is there a way to revert the dephasing of spin ensembles ?

spin echoes (2)

rephasing of spin ensembles:

applying a 180° HF pulse after FID signal has died out leads to rephasing
$\Rightarrow$ measurable signal in antenna = SPIN ECHO

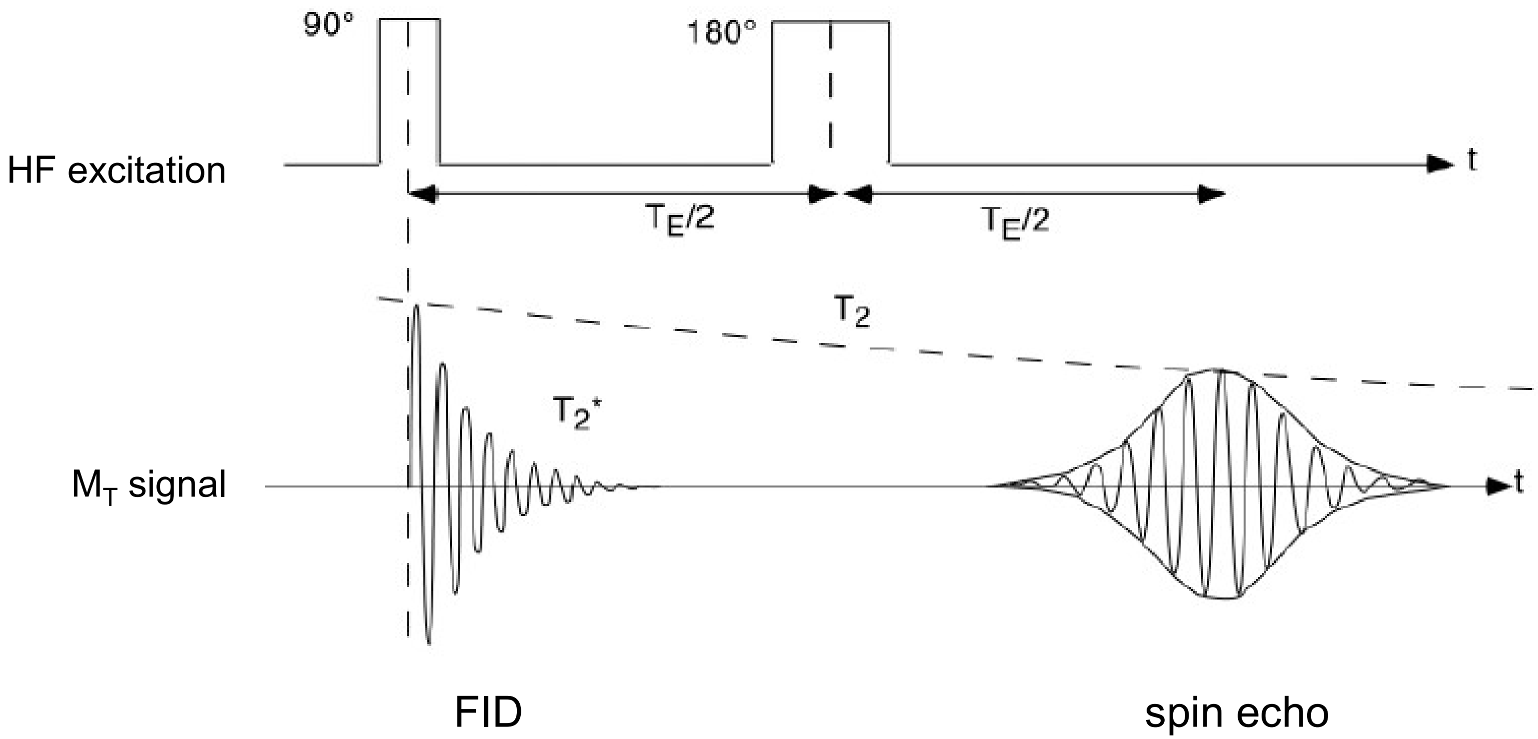

T_E = echo time

$T_E/2$ freely adjustable

spin echoes (3)

rephasing of spin ensembles with 180° HF-pulse (phase ψ = 0°)

(1) 90°HF-pulse: turn down magnetization into +y‘-direction

(2) dephasing:
clockwise:
some spin ensembles lead
some spin ensembles are behind

(3) after T_E/2 180° HF-pulse (Ψ=0°):
rotate spins by 180° around x‘-axis

(4) too slow spins still too slow,
faster spins still too fast
(clockwise !) $\Rightarrow$ rephasing!

(5) after T_E: all magnetic moments again in-phase
$\Rightarrow$ measureable transversal magnetization
(in –y‘-direction) $\Rightarrow$ **spin echo**

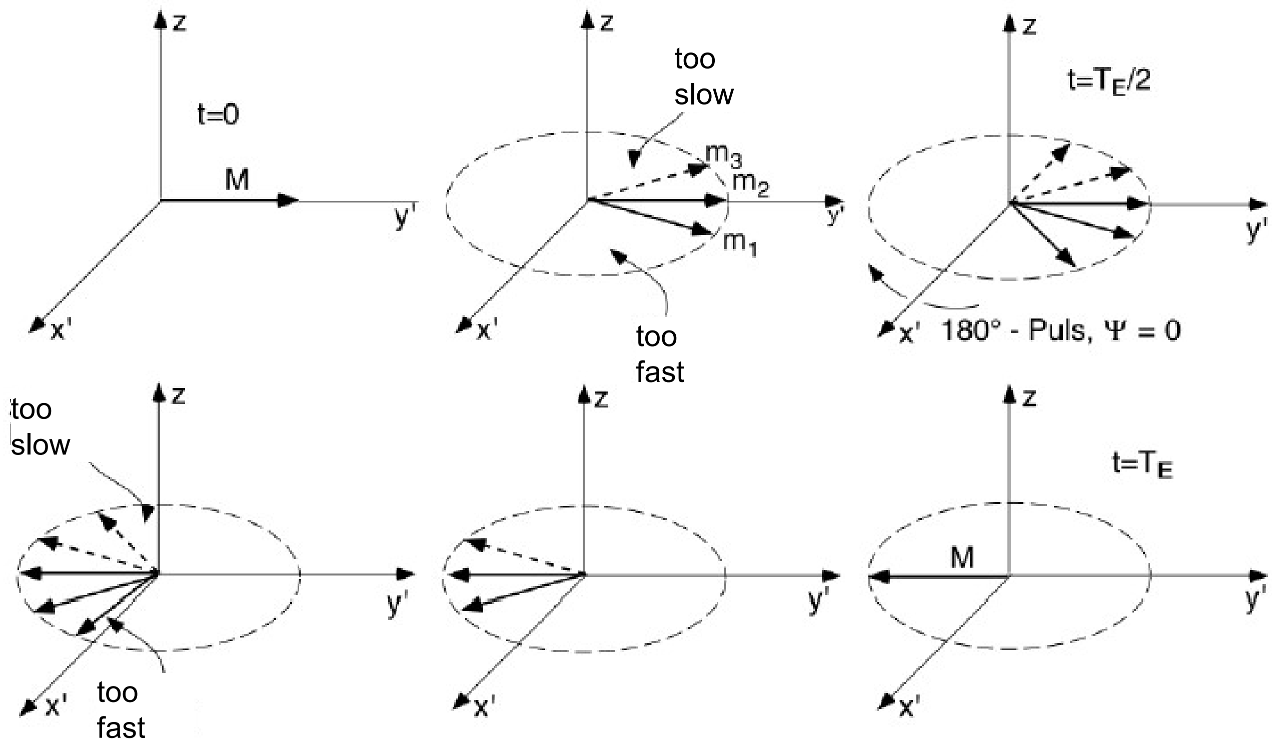

spin echoes (4)

rephasing of spin ensembles with 180° HF-pulse (phase ψ = 90°)

(1) 90°HF-pulse: turn down magnetization into +y'-direction

(2) dephasing:
clockwise:
some spin ensembles lead
some spin ensembles are behind

(3) after $T_E/2$ 180° HF-pulse (Ψ=90°):
rotate spins by 180° around y'-axis

(4) too slow spins still too slow,
faster spins still too fast
(clockwise !) $\Rightarrow$ rephasing!

(5) after T_E: all magnetic moments again in-phase
$\Rightarrow$ measureable transversal magnetization (in +y'-direction) $\Rightarrow$ **spin echo**

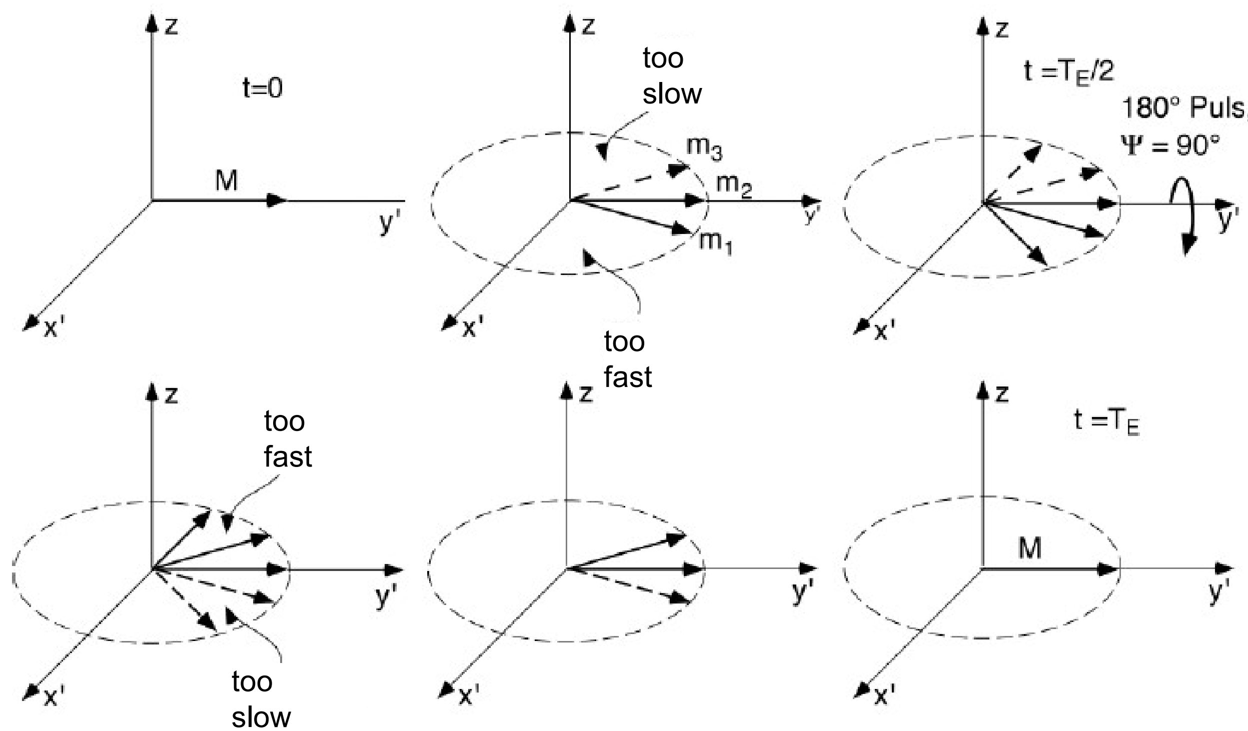

spin echoes (5)

rephasing spin ensembles with Inversion-Recovery pulse sequence

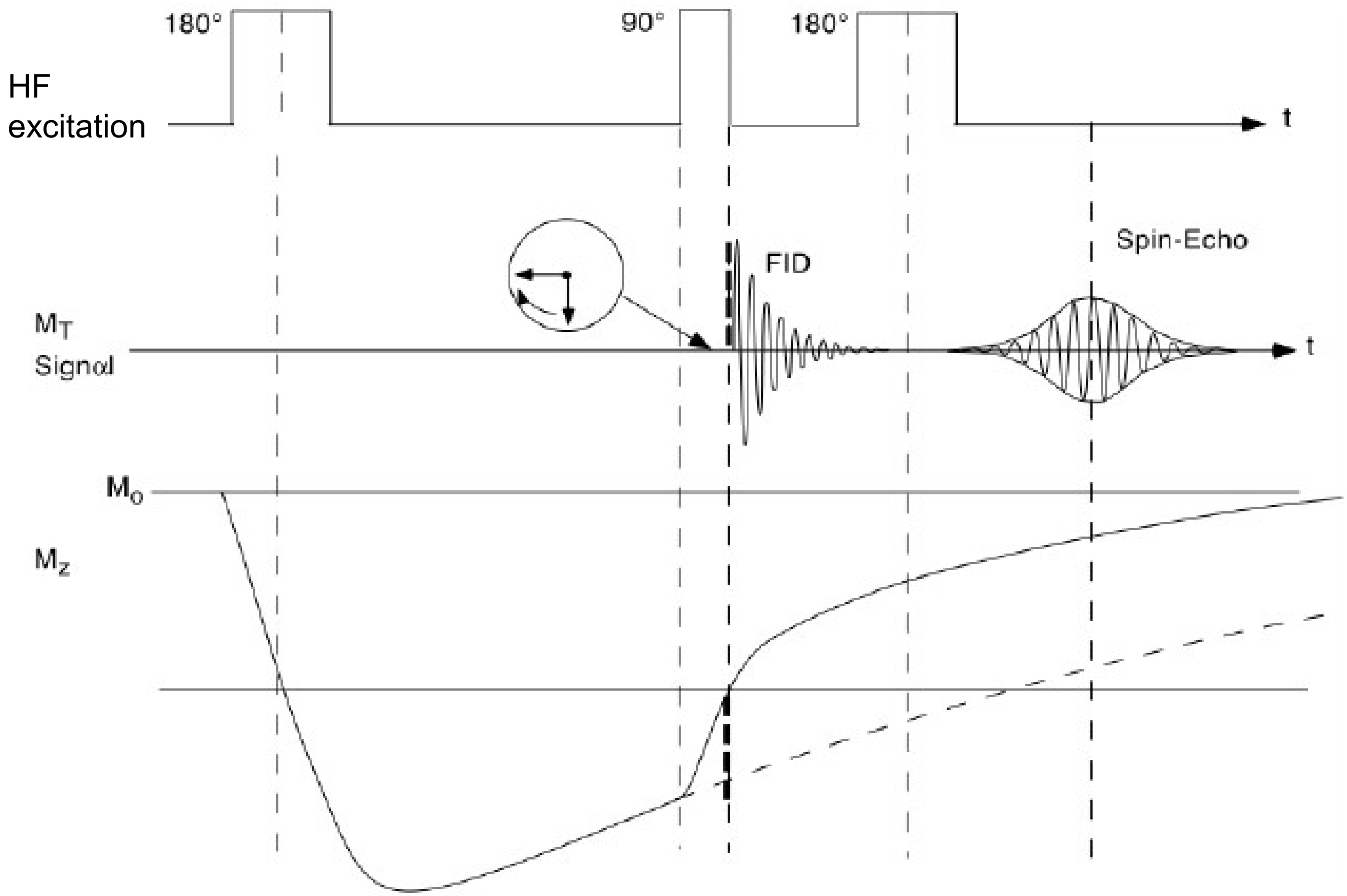

spin echoes (6)

multiple spin echoes

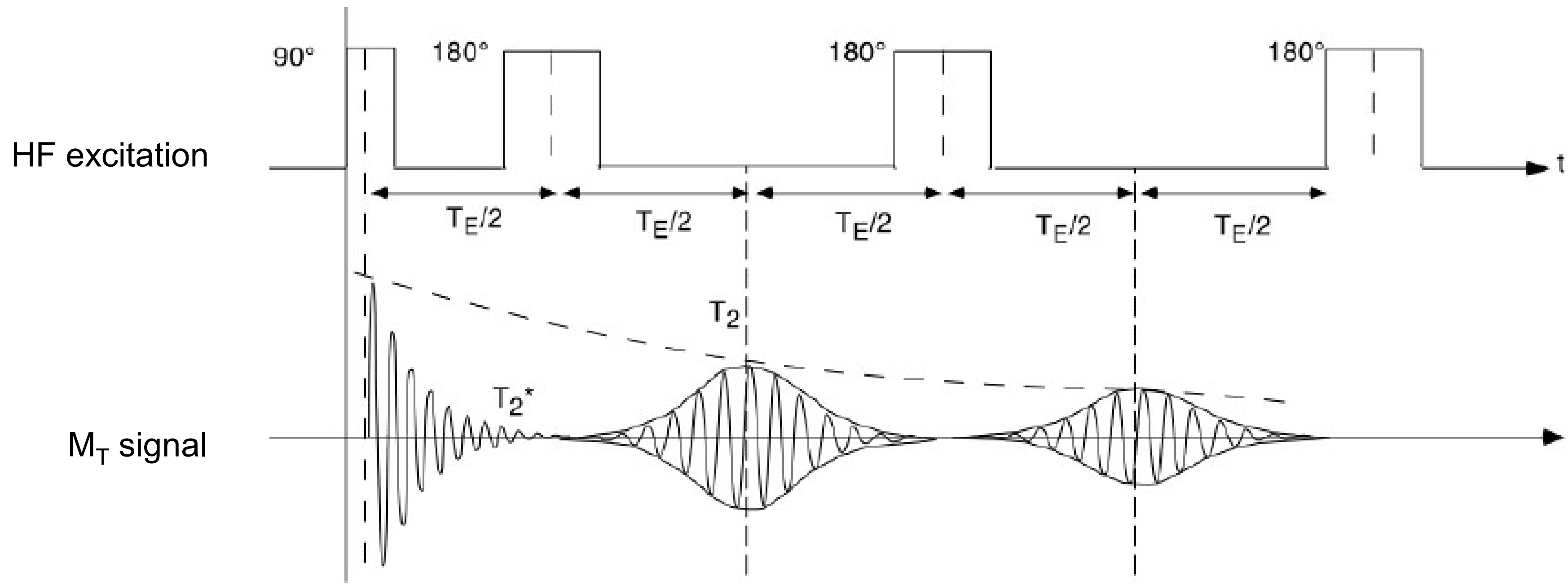

- statistical dephasing of spins within an ensemble (T_2 time)
- amplitude of spin echoes ~ $\exp(-t/T_2)$
- if $T_E > T_2$ ⇒ small spin echo amplitude
- if $T_2 >> T_2^*$ ⇒ multiple spin echoes using 180° HF pulses

spin echoes (7)

FID signal amplitude decays with T_2^*

spin echo signal decays with T_2^* (recovered FID)

maximum amplitude of spin echo signal decays with T_2

in general, we have: $T_2^* < T_2 < T_1$

T_2^* generally harder to measure

$\Rightarrow$ echoes preferred for imaging !

Hahn echoes

rephasing of spin ensembles using two 90° HF pulses

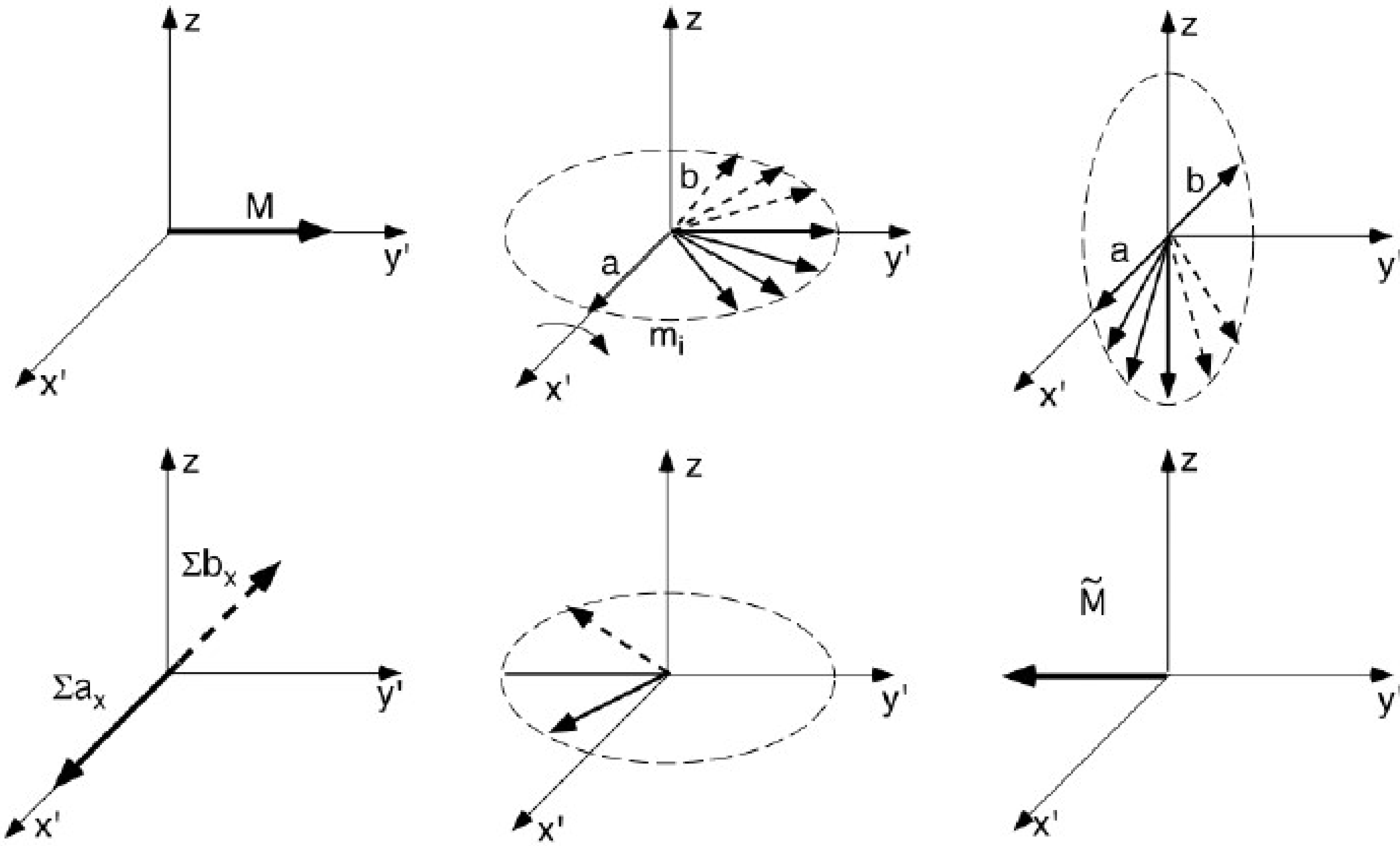

gradient echoes

given:
$B_z = B_{00} + G_z z$ and
$B = (0,0,B_z)$ field gradient in z-direction

precession frequency of spin ensembles differs for different z

for $G_z > 0$:
spins lead if above $z = 0$
spins are behind if below $z = 0$

rephasing using 180° HF pulse or using **polarity reversal of gradient field**

for $G_z < 0$:
spins are behind if above $z = 0$
spins lead if below $z = 0$

after T_E all magnetic moments in-phase
⇒ measurable transversal magnetization
⇒ **spin echo**

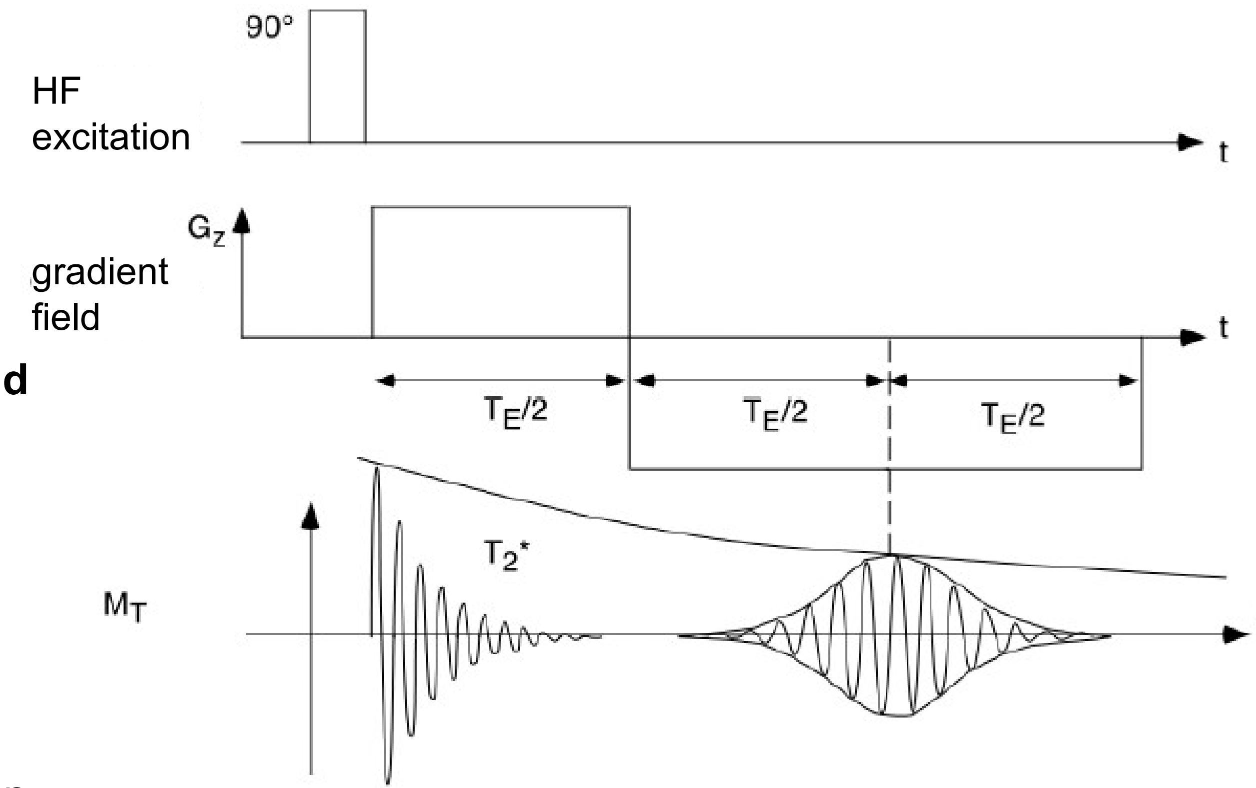

basics of tomography

given: human body in strong B_0 field
- sequence of HF pulses induces rotating transversal magnetization M_T
- M_T differs for different tissues $\Rightarrow$ location-dependent observable: $M_\mathrm{T}(x,y,z)$
- small volume elements (voxel) have their own M_T
- but: all voxel contribute to signal in antenna

purpose of MRI:

generate sectional image of transversal magnetization $M_\mathrm{T}(x,y)$
by
encoding signals from each voxel
using appropriate pulse sequences

basics of tomography

pulse sequences

sequence	slices	matrix	acquisition time
Spinecho	Multi	256	3-12 min
Turbo SE	Multi	256	1-4 min
HASTE	Single Shot	128-256	0,7-1,2 sec
Gradientenecho	Multi / 3D	256	7 sec - 10 min
Turbo FLASH	sequentiell	64-128	300 ms - 2 sec
EPI	Single Shot	64-128	50-200 ms
Turbo GSE	Multi / Single Shot	256	360 ms - 4 min

basics of tomography

basic schemes of MRI pulse sequences:

***spatial encoding*:**

selective excitation of a slice (often using G_z-gradient fields)

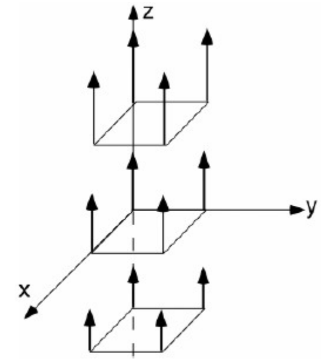

***signal encoding with a slice*:**

phase encoding (often using G_y-gradient fields)
(halfway between excitation and read-out of antenna signals)

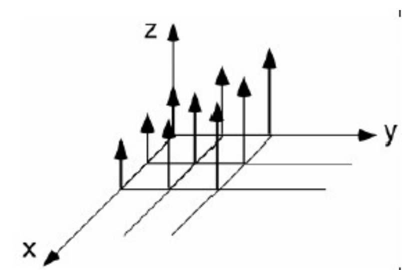

frequency encoding (often using G_x-gradient fields)
(during read-out of antenna signals)

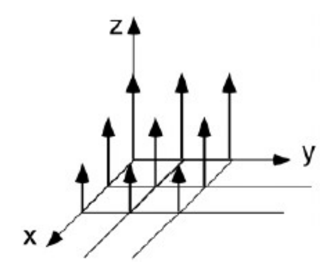

characteristic strength of gradient fields: ~ 40 mT/m

basics of tomography

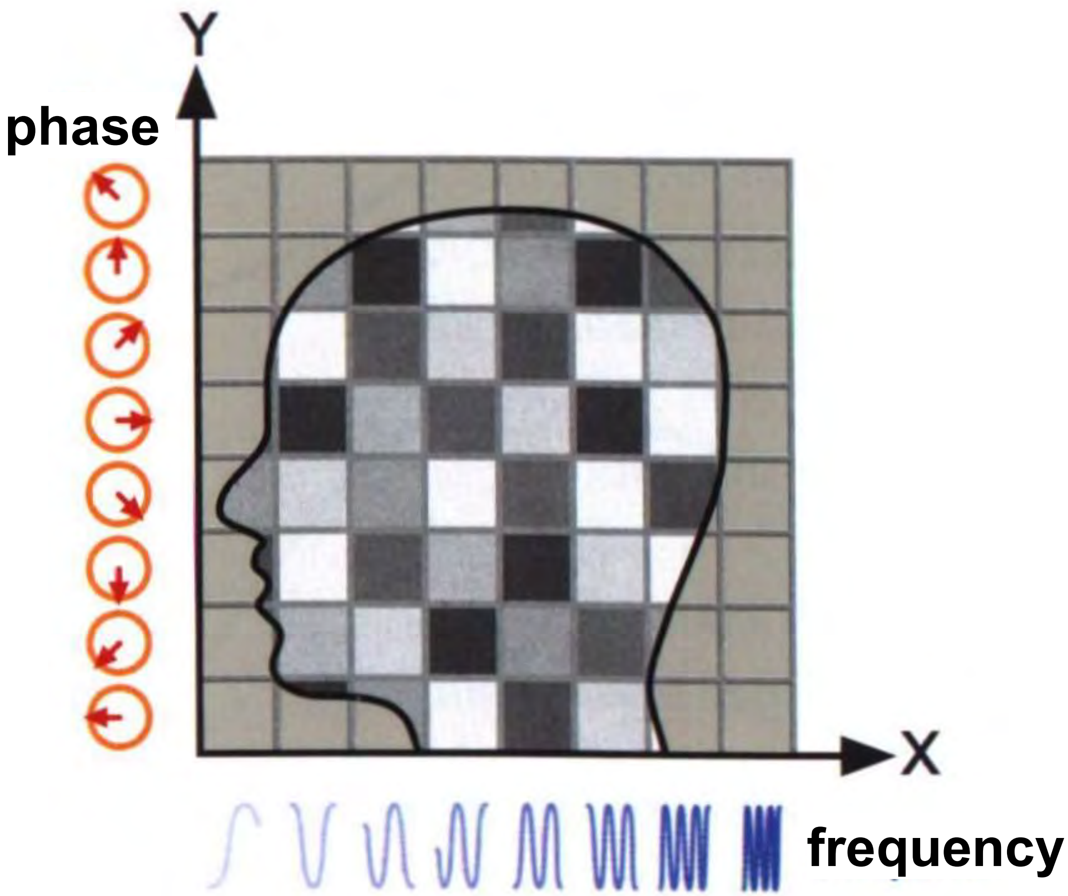

G_z:
slice selection (z-direction)

G_y:
phase encoding (y-direction)

G_x:
frequency encoding (x-direction)

signal per voxel:
frequency- and phase-modulated
FID or spin echo (depending on T1, T2)

basics of tomography

spatial encoding via selective excitation (1)

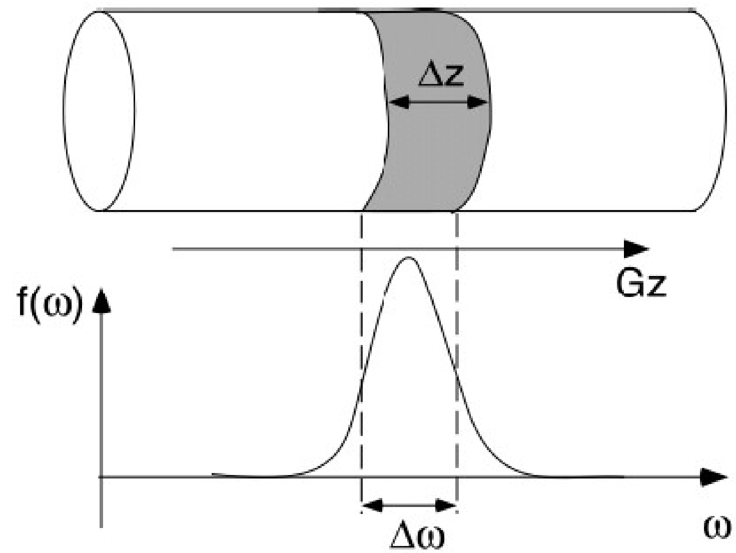

- HF-pulse turns spins into x-y-plane ⇒ measurable M_T
- G_z-field || B_0-field ⇒ ω_0 differs in each z-slice

$$\omega_0 = +\gamma(B_{00} + G_z z)$$

- excitation = resonance phenomenon
  ⇒ turning of spins with proper ω_0
- resonance line has finite width (Lorentzian)
  ⇒ no exact frequency matching of HF wave required

- exciting HF wave has finite spectral width $\Delta\omega$ (short pulse)

⇒ HF excitation with gradient field turns spins in a slice of thickness:

$$\Delta z = \frac{\Delta\omega}{\gamma G_z} = \frac{2\pi\Delta f}{\gamma G_z}$$

slice thickness Δz :
change bandwidth Δf of HF pulse
($\Delta z \rightarrow 0$? caveat: Boltzmann statistics!)

positioning of slice:
change strength of gradient field G_z

basics of tomography

spatial encoding via selective excitation (2)

different gradient field strengths map the same pulse onto slices with different slice thickness

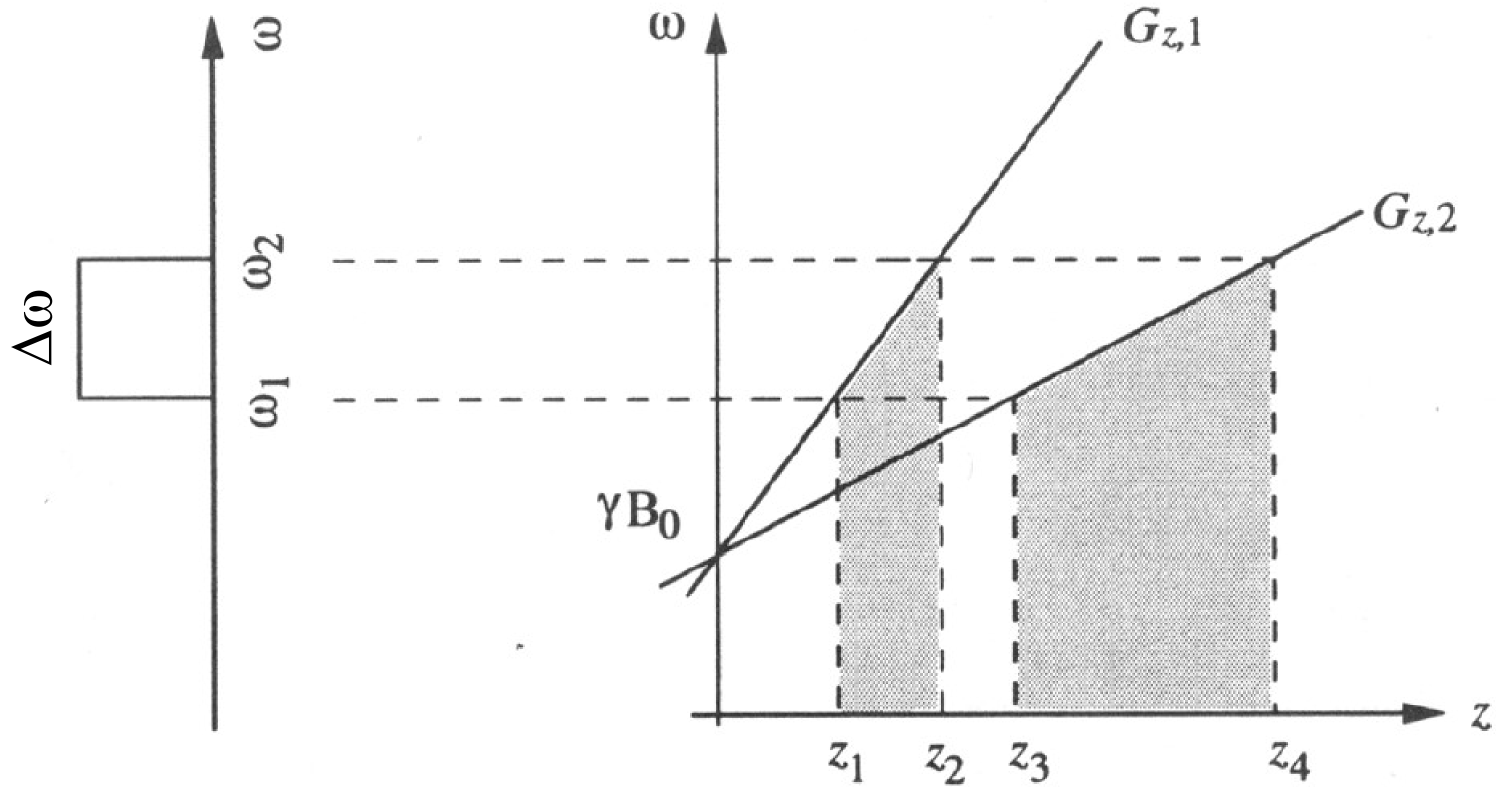

basics of tomography

spatial encoding via selective excitation (3)

a sharp boundary between excited slice and neighboring non-excited areas can be achieved using a $\sin(x)/x$ amplitude function $B(t)$ of the HF pulse:

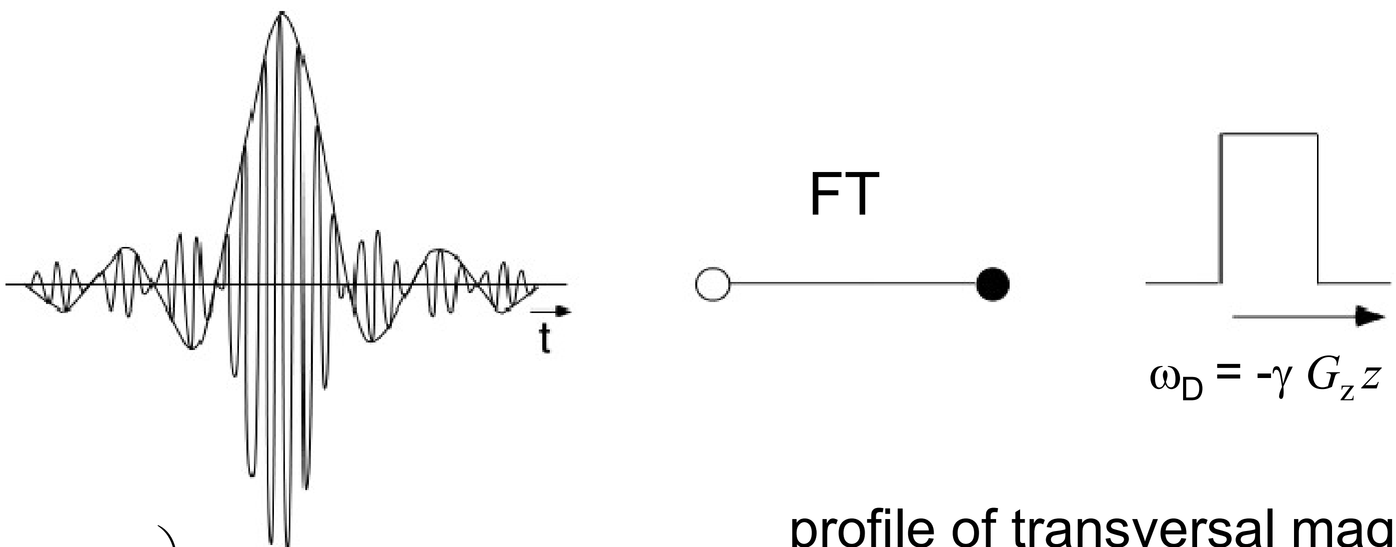

$$B(t) = A\frac{\sin\left(\frac{1}{2}\gamma G_z \Delta z t\right)}{\frac{1}{2}\gamma G_z \Delta z t}$$

profile of transversal magnetization with ω_D = difference of angular velocity wrt Larmor frequency at z=0

basics of tomography

spatial encoding via selective excitation (4)

use of unipolar pulse leads to inhomogeneous transversal magnetization

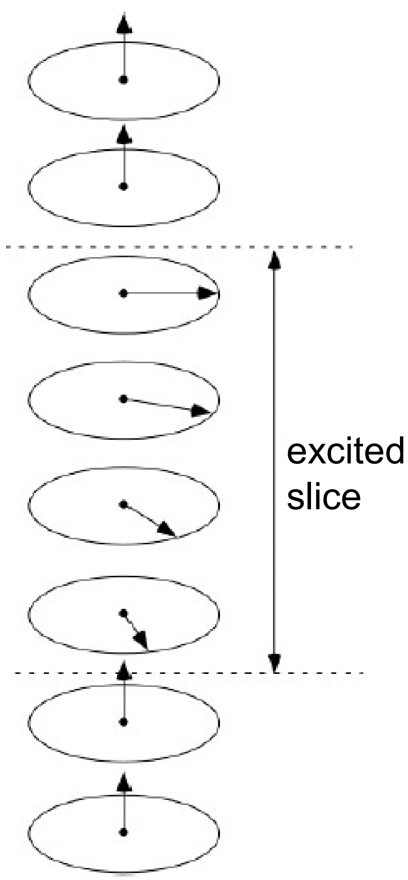

z-gradient and HF pulse lead to homogeneous transversal magnetization

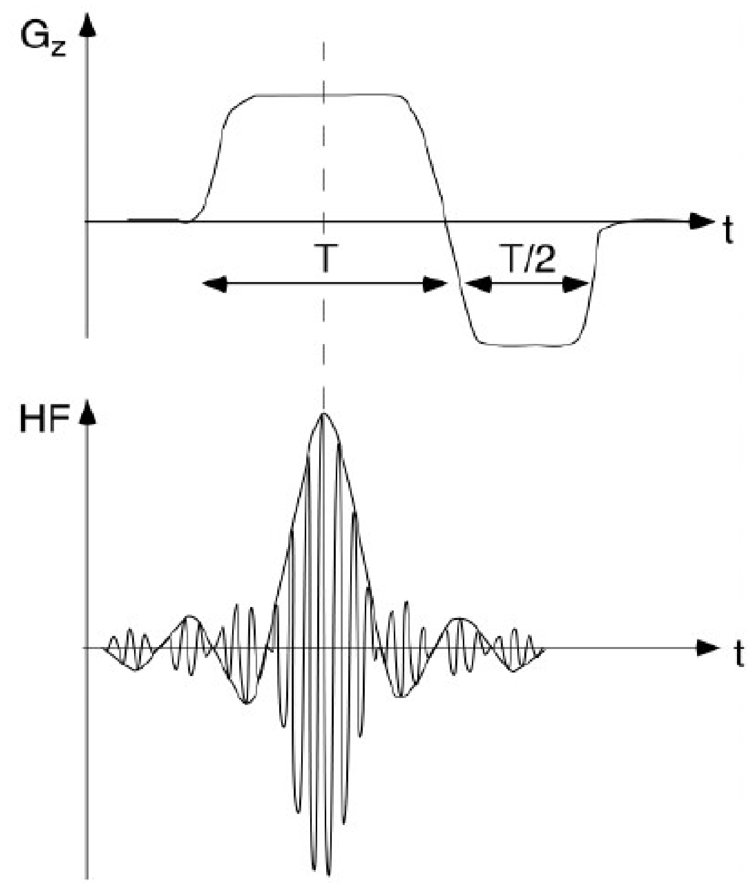

basics of tomography

spatial encoding via selective excitation (5)

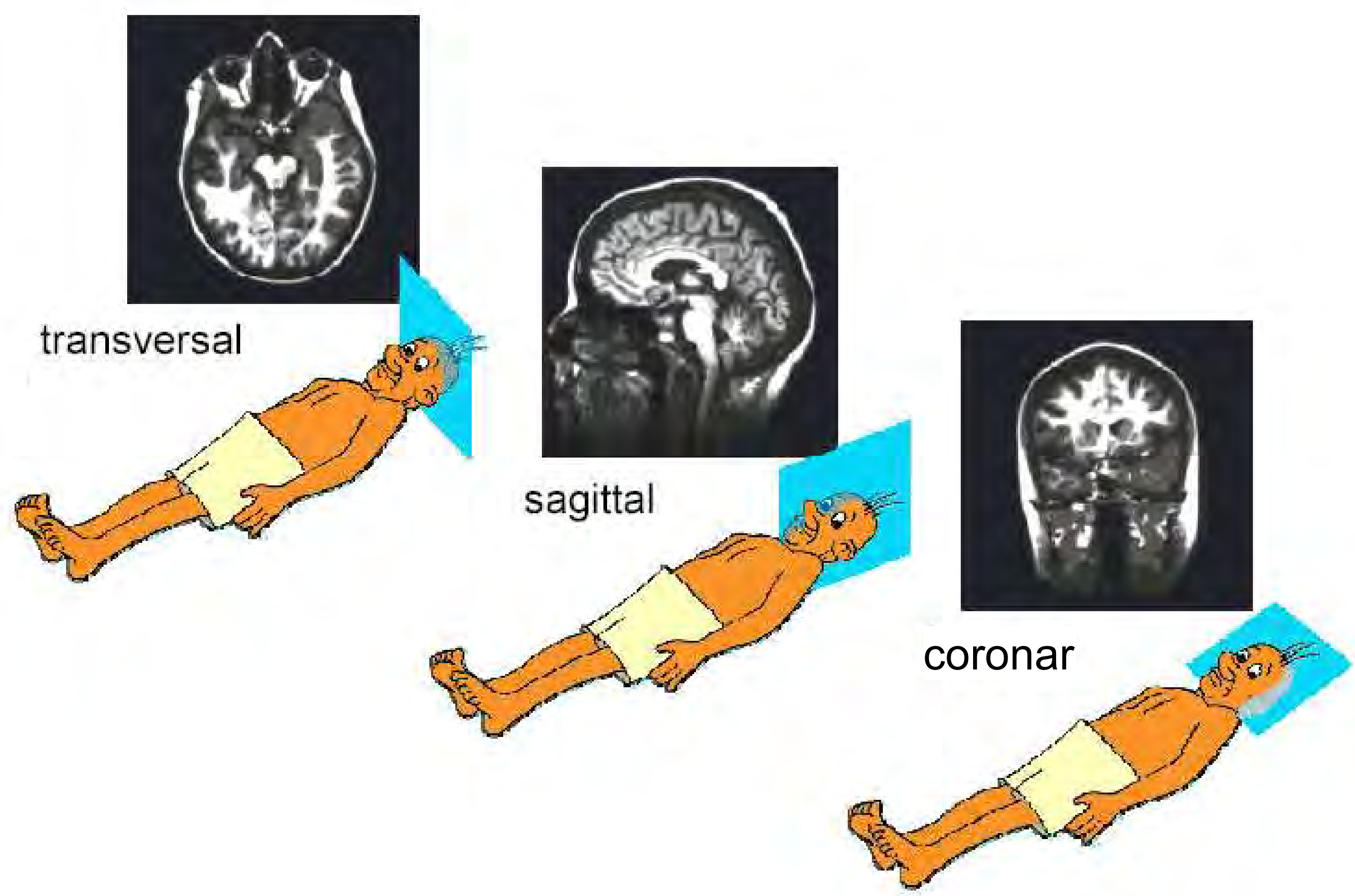

basics of tomography

phase coding (1)

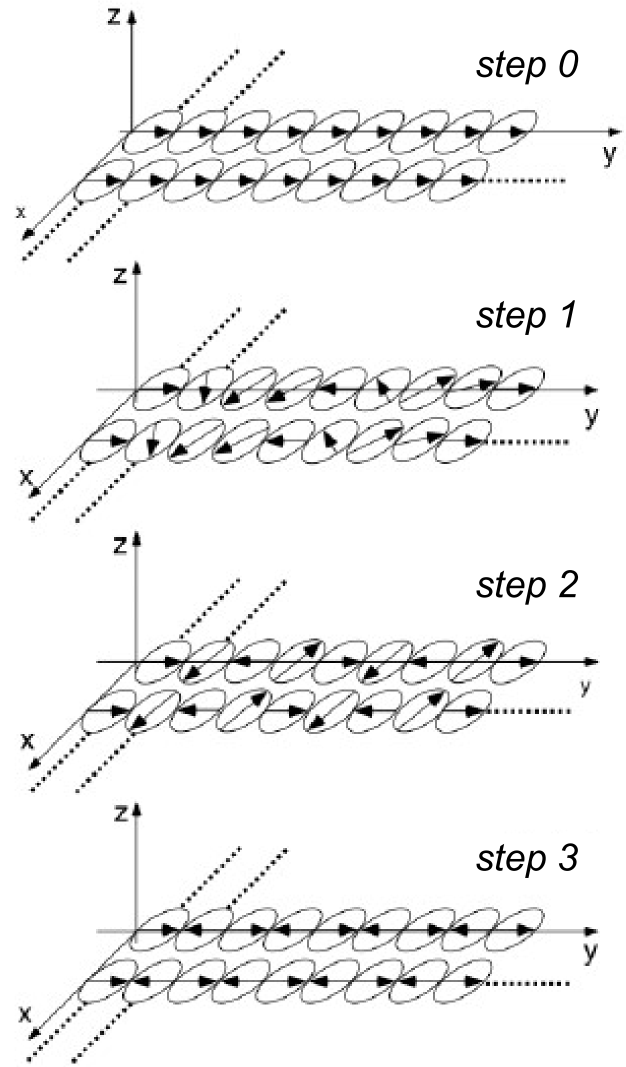

- HF-pulse turns spins into x-y-plane
  assumption: there are no relaxation phenomena

- apply G_y field halfway between excitation and read-out

- *step 0:* G_y-field on for time $T_y \Rightarrow$ precession velocity is function of y;
  choose G_y such that magnetization is antiparallel a left and right boundary of image;
  turn-off gradient $\Rightarrow$ precession velocity unaltered
  ("freeze" spin orientation)

- *steps 1 – 3*: *n*-fold repetition (stepwise increase of G_y) until magnetization in neighboring voxel antiparallel
  (image-size 256 *x* 256 $\Rightarrow$ *n*=256 !)

$\Rightarrow$ coding of spatial information (y-direction) via phase !

- number of phase coding steps defines recording duration !

basics of tomography

phase coding (2)

- angular velocity of phase

$$\omega_p = -\gamma(B_{00} + G_y\, y) + \gamma B_{00} = -\gamma G_y\, y$$

- phase angle after T_y:

$$\varphi_p = -\gamma \underline{G_y}\, y \underline{T_y} \longrightarrow$$

strong gradients + short times
or
small gradients + long times

- magnetization in *y*-direction at time T_y:

$$M'_T(y) = M'_{T_0}(y)e^{-i\gamma G_y y T_y}$$

caveat: $M'_T(y)$ complex-valued !

- maximally required gradient (for antiparallel orientation):

$$\varphi_{p,\max} = \pi = -\gamma G_{y,\max} \Delta y T_y$$

Δy = distance between pixel

$$\frac{1}{\Delta y} = 2\gamma^* G_{y,\max} T_y = \frac{\#\,\text{pixel in y-direction}}{\text{image size in y-direction}}$$

γ^* in [MHz/T]

basics of tomography

frequency coding

- HF-pulse turns spins into x-y-plane
  assumption: there are no relaxation phenomena

- apply G_x-field during read-out:
  faster precession of spins in +x-direction
  slower precession of spins in -x-direction

- each voxel emits signal with different frequency
  during measurement

  $\Rightarrow$ coding of spatial information (x-direction)
  via frequency !

- magnetization in x-direction: $M'_T(x) = M'_{T_0}(y)e^{-i\gamma G_x x t}$

- antenna records mixture of frequencies
  $\rightarrow$ decoding via Fourier-transform

- bandwidth of antenna = $\gamma\ G_x$ times size of image in x-direction

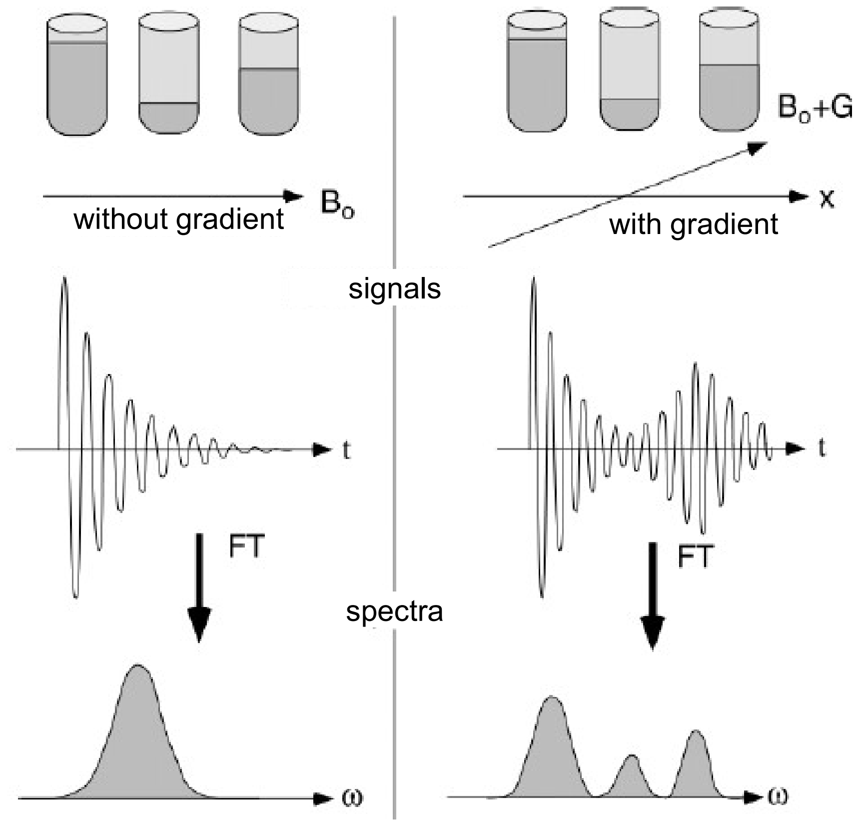

caveat: $M'_T(x)$ complex-valued !

basics of tomography

signal in antenna

- slice selection with z-gradient (signal = transversal magnetization)

- x-y-coding with x-gradient (frequency) and y-gradient (phase)

- total signal in antenna:

$$S_t(t,T_y) = \iint M'_{T_0}(x,y)\, e^{-i\gamma G_x x t - i\gamma G_y y T_y}\, dx dy$$

- with $k_x = \gamma\, G_x\, t$ und $k_y = \gamma\, G_y\, T_y$ ("normalized" time; unit m^{-1}), we have:

$$S(k_x,k_y) = \iint M'_{T_0}(x,y)\, e^{-i(k_x x - k_y y)}\, dx dy$$

caveat:
since $M'_T(x,y)$ complex-valued
$\Rightarrow$
$S(k_x,k_y)$ complex-valued !

$\Rightarrow$

$$M'_{T_0}(x,y) \;\overset{\text{2D-FT}}{\circ\!\!-\!\!-\!\!-\!\!\circ}\; S(k_x,k_y)$$

signal in antenna (quadrature detector) is Fourier-transform of images

basics of tomography

k-space (1)

- $k_x = \gamma\, G_x\, t$ and $k_y = \gamma\, G_y\, \mathrm{T}_y$ (normalized time; unit m^{-1})

- from time-domain to position-frequency-domain

- *k*-space identical to u-v-plane for Fourier-transform of image in x-ray imaging:

$$k_x = 2\pi u,\ k_y = 2\pi v$$

- the longer the recording time the more contributes the signal to increasing spatial frequencies (resp. phases) in the image

$\rightarrow$ more detailed structures having shorter wavelengths:

$$k_\mathrm{x} = 2\pi/\lambda_\mathrm{x},\ \ k_\mathrm{y} = 2\pi/\lambda_\mathrm{y}$$

basics of tomography

k-space (2) *spatial frequencies*

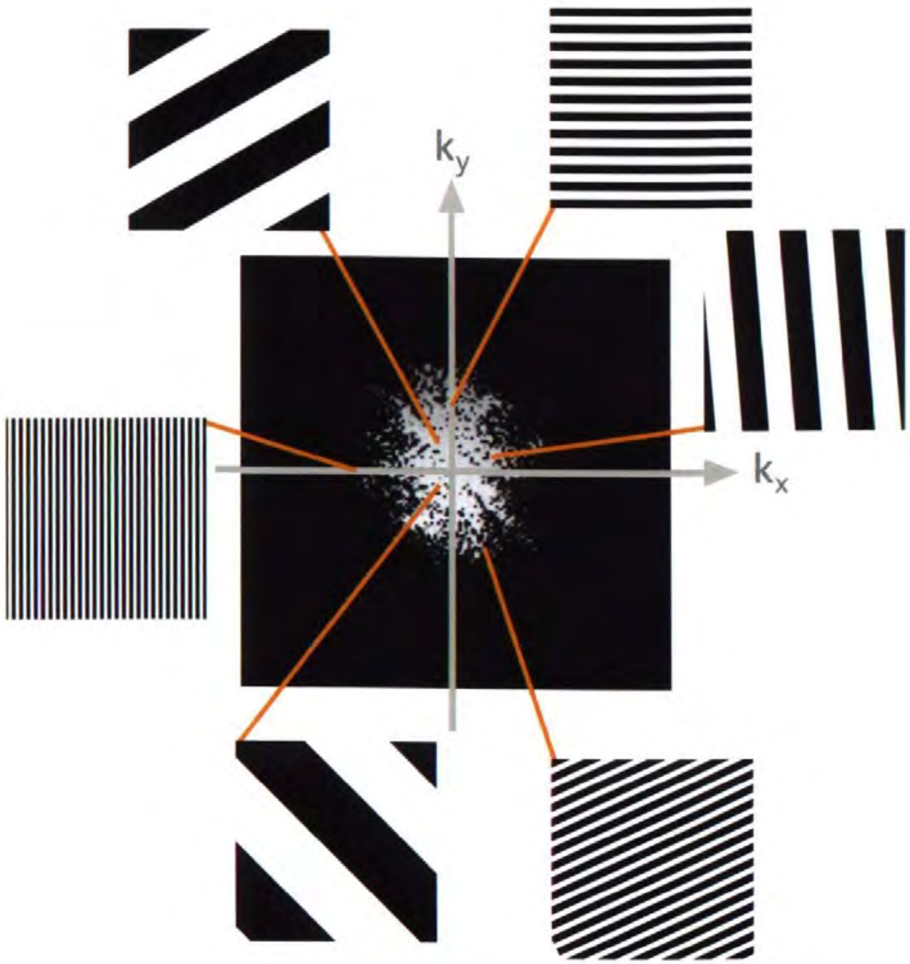

entry in *k*-space determines the contribution of some stripe pattern to the image

coarse stripe pattern:
low spatial frequencies
(near origin of coordinate system)

fine stripe pattern:
high spatial frequencies
(at higher values of k_x, k_y)

basics of tomography

k-space (3a) spatial frequencies

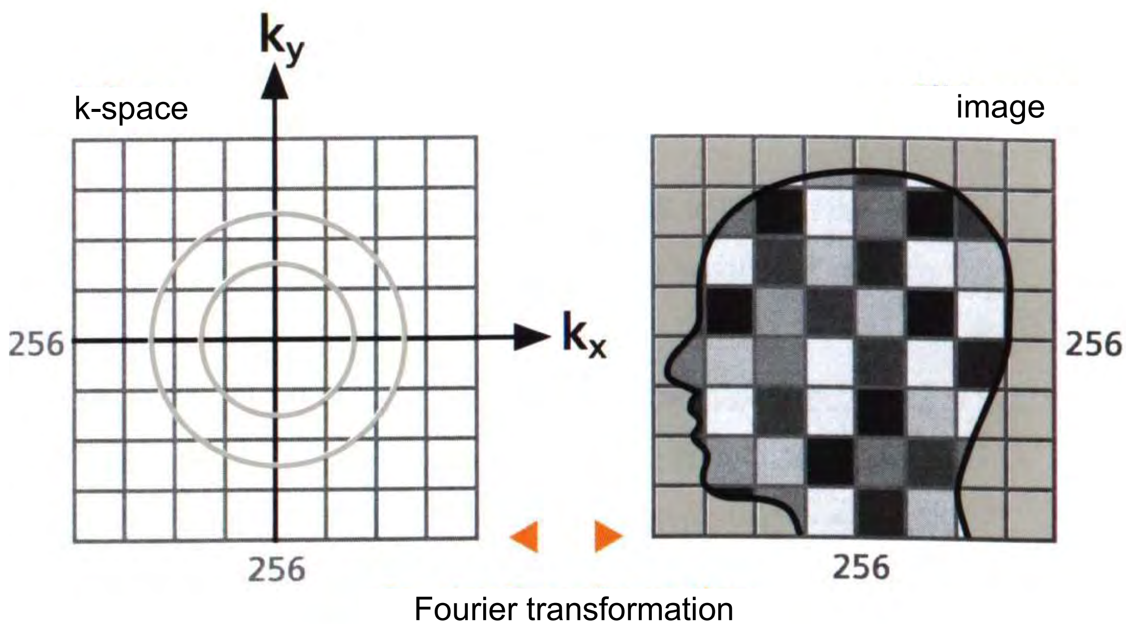

basics of tomography

k-space (3b) spatial frequencies

*an entry in k-space does **not**! correspond to a pixel in image*

*entries in k-space near the origin define coarse structures and thus **contrast***

*entries at the boundaries of k-space define fine structures (edges, contours, etc.) and thus **resolution***

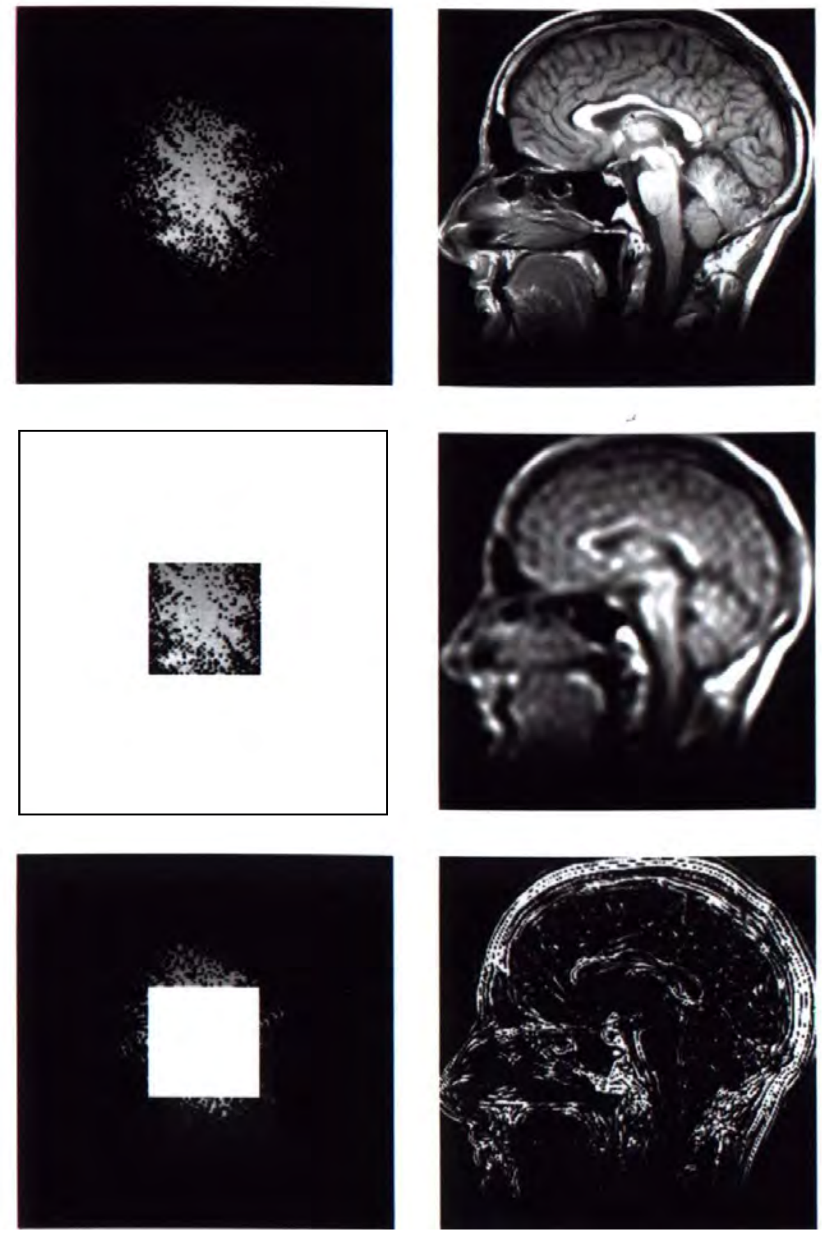

basics of tomography

Caveat: filtering of *k*-space data !

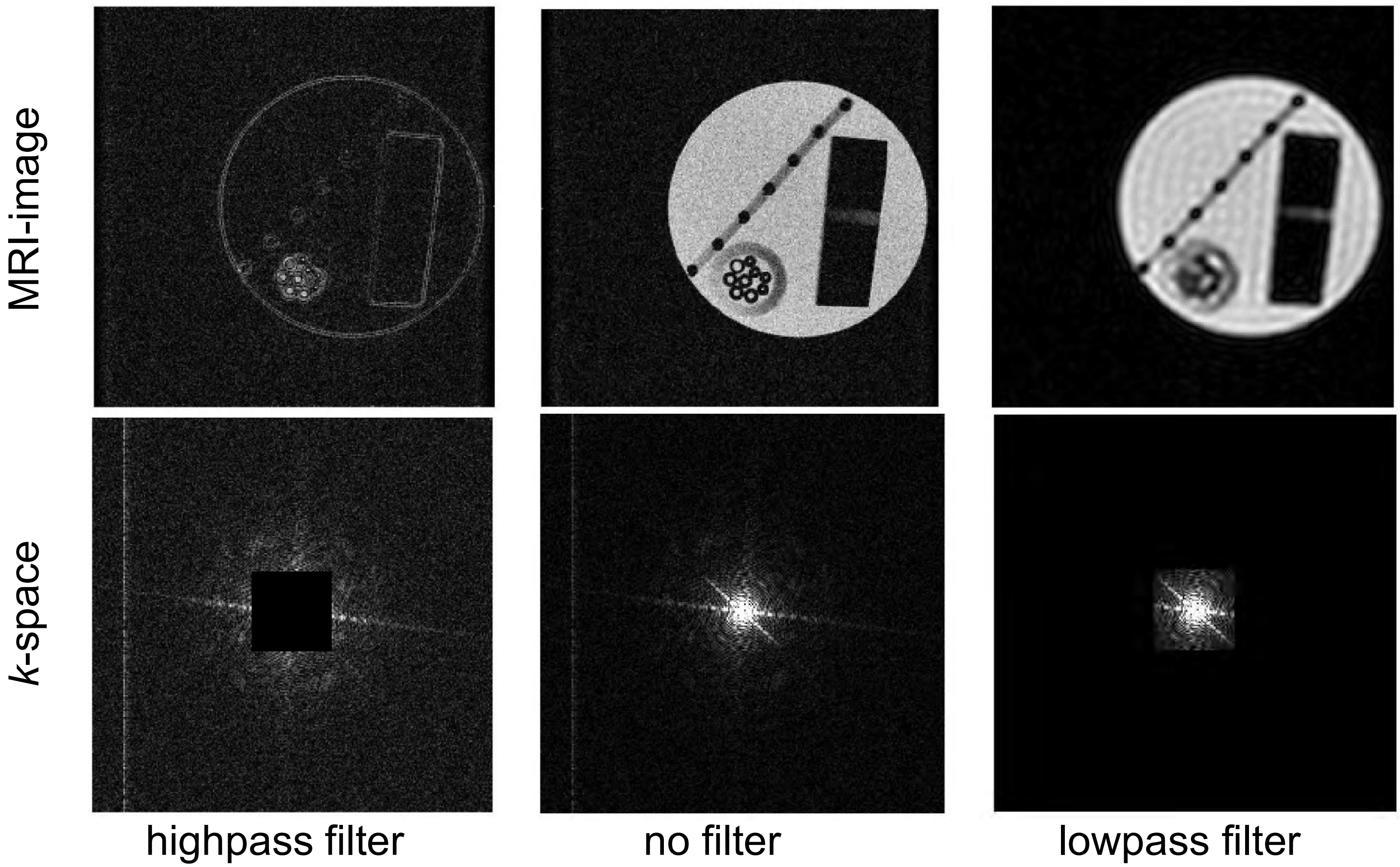

basics of tomography

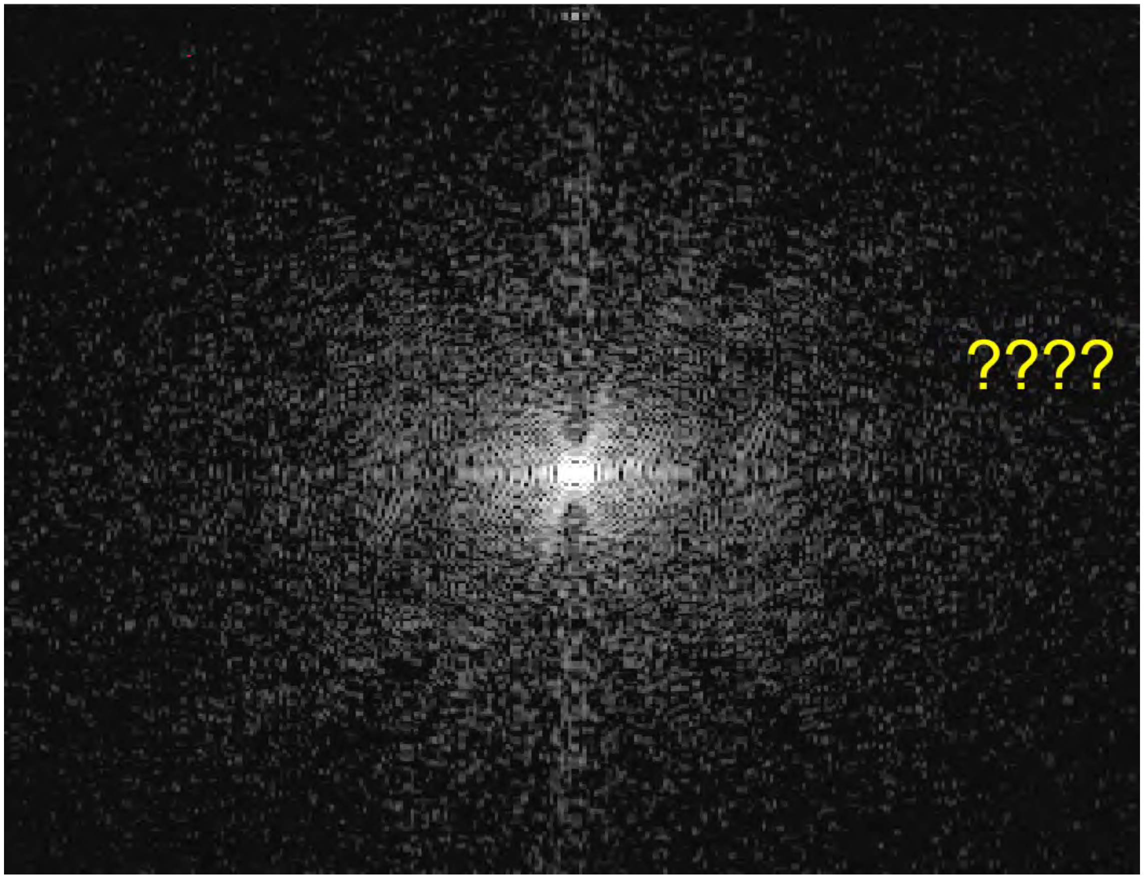

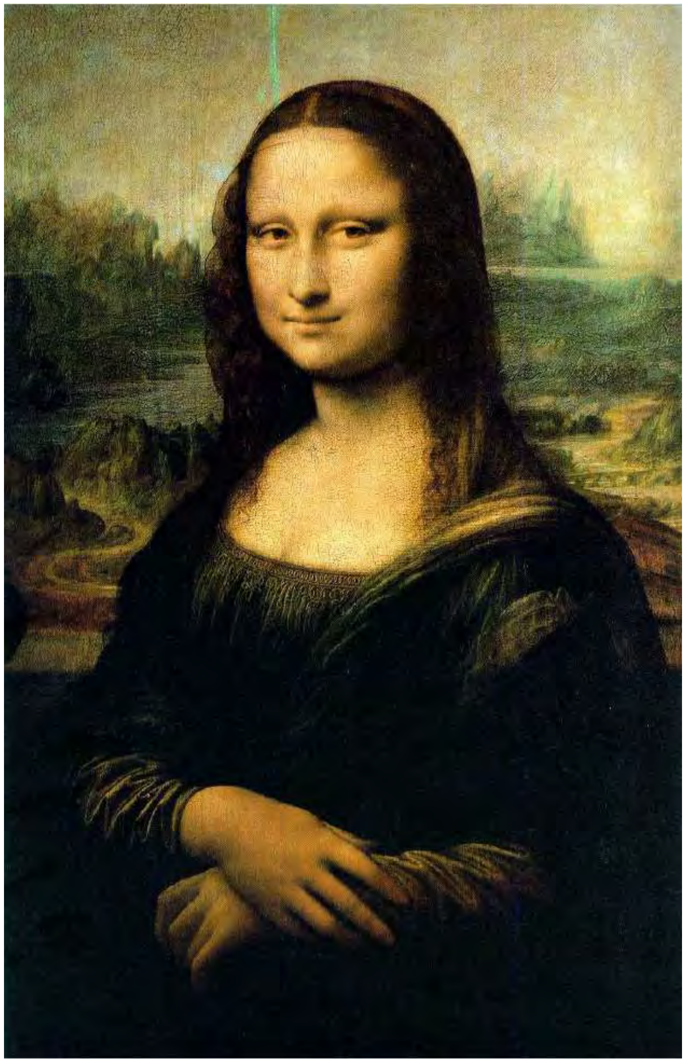

basics of tomography

k-space (4)

Cartesian sampling of *k*-space using Spin-Echo pulse sequence

Note:

previous assumption: no relaxation phenomena!

Now: use echoes !

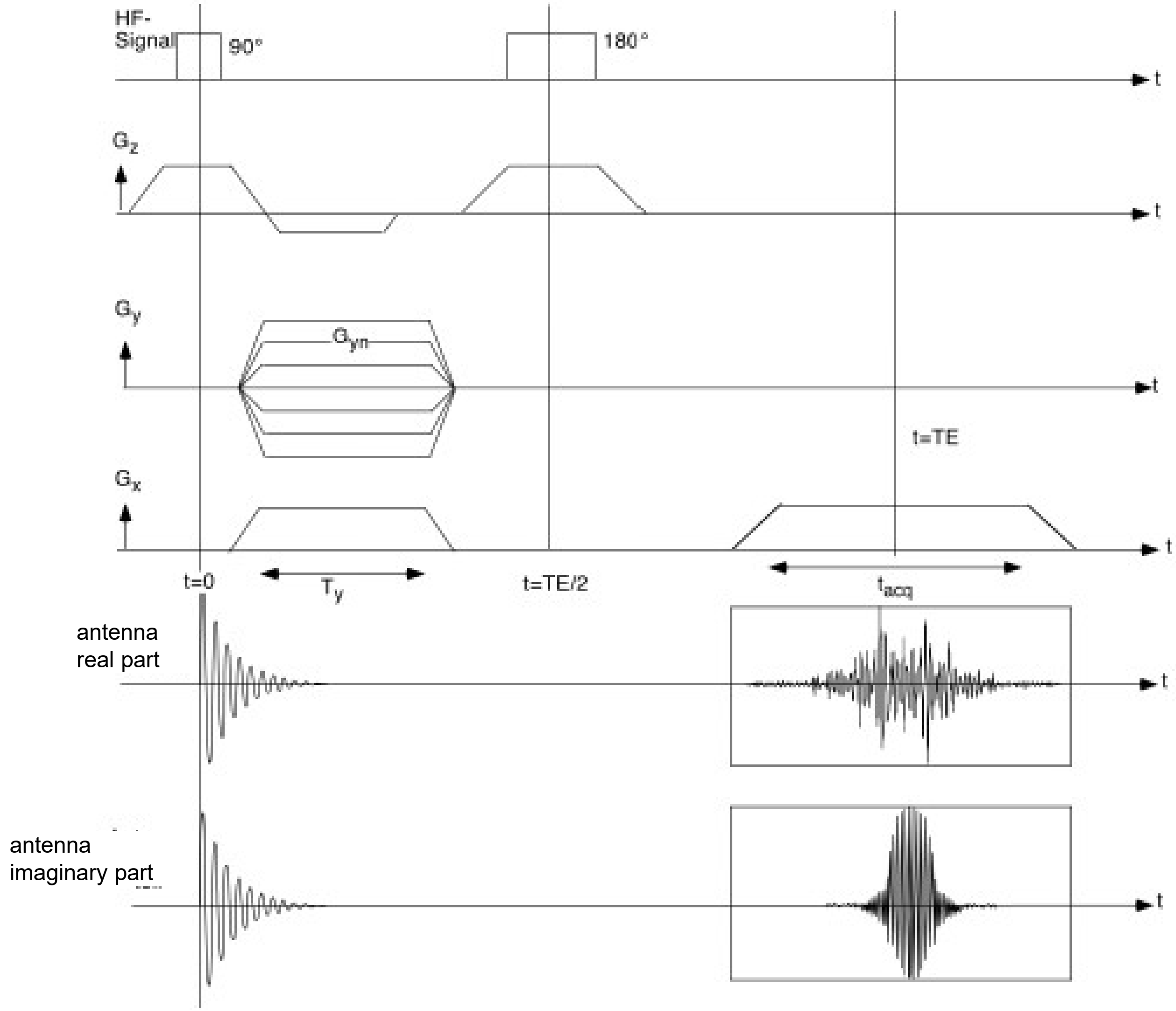

basics of tomography

k-space (5)

from signal via *k*-space to image

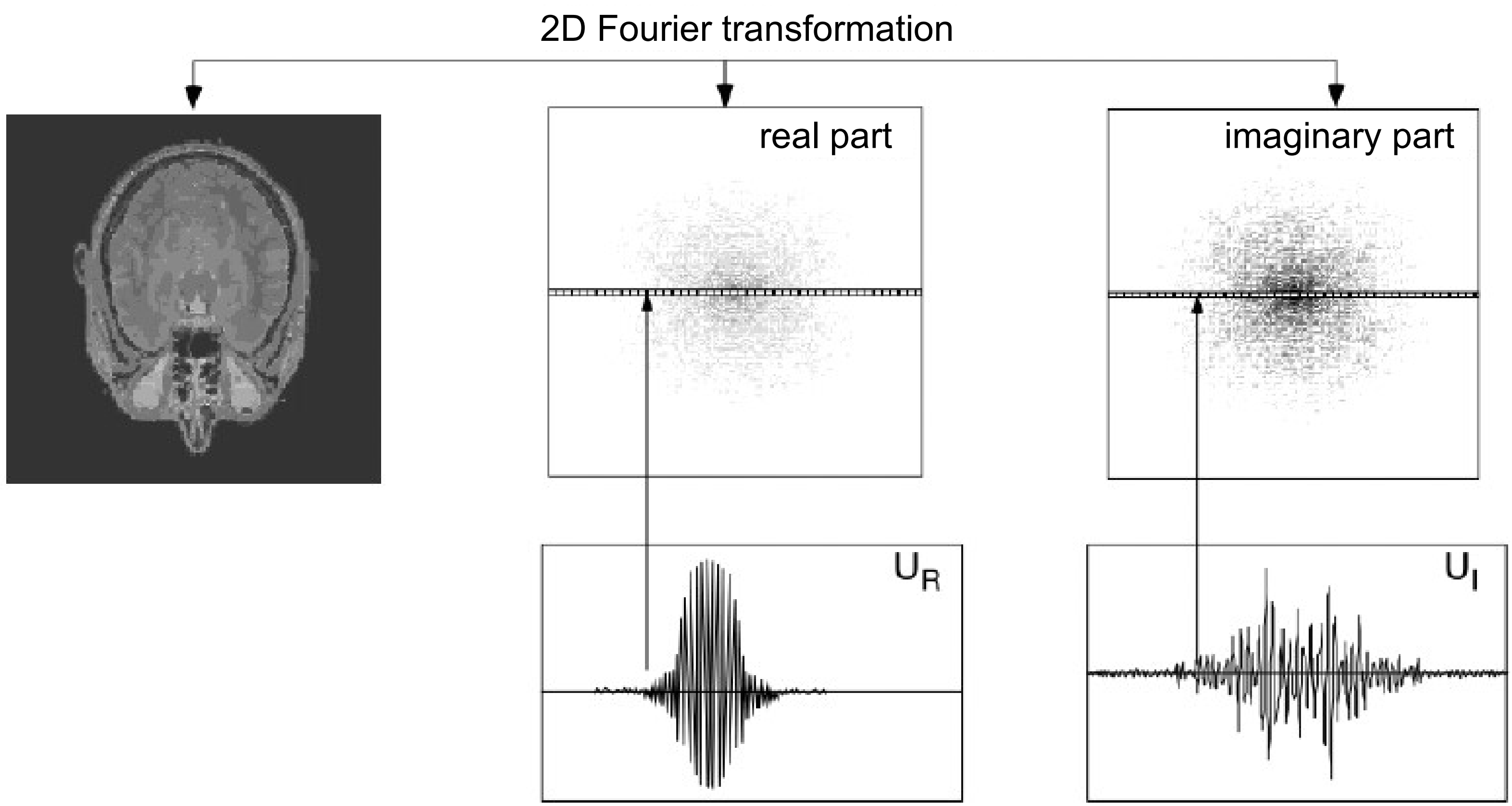

basics of tomography

k-space (6) relation to Radon transformation

assumption: no phase coding (G_y=0)
⇒ signal in antenna:

$$S_{t_0}(t) = \iint M'_{t_0}(x,y) e^{-i\gamma G_x x t} dx dy$$

⇒ in *k*-space:

$$S_0(k_x) = \int \Big(\underbrace{\int M'_{t_0}(x,y) dy}_{} \Big) e^{-ik_x x} dx$$

equivalent to projection in CT
under angle Θ=0° and *x* variable
$p_0(x)$

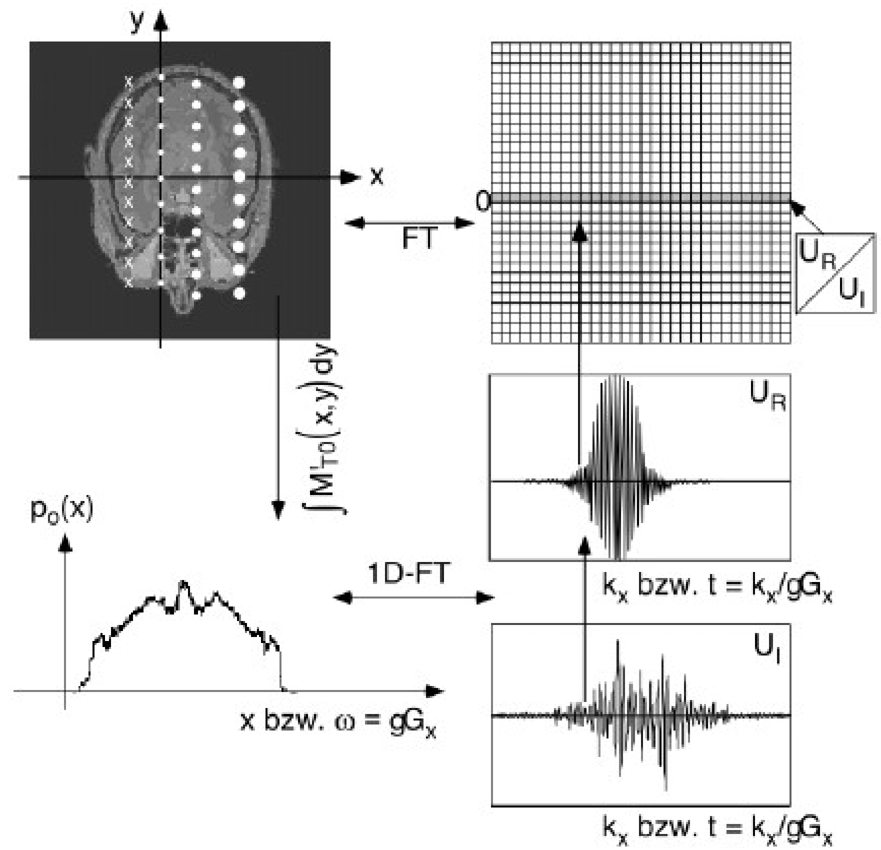

$S_0(k_x)$ is 1D-Fourier transform of projection

basics of tomography

k-space (7) relation to Fourier-slice theorem

recap: 1D-Fourier transform of projection provides data for Fourier-transformed image of a beam passing through the origin of coordinate system

CT:

- *complete dataset in k-space via recording sufficiently many projections under different angles Θ*
- *recorded projections need to be Fourier-transformed, before assigning them to the Fourier-transformed image*

MRT:

- *complete dataset in k-space via simultaneous switching of G_x- and G_y-gradients during read-out (tilted projections in k-space)*
- *continued rotation: G_x-gradient in rotated system via rotating the coordinate systems around z-axis*
- *data are the (complex-valued) Fourier-transform of projections and can thus directly be assigned to "image" in k-space*

basics of tomography

k-space (8) relation to Fourier-slice theorem

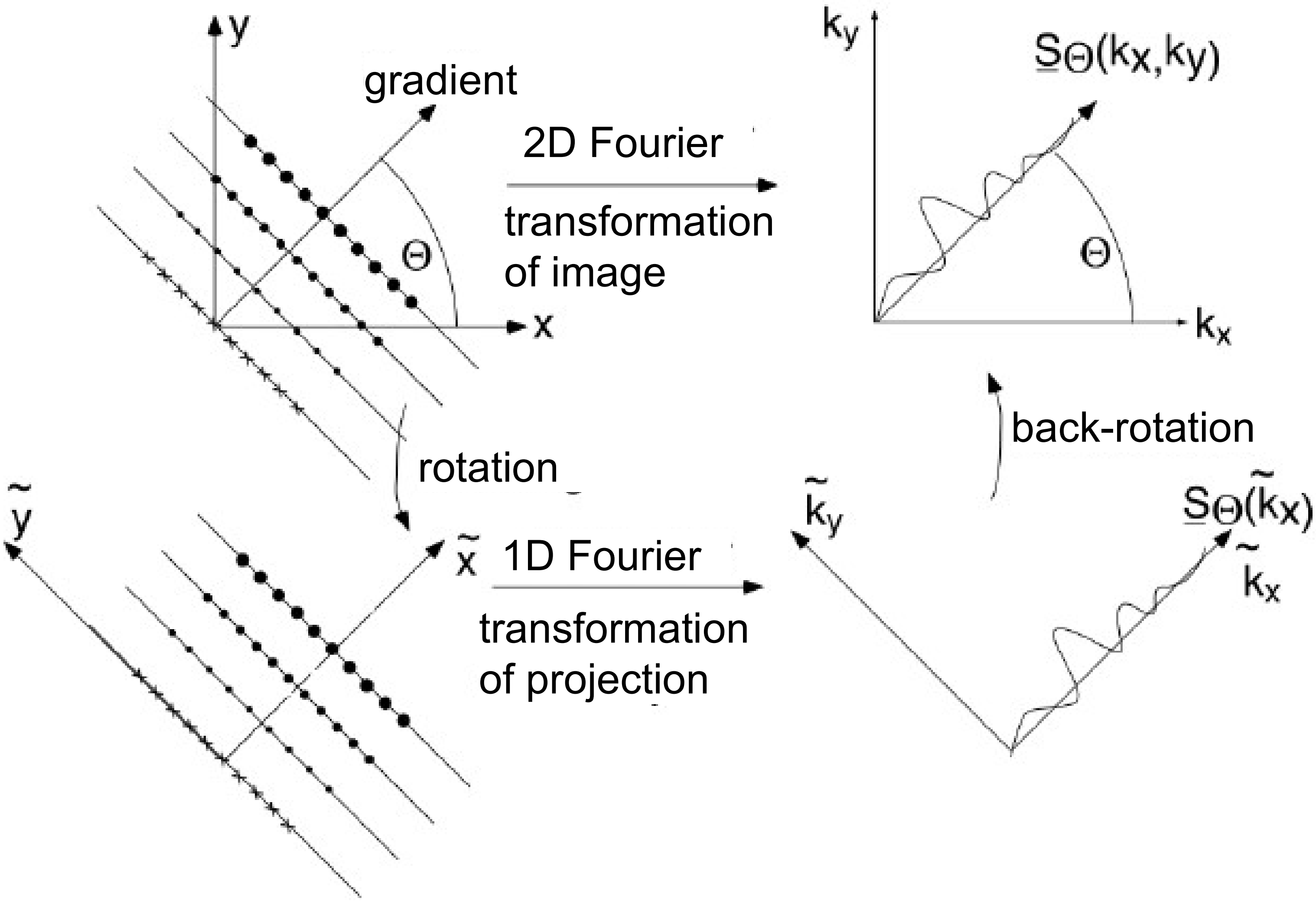

basics of tomography

k-space (9) relation to Fourier-slice theorem

- *we have:* ***the Fourier transform (FT) of a rotated image results in a Fourier-transformed image rotated by the same angle***

$\Rightarrow$

- Fourier transform of a rotated projection delivers values of a Fourier-transformed images on a rotated beam through the origin of coordinate system

- sampling of Fourier space of an image by successively rotating the field gradient

- image construction via inverse Fourier transformation

basics of tomography

k-space (10) Cartesian sampling

1) choose arbitrary initial value in k-space via phase-coding

2) k_y varies (due to G_y-gradient), however, k_x remains constant at each sampling point (magnetization vector varies with $k_y = \gamma G_y T_y$)

3) switch on G_x-gradient (frequency-coding) read-out along line parallel to k_x-axis

4) etc.

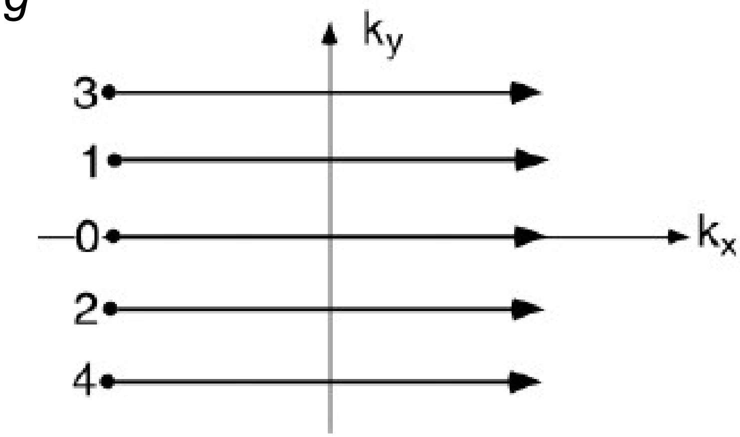

basics of tomography

k-space (11) sampling with projections

1) fixed initial value in k-space (e.g. origin), since no phase-coding

2) tilted field-gradients (G_x- and G_y-gradient): alignment of magnetization vectors towards border of k-space

3) sampling on radial beam

4) etc.

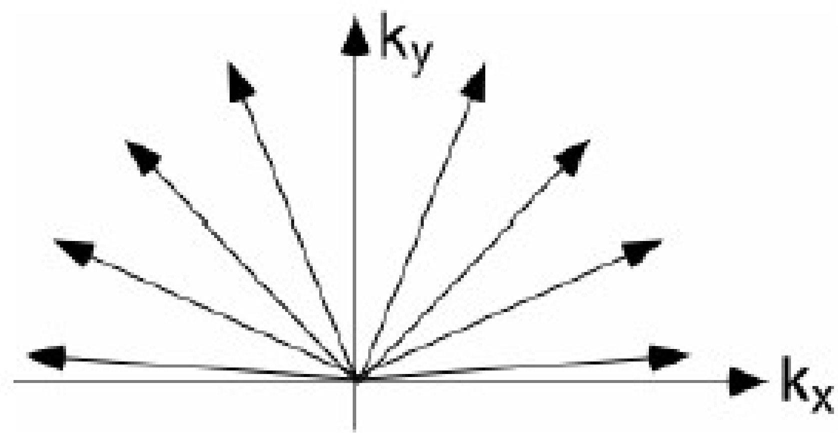

basics of tomography

k-space (12) "spiral imaging"

1) fixed initial value in k-space (e.g. origin), since no phase-coding

2) sampling along arbitrary trajectories via altering G_x- and G_y-gradients during read-out

- ramp-like
- sinusoidal-like
- etc.

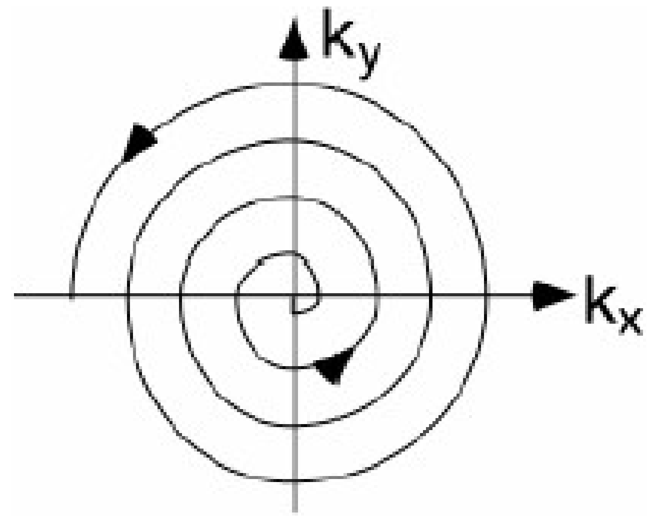

components of an MRI system

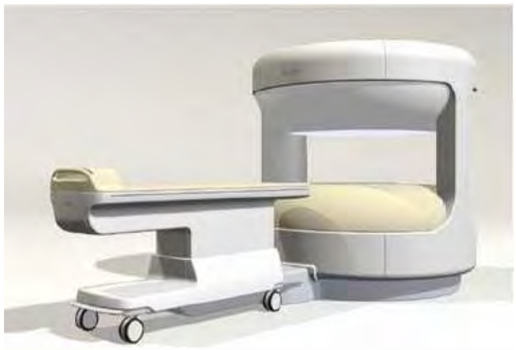

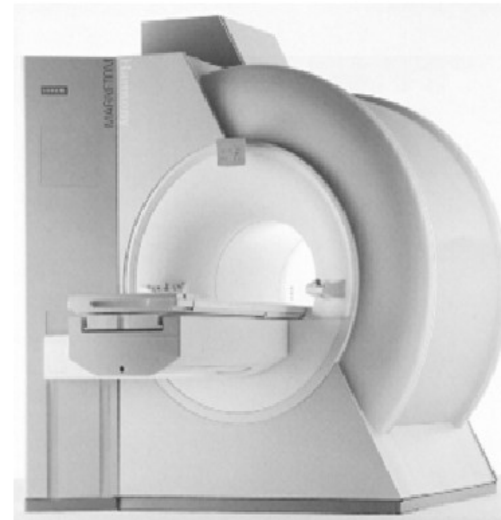

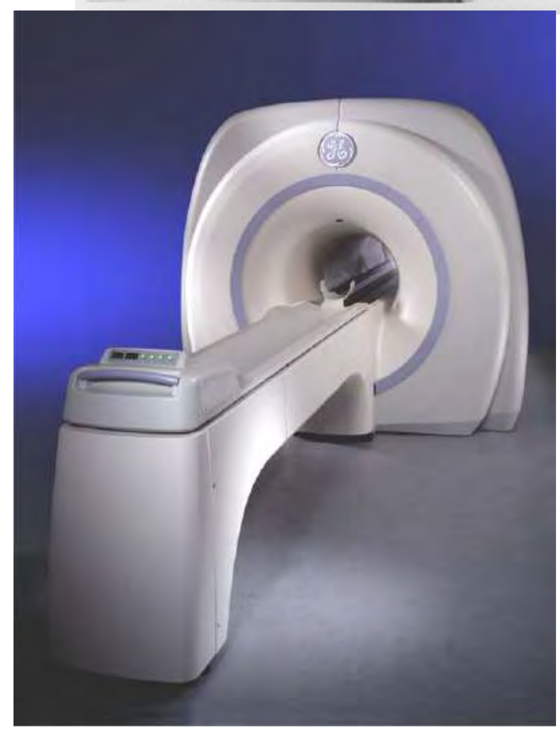

components of an MRI system

- strong magnet to generate static homogeneous magnetic field
  (0.1 – 4.0 T; for comparison: earth magnetic field 30 μT - 60 μT)
- HF generator and transmitter coil to generate oscillating magnetic field for excitation
- gradient coils to generate magnetic field gradients for spatial encoding (~ 40 mT/m)
- receiver coils for HF signals
- control computer
- console for data input/output and control of system functioning

magnetic resonance imaging (MRI) *system components*

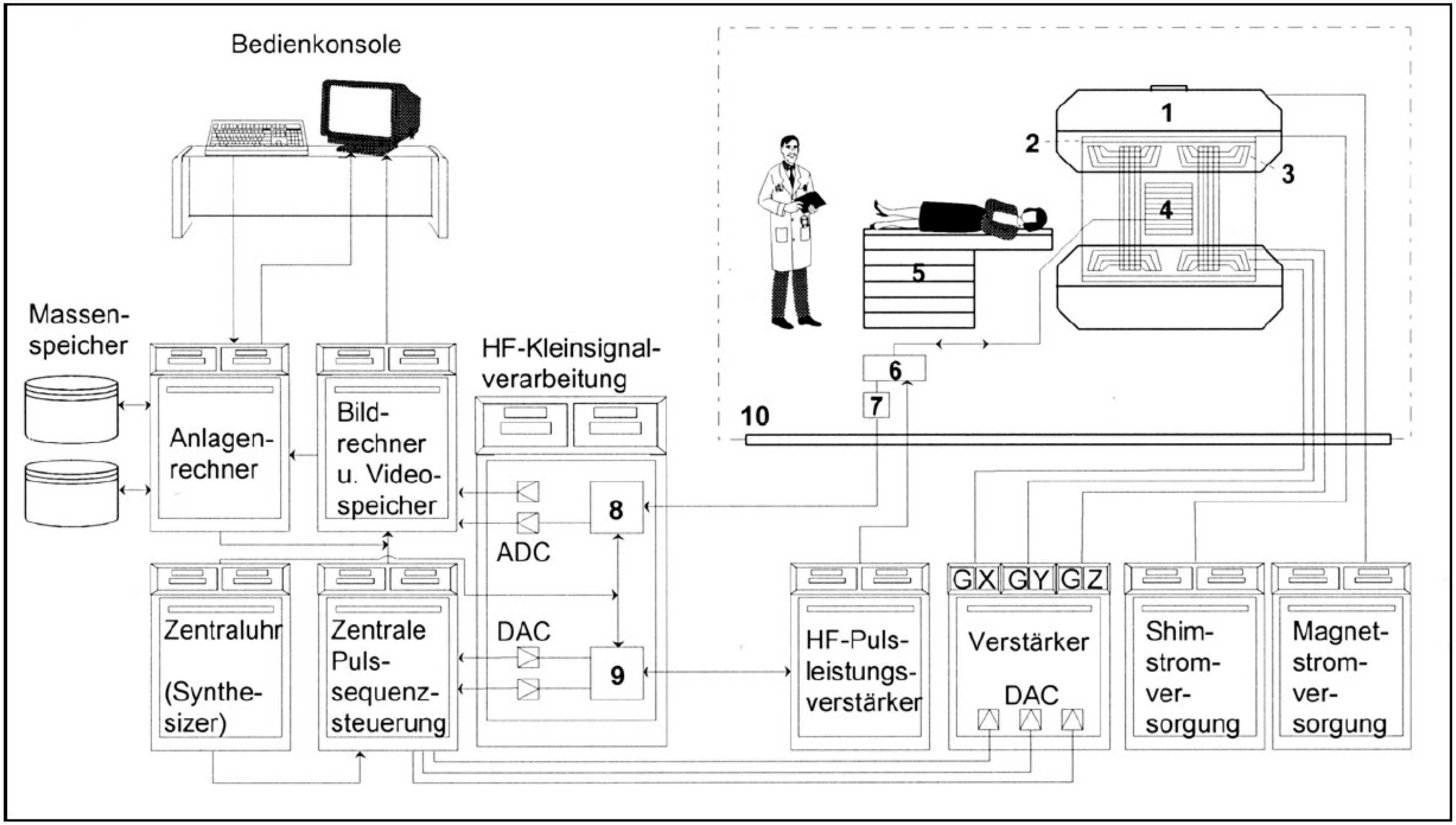

1 Magnet mit Kryotank und Kälteschild
2 Shimspulensystem
3 Gradientenspulensystem
4 HF-Resonator
5 Patientenliege
6 Sende-Empfangsweiche
7 Vorverstärker
8 Quadraturdemodulator mit 2 Tiefpässen
9 ESB-Modular
10 HF-dichte Durchführungen

magnet

largest and heaviest system component (characteristic: 5 – 10 tons)

magnetization in body ~ field strength
⇒ improvement of signal-noise-ratio ~ field strength

but: with increasing field strength:
- prolongation of T_1 time
- prolongation of recording duration
- increase of chemical shift ⇒ more artifacts

chemical shift:
- shift of resonance frequency of nucleus depending in chemical bond (e.g., structure of molecule)
- weakening of applied magnetic field by electron shell proportional to magnetic field strength

magnet

range	field strength	Larmor-frequency	T1 white matter brain	chemical shift fat/water (3.5 ppm)	SNR white matter brain (rel. units)
very small	0,02 T	852 kHz	?	3 Hz	≈ 0,02
small	0,5 T	21,3 MHz	540 msec	75 Hz	0,6
medium	1 T	42,6 MHz	680 msec	149 HZ	1
large	4T	170,4 MHz	1080 msec	595 Hz	2,3

for ω_0>40 MHz: shading due to skin effect !
(i.e., weakening of external field due to eddy currents induced by HF field)

magnet

identical
recording
parameter

different impression
of images
due to field-strength
dependent
signal-to-noise
ratio

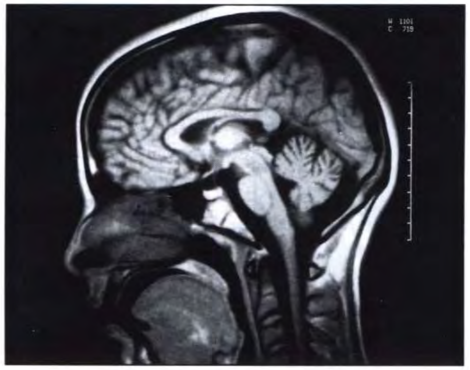

0.2 T

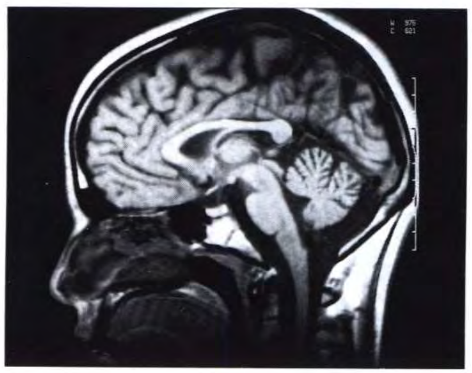

1.0 T

1.5 T

recording parameter
optimized
(wrt field strength)

homogeneous
impression
of image

magnet - requirements

requirement	**range****	**problem**
homogeneity	1ppm (20 cm sphere) 10 ppm (40 cm sphere)	shortening of T_2 image distortions
long-term stability	0.1 ppm / h	Larmor frequency unstable (drift)
short-term stability		phase coding unstable (drift)
scatter field	0.5 mT-limit* in lateral direction at 3 m in longitudinal dir. at 5 m	disturbs functioning of other devices (e.g. pace maker) dangerous attraction of iron-bearing materials

* 0.5 mT = limit for heart pace maker

**reported values are orders of magnitude only

magnetic resonance imaging (MRI)

magnetic resonance imaging (MRI)

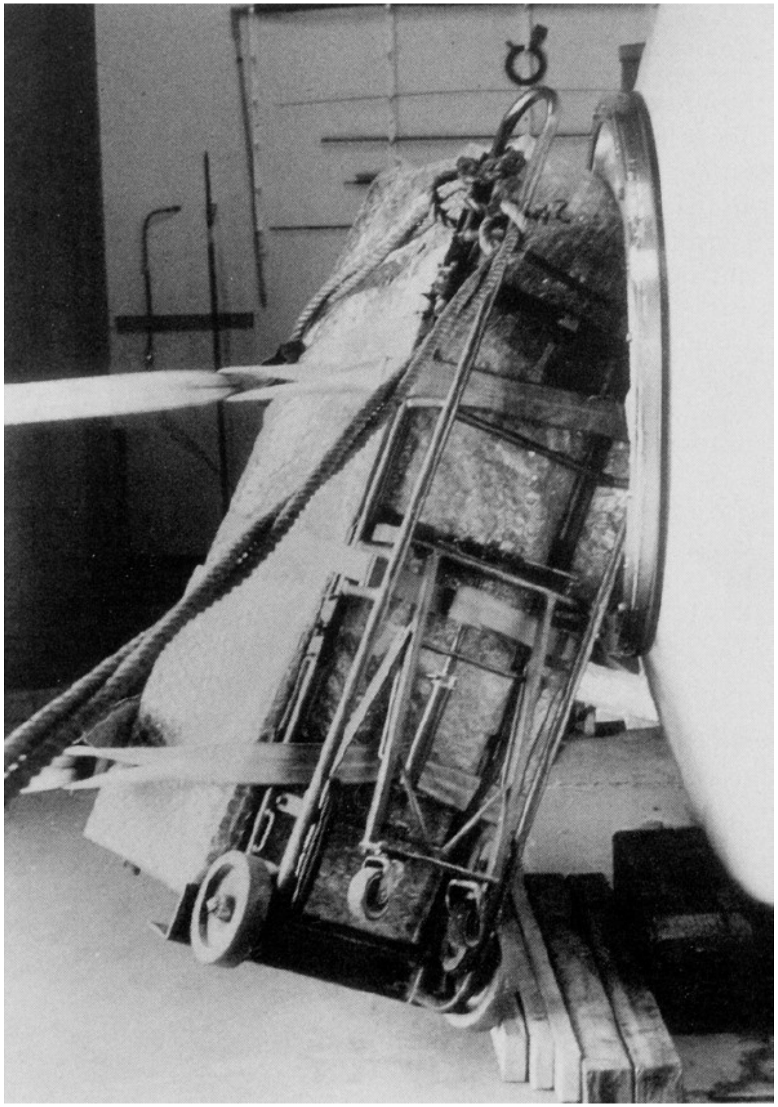

Junge stirbt im Tomographen

New York. (dpa/tlz) Tödliche Kräfte eines Kernspintomographen: Ein Sechsjähriger wurde von einem Sauerstoffkanister getroffen, den das Gerät angesogen hatte.

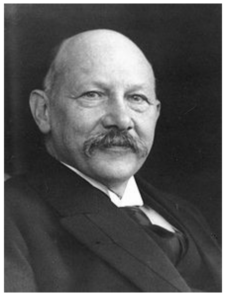

Heike Kamerlingh Onnes

magnet

best suited: ***superconducting magnets***

characteristic: cylindrical coil, patient in center

multi-filament-wire: niobium-titanium-alloy (embedded in copper matrix)
- single wire consists of ~ 30 filaments (each 0.1 mm diameter)
- diameter of Cu-matrix: ~ 2mm
- for 1T field strength: 10 km length of wire with mean radius of 550 mm
- lossless transport of currents of up to 500 A (characteristic: 200 A)
- stored magnetic field energy ~ 4 MJ (@200 A)

Nb-Ti is superconducting below critical temperature T_c ~ 4.2 K (liquid He):
- induced current indefinitely (almost) persists with no power source

Meißner-Ochsenfeld effect:
- perfect shielding of external magnetic fields

magnet ("charging")

a magnet can be charged within in hour due to $U = L\,\mathrm{d}I/\mathrm{d}t$:

example:
- current source with 10 V, 200 A, 2000 W
- heating of a jumper in magnet above Tc
- if induced current reached (e.g.) 200 A, turn off heating
- magnet becomes superconducting (in liquid He)
- remove current source

magnet (shimming)

- magnet does not provide required homogeneity (e.g. after heating,…)

- field balancing (*shimming*) through mounting of iron sheets and/or correction with dedicated shim coils

- field in open inner area of magnet must follow Laplace equation.
  We have: $\vec{\nabla} \text{x} \vec{B} = 0 \quad \text{and} \quad \vec{\nabla} \cdot \vec{B} = 0$

- In general, we have: $\vec{\nabla} \text{x} (\vec{\nabla} \text{x} \vec{B}) = \vec{\nabla} \cdot (\vec{\nabla} \cdot \vec{B}) - \Delta \vec{B} \Rightarrow \Delta \vec{B} = 0$

- find solutions for B_z through expansion in spherical harmonics

- recording B_z on central axis an on sphere (different angles θ and φ) allows estimation of low-order coefficients of expansion

- compensation of all coefficients with iron sheets and shim coils

gradient coils (1)

important characteristics of gradient coils	**typical orders of magnitude for a coil diameter of 80 cm**
gradient circuit time	10 mT/m in 0.5 s
inductance	200 µH = 200 Vs/A
current / gradient	30 A(mT/m)
maximum current	300 A
current circuit time	600 kA/s
peak performance of amplifier (excl. ohmic loss in coil)	36 kW

fast pulse-sequences:
up to 20 mT/m

small inductance:
rapid switching, but:
low number of turns

fast switching of gradient coils causes strong knocking noise !
(mechanical forces that act on coils, cf. loudspeaker)

gradient coils (2)

most often used coil configurations

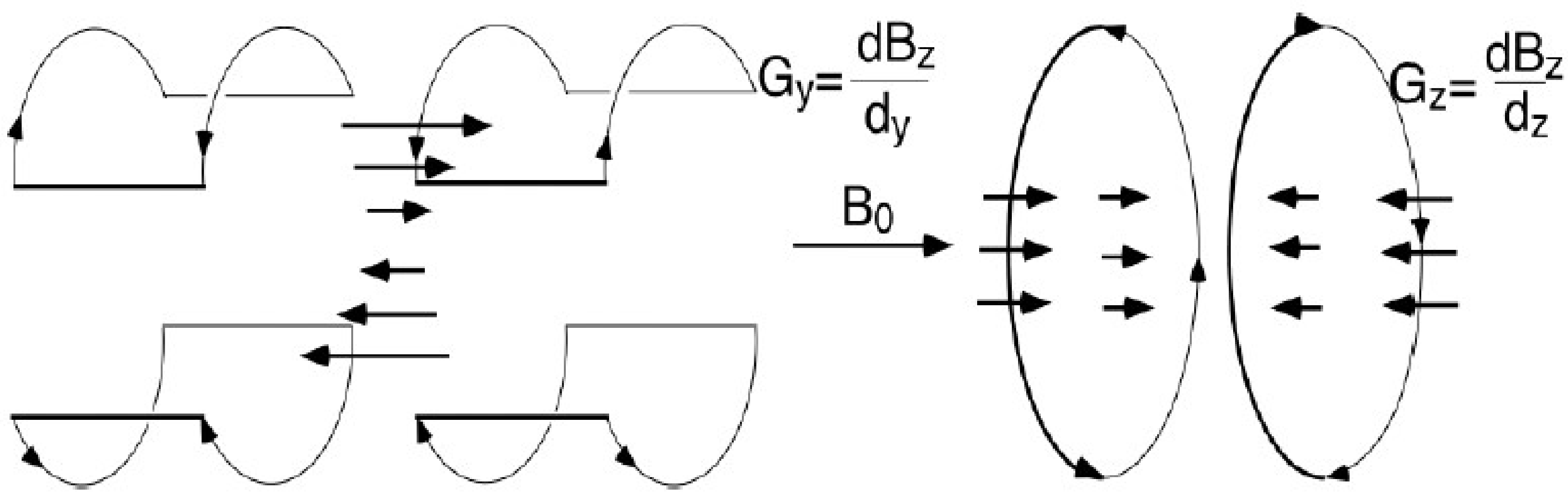

G_x-coil tilted by 90°

estimation of field using Biot-Savart law: $d\vec{B} = \frac{\mu_0 I}{4\pi r^3}\vec{r} \times d\vec{I}$

gradient coils (3)

1984: Jedi-helmets

gradient coils (4)

compensation for eddy currents
(many components of magnet contain aluminum $\rightarrow$ eddy currents !)

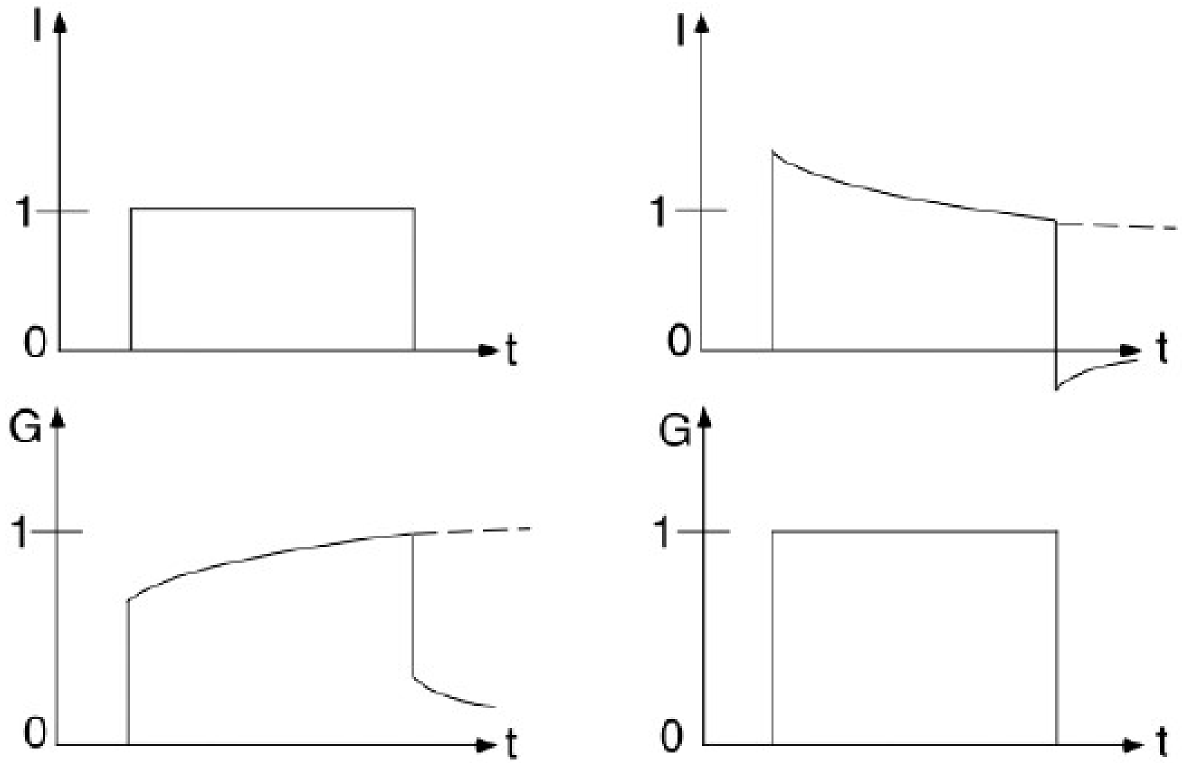

without compensation　　with compensation

transmit/receive coils (1)

requirements:

- generation and detection of oscillating B-field transversal to longitudinal direction of magnet (z-axis)

- frequency depends on B_0
(21.3 MHz @ 0.5 T; 42.6 MHz @ 1.0 T; 63.9 MHz @ 1.5 T)

- homogeneous excitation (smooth flip angles)

problems:

- dimensions of coil > wavelength

- conducting components typically have parasitic capacitances and inductances

- impedance adjustment to transmitter/receiver

transmit/receive coils (2)

saddle-like coil

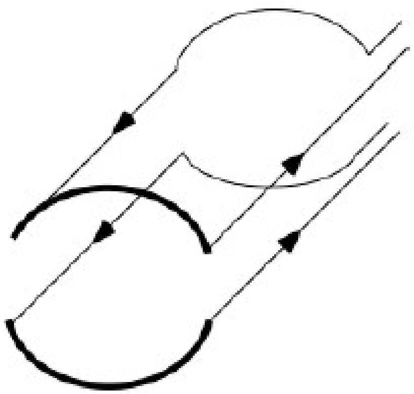

"birdcage" coil

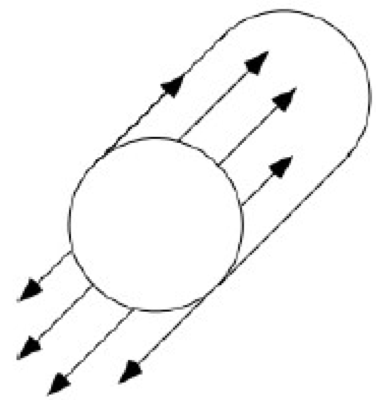

very small magnetic field strengths
resp.
very low frequencies

(principle: pair of Helmholtz coils)

strong magnetic field strengths
resp.
high frequencies
(principle: sinusoidal distribution of currents along cylinder barrel generates homogeneous field inside cylinder)

sizing of coil such that noise as small as possible
in general: the smaller the coil coverage the lower the noise !

transmit/receive coils (3)

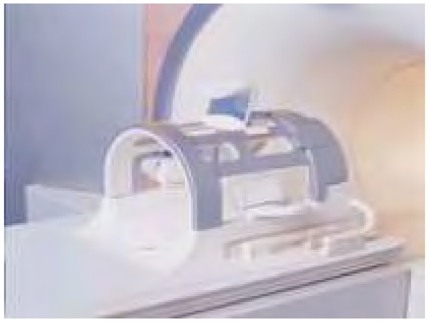

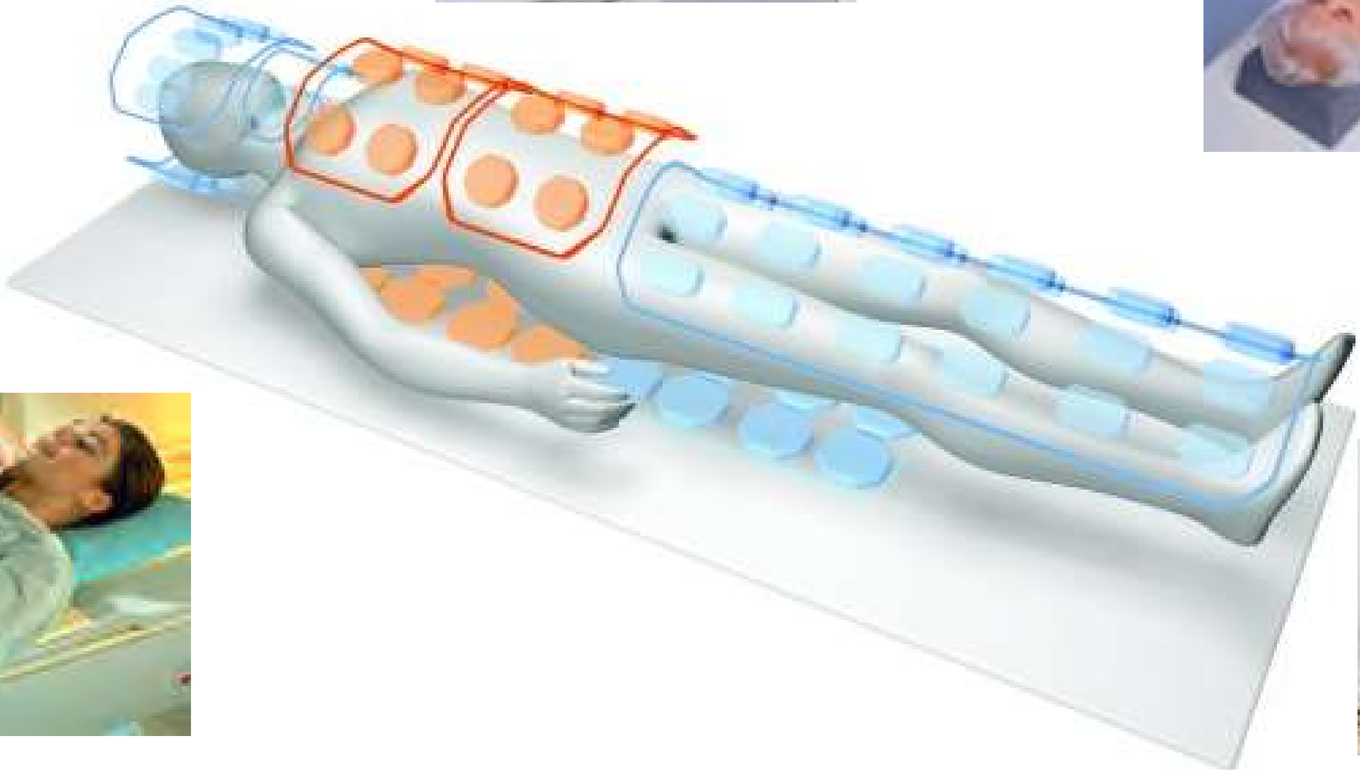

from: Siemens + Philips

- MRI-images depict the local strength of the transversal magnetization $M_T(x,y)$ at the time of maximum amplitude of an echo

- $M_T(x,y)$ depend on properties of the tissue and on control parameter of a pulse sequence

- def. contrast: $K = \frac{I_1 - I_2}{I_1 + I_2}$ where $I_{1,2}$ = signal of tissue 1,2

- K depends on noise in $I_{1,2}$

- the larger a pixel the higher the signal amplitude and the smaller the noise

- but: diminished spatial resolution!

$\Rightarrow$

strong mutual dependence of contrast, noise, and spatial resolution

influencing variables

tissue properties	**MRI system parameter**
proton density ρ	repetition time T_R
long. relaxation time T_1	echo time T_E
transv. relaxation time T_2	flip angle α
chemical shift	
field inhomogeneities T_2^*	inversion time T_i
transport and movement	field data (B_0, G_x, G_y, G_z)
uptake contrast agent	sequence (spin-echo, etc.)

influencing variables T_E and T_R

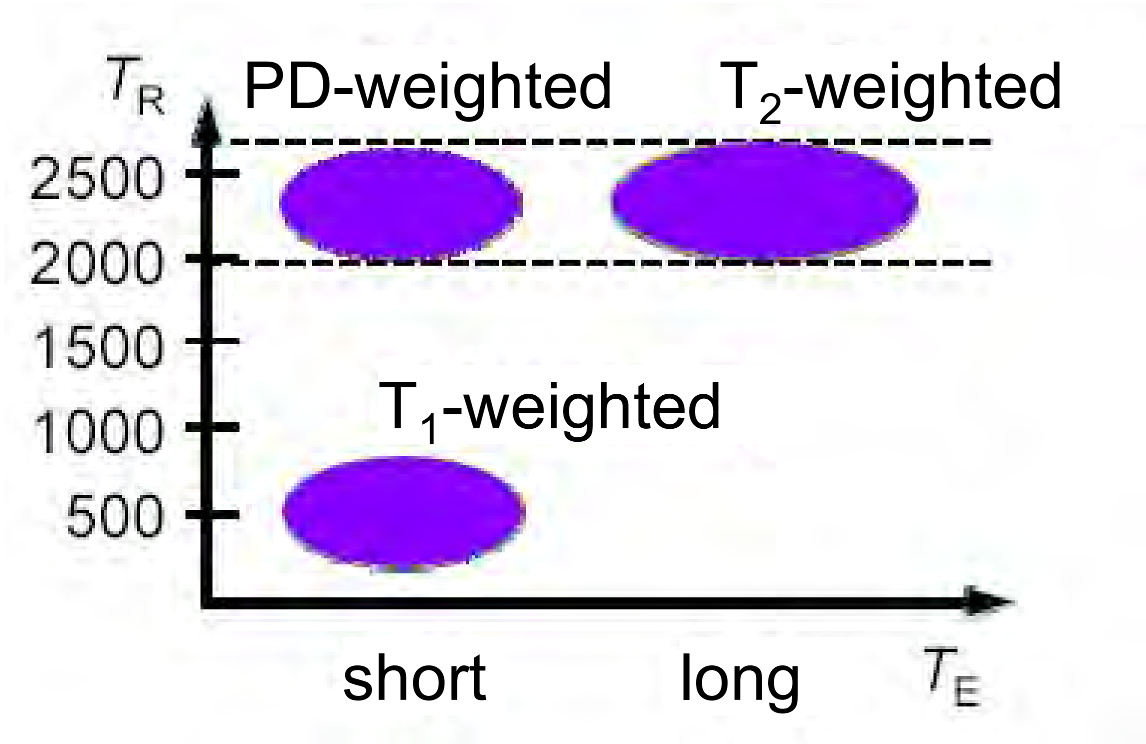

sequences: proton density weighting

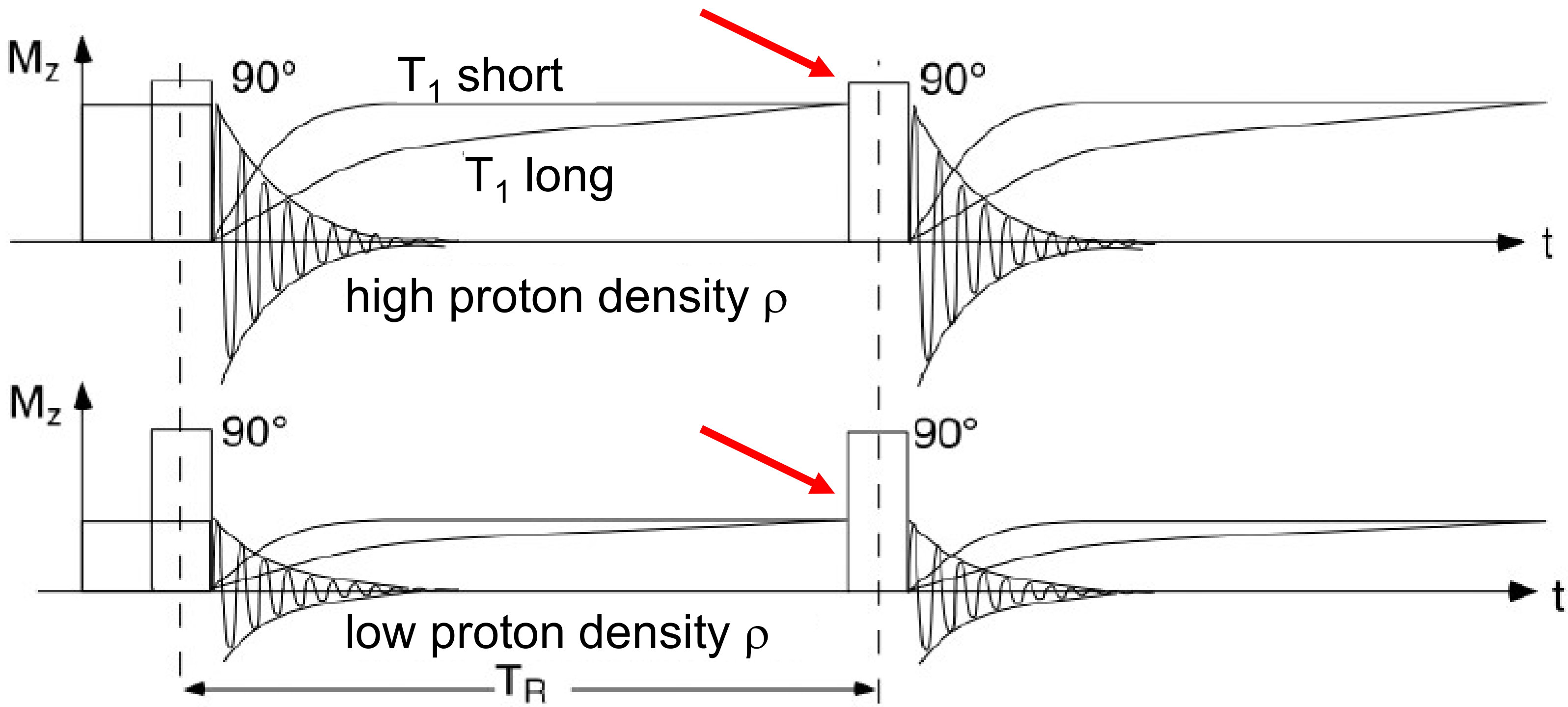

choose $T_E << T_2$ and $T_R >> T_1$

sequences: T_1-weighting

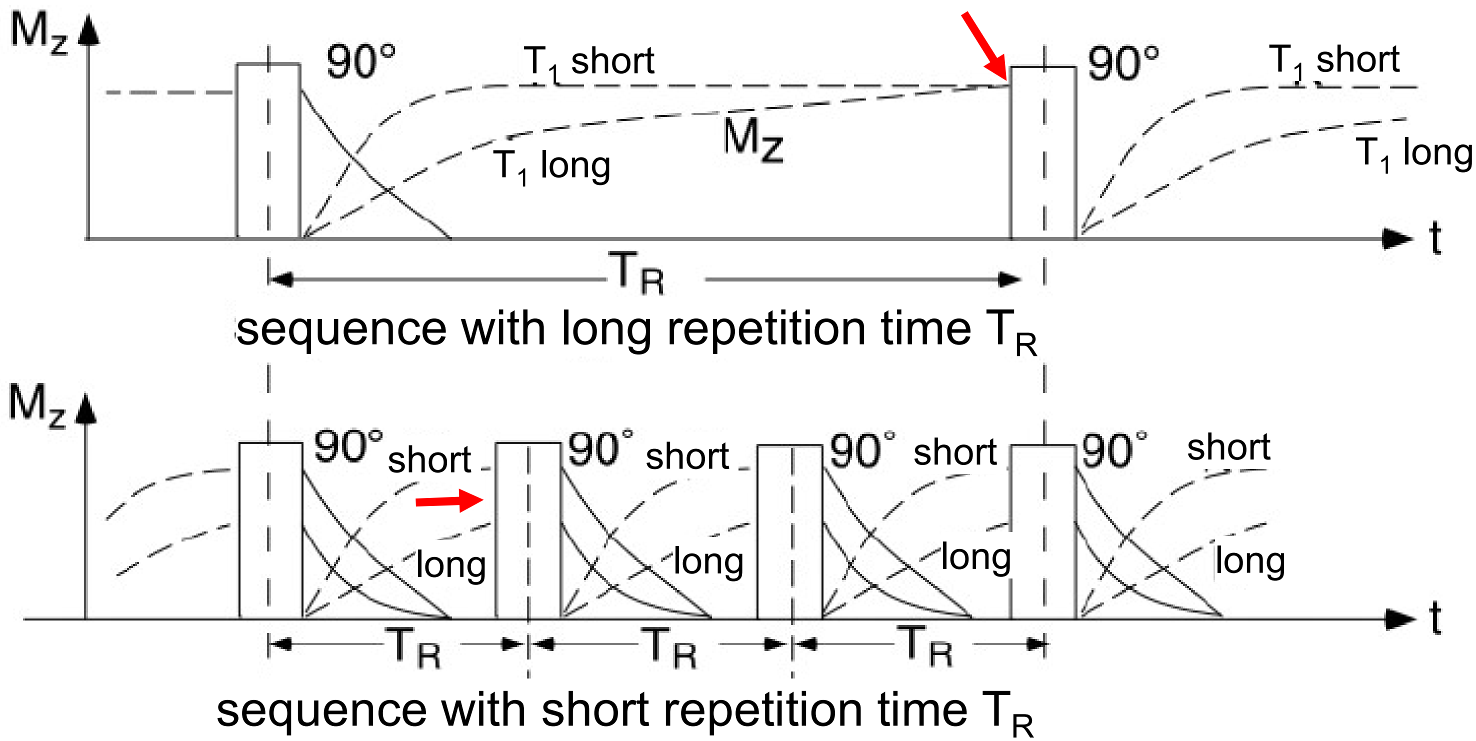

a short repetition time T_R allows for T_1-weighted images

sequences: T_2-weighting

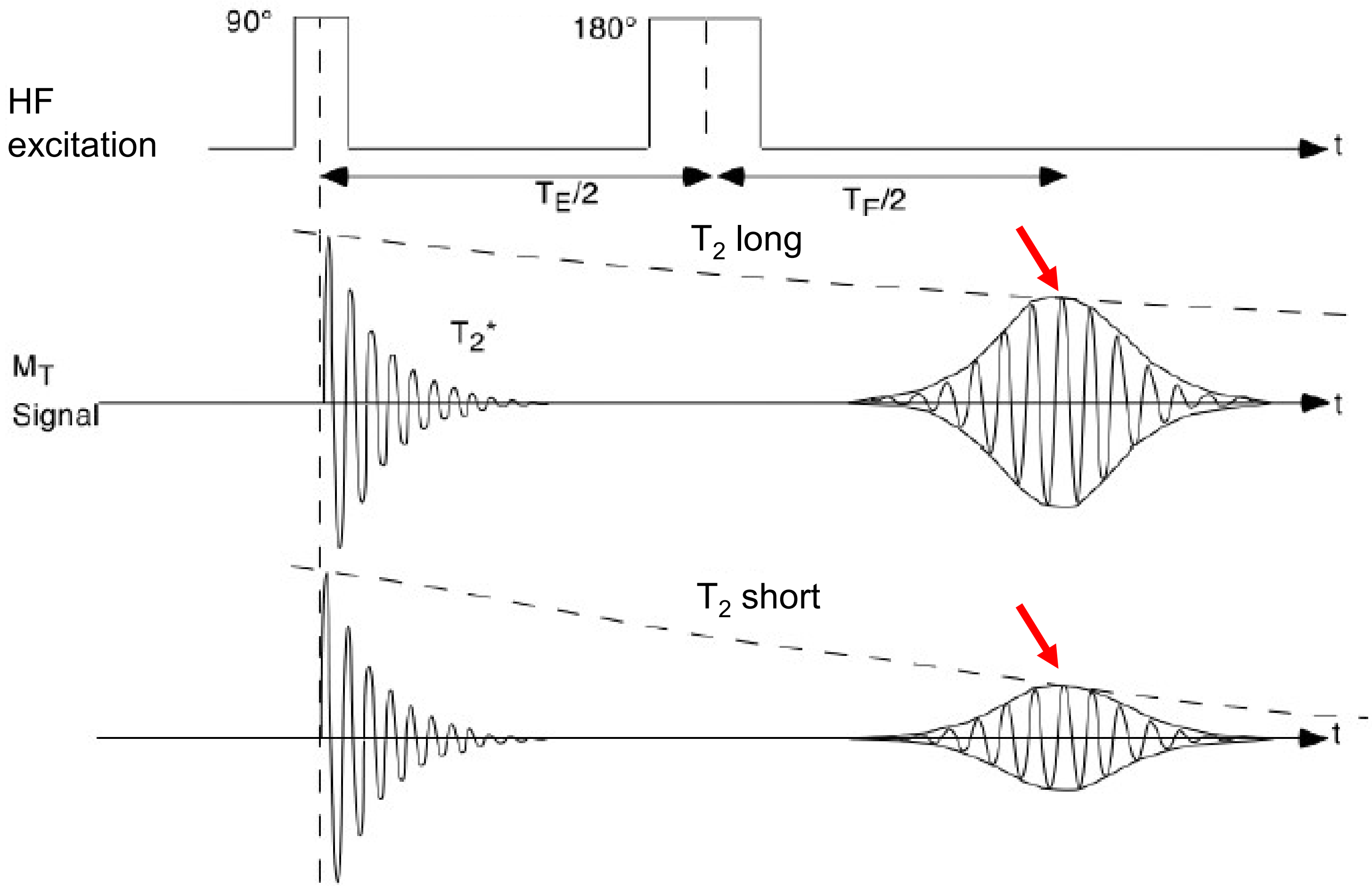

a long echo time T_E allows for T_2-weighted images

different weightings using a saturation-recovery sequence

proton density-weighted	**T_1 - weighted**	**T_2 - weighted**
T_R long (e.g. 2000 ms)	T_R short (e.g. 500 ms)	T_R long (e.g. 2000 ms)
T_E short (e.g. 15-30 ms)	T_E short (e.g. 15-30 ms)	T_E long (e.g. 100-200 ms)

different weightings allow for different contrasts
→ potential of MRI !
→ contrast optimization is application-dependent !

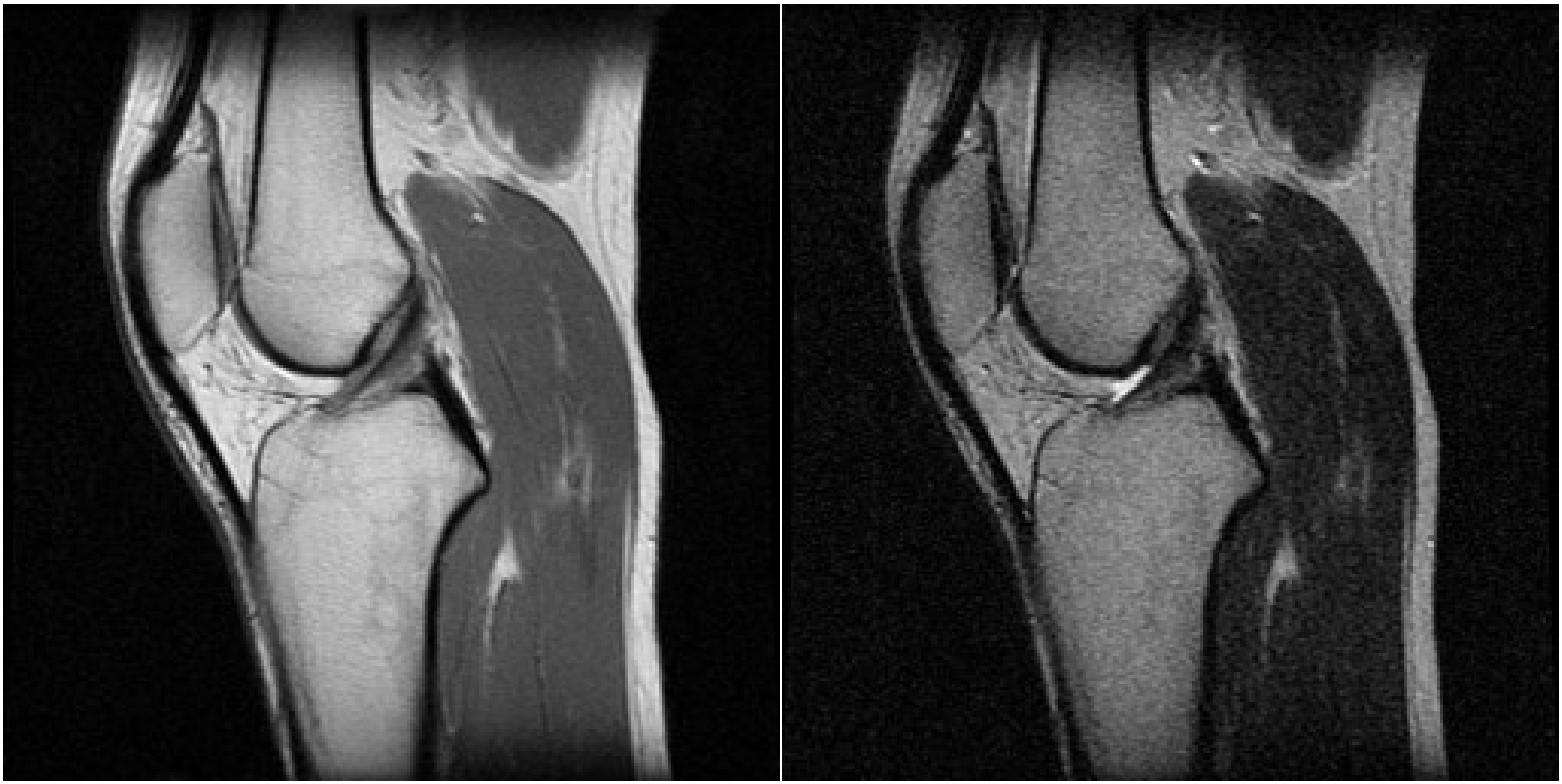

proton density-weighted T_2-weighted

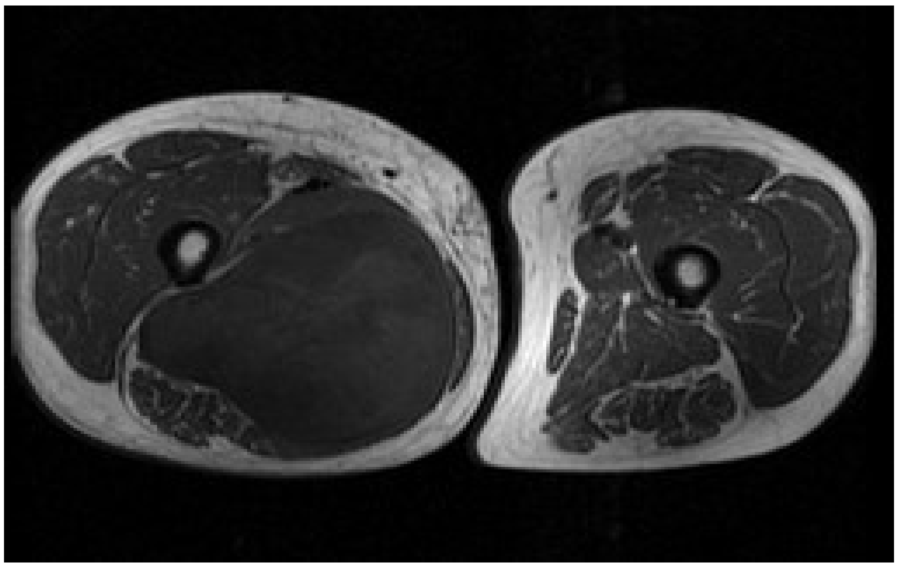

T_1-weighted

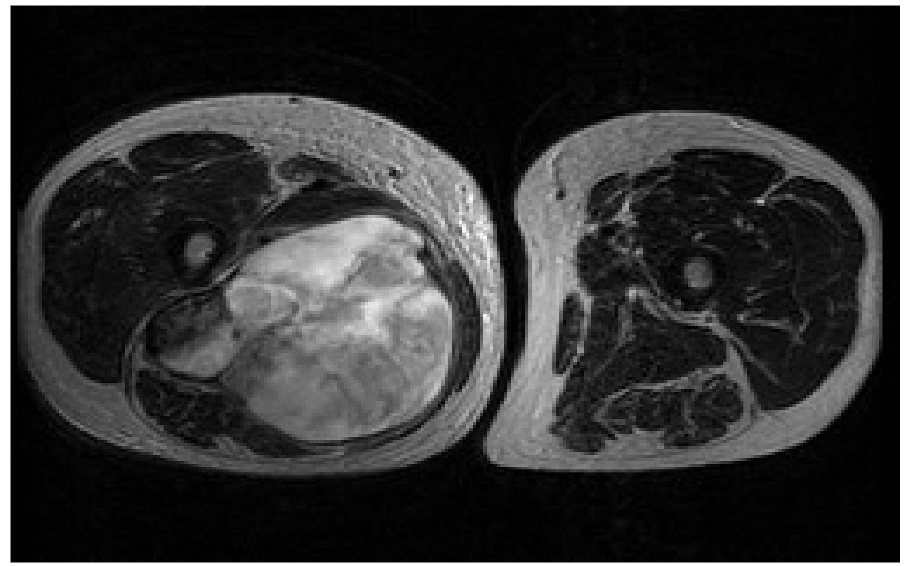

T_2-weighted

magnetic resonance imaging (MRI) *contrast*

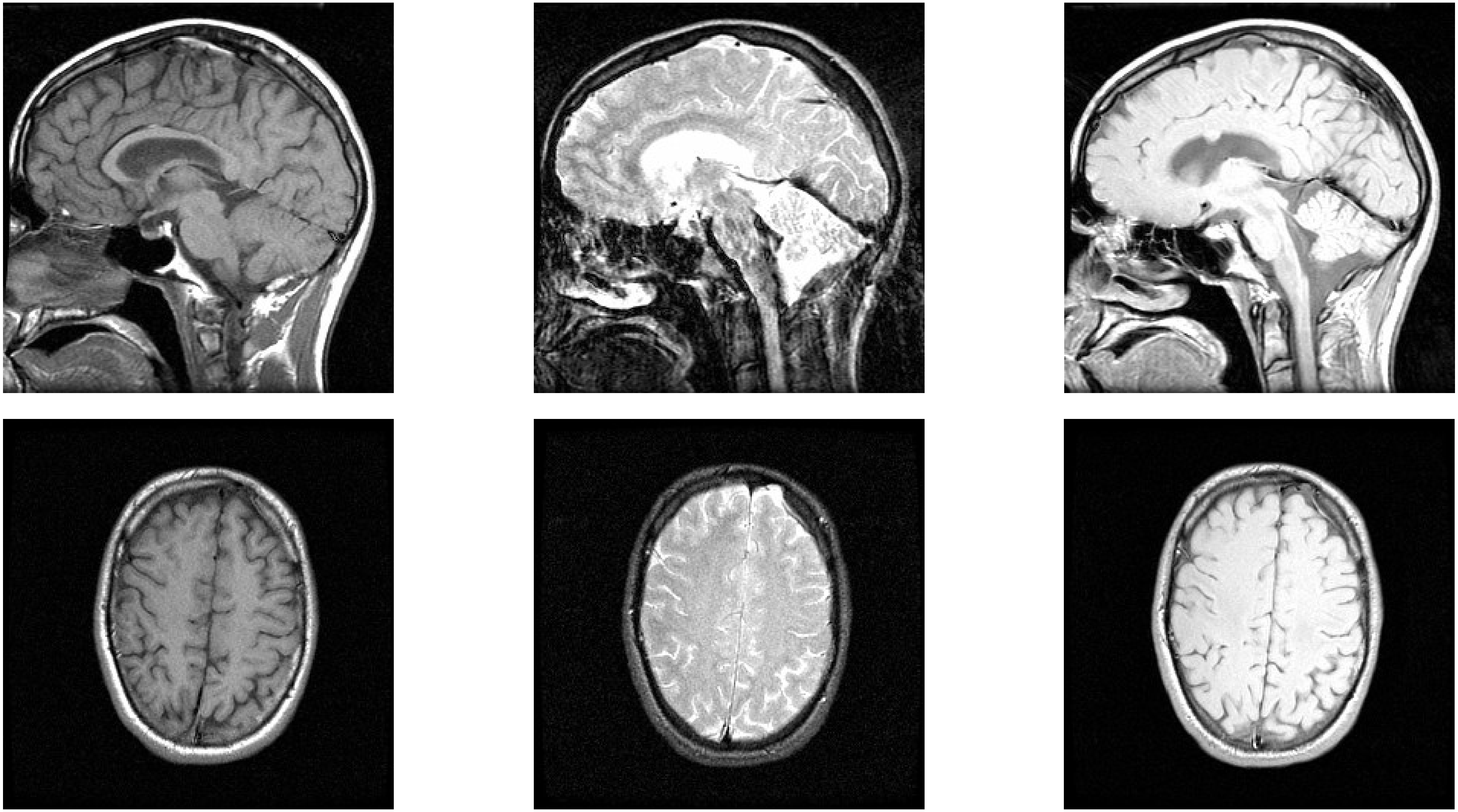

T_1-weighted | T_2-weighted | proton density-weighted in general, we have:

envelope of spin echo corresponds to modulation transfer function (MTF)

thickness of excited slice (z-direction):

- the steeper the G_z-gradient field resp. the smaller the bandwidth of HF signal the thinner the slice

$$\Delta z = \frac{\Delta\omega_s}{\gamma G_z}$$

characteristic values: few mm

lateral resolution (x-, y-direction):

- depends on G_y- and G_x-gradient fields (phase- and frequency-coding) and their related recording times T_y und T_s

$$\Delta y = \frac{\pi}{\gamma G_{y,\max} T_y} \qquad \Delta x = \frac{\pi}{\gamma G_x T_s}$$

typically: (Δx, Δy) ≥ Δz

limiting factors for lateral resolution:

- relaxation phenomena (signal indistinguishable from noise after long times)
- frequency resolution and bandwidth of detector
- processing speed of AD-converter (avoidance of aliasing artifacts)
- technical limits for the generation of gradient fields

further influencing factors:

- homogeneity of magnet (image distortions)
- linearity of gradients (image distortions)
- chemical shift

  proton Larmor frequency differs in different environments

  fat image and water image shifted relative to each other (for field strengths > 3T)

  $\rightarrow$ diminished detail discrimination

$$SNR = M_{T_0}(\vec{r})\sqrt{\frac{\omega_0\mu_0 Q}{4kTV_{eff}\Delta f}}\sqrt{N_m N_p N_a}\;10^{\left(-(\delta+F_r)/20\right)}\;e^{\left(-T_E/T_2\right)}dv$$

important influencing factors :

- saturation magnetization $M_{T0}(\mathrm{r})$ (increases with B_0)
- quality Q of coil: ohmic resistance of coil, bandwidth of detector, ohmic resistance due to eddy currents induced in body !
- effective volume V_{eff} “seen” by the coil
- recording bandwidth Δf (Nyquist theorem)
- number of samples N_{m}, of phase coding steps N_{p} and total averaged samples N_{a} (assumption: statistically independent individual recordings !)
- noise in recording circuit (damping @ input δ und noise figure F_{r}) in dB
- ratio echo time T_{E} and relaxation time T_2
- volume of recorded voxel dv

movement/transport	**no movement**

- phase effects
- amplitude effects
	- device
	    - sampling error (truncation, aliasing)
	    - B_0-inhomogeneities
	    - eddy currents
	    - insufficient field-of-view
	    - cross-talk between neighb. slices
	
	- patient
	    - chemical shift
	    - strong susceptibility gradients

movement artifacts (1)

rigid (global movements, breathing):
phase shift in Fourier data

elastic (local movements, e.g. heart):
practically not correctable

possible solutions:
- fixate patient
- reduce recording time
- external triggering (EKG)
- image processing

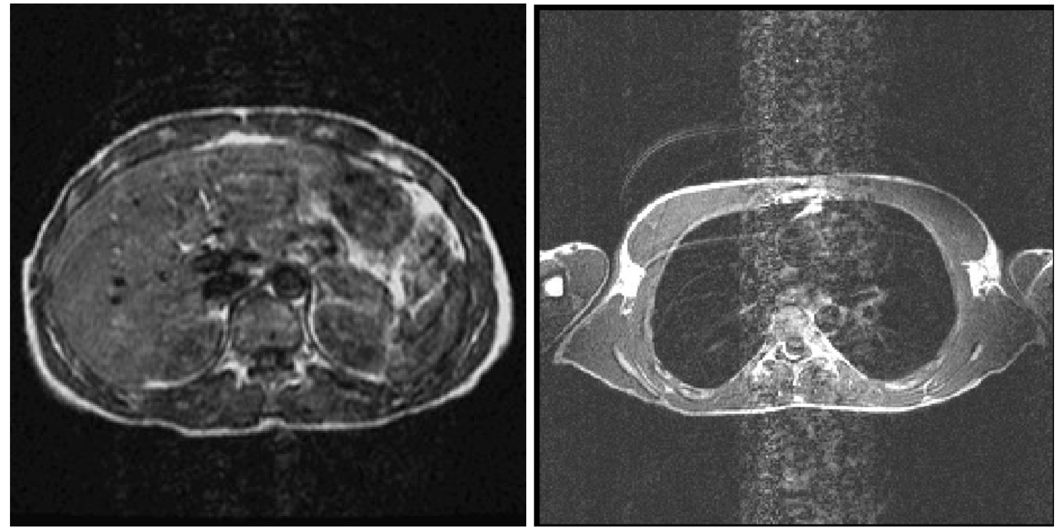

movement artifacts due to breathing

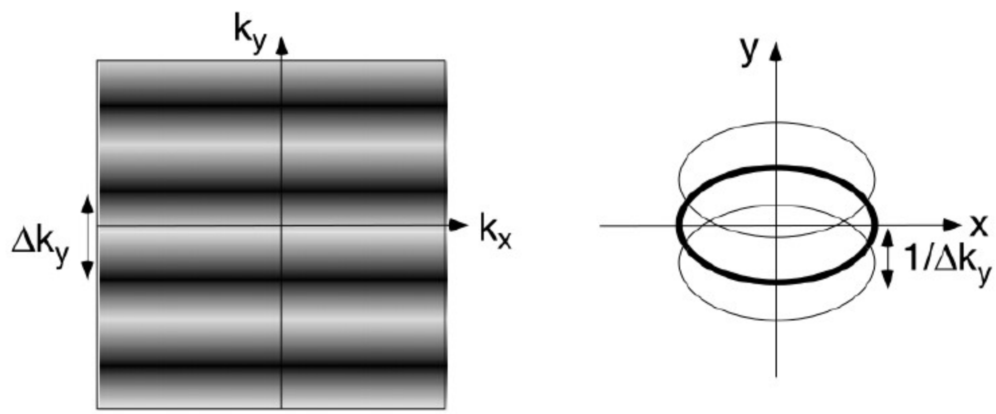

intensity modulation in *k*-space due to breathing and “ghost images”

movement artifacts (2)

global movement: patient leaves scanner during recording

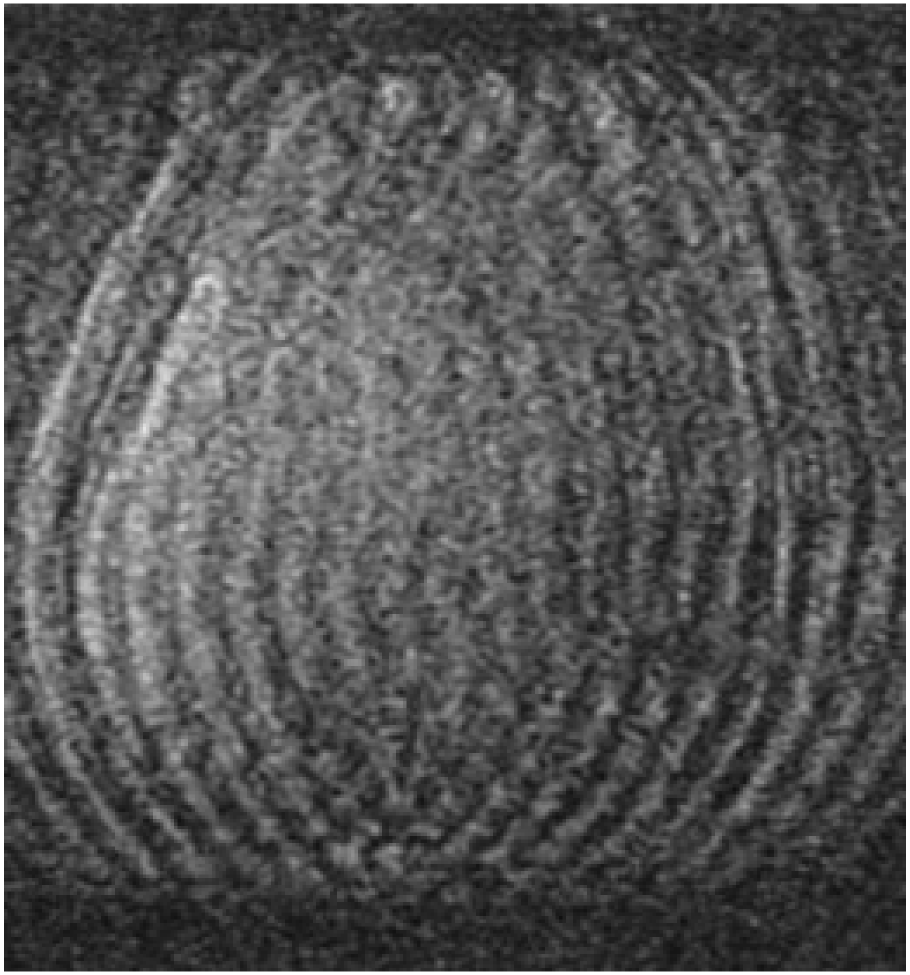

movement artifacts (3)

- spins change either their position during measurement or their velocity (blood, CSF !)

- ghost images or complete signal loss

- potential solutions with dedicated sequences:
    - flow rephasing via pre-saturation
    - flow compensation via double- or triple-gradient pulse

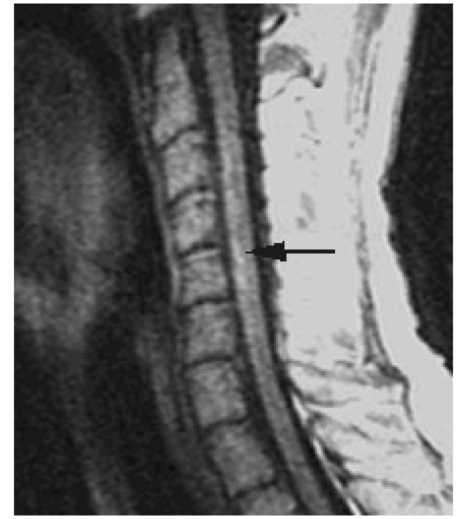

swallow

no swallow

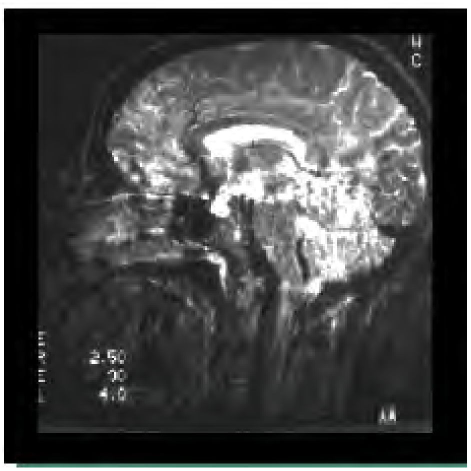

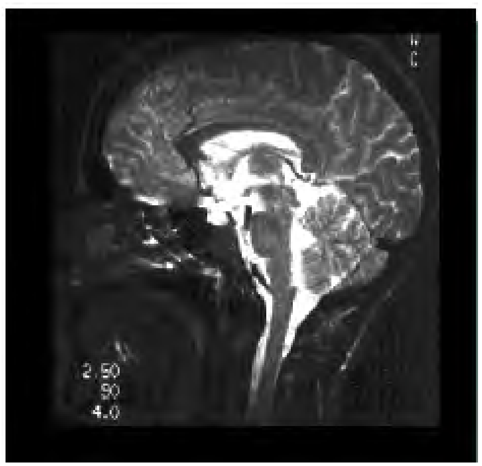

without　　　　with
flow rephasing

field inhomogeneities from materials with different susceptibilities

- spin-spin coupling (T2 time) changes magnetic field locally

- modification of Larmor frequency

- spatial assignment distorted
  $\Rightarrow$ geometric distortion

- relaxation effect differ
  $\Rightarrow$ inhomogeneous intensities

e.g.
μ_1 = air
μ_2 = tissue

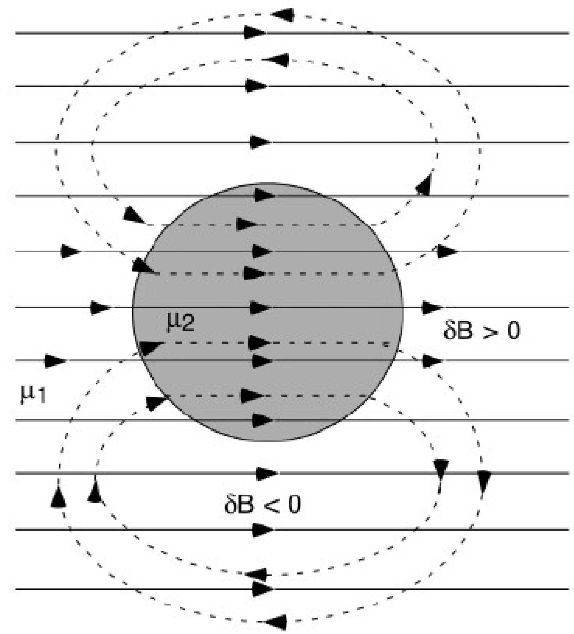

positive usage:
imaging with susceptibility parameter !

field inhomogeneities from materials with different susceptibilities

when using long echo times, local dephasing effects can lead to signal loss in areas between tissues having different susceptibilities

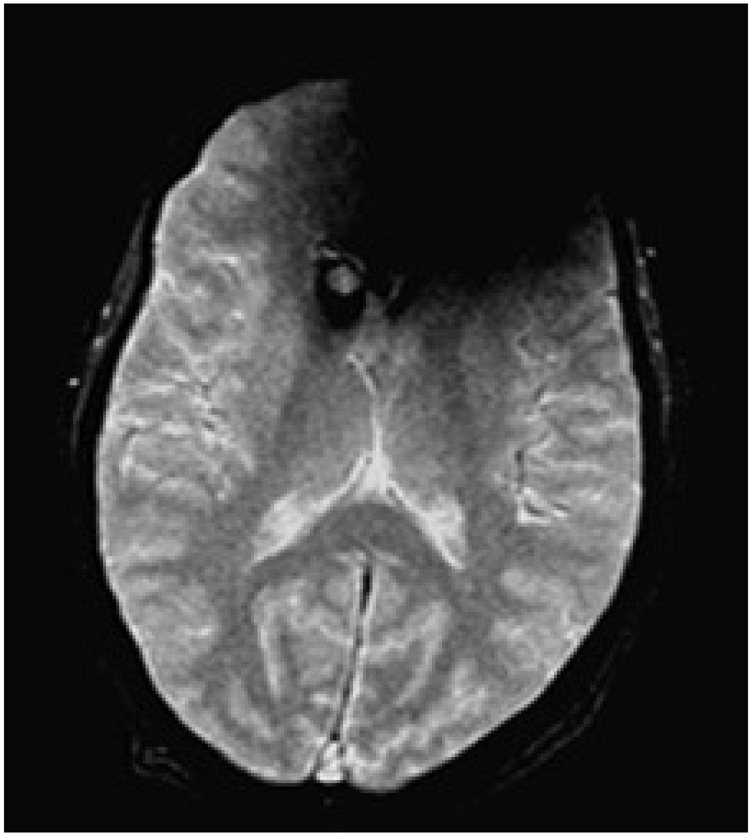

dental filling

field inhomogeneities from materials with different susceptibilities

massive susceptibility artifacts

metal clip in hair band
("cone-head")

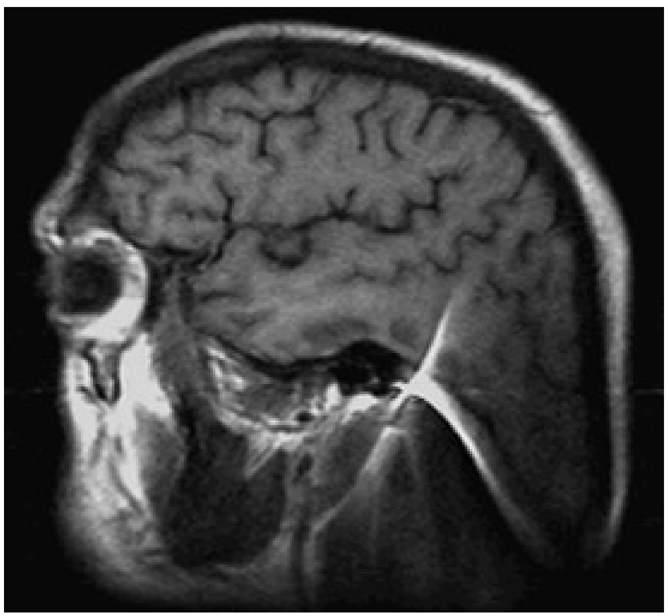

brace

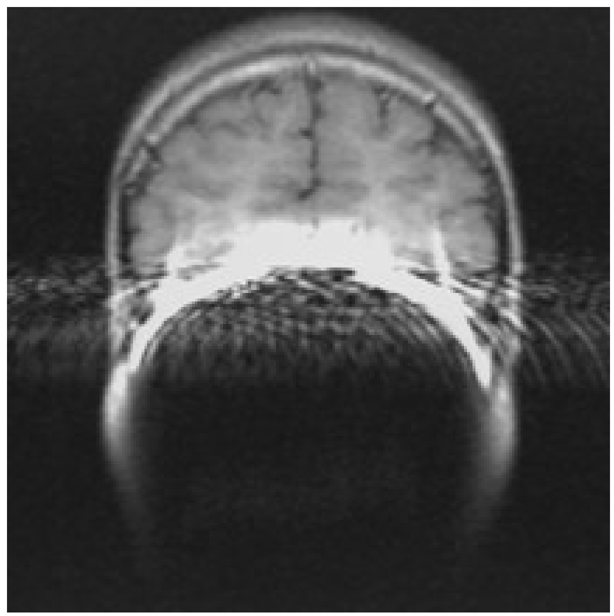

belt

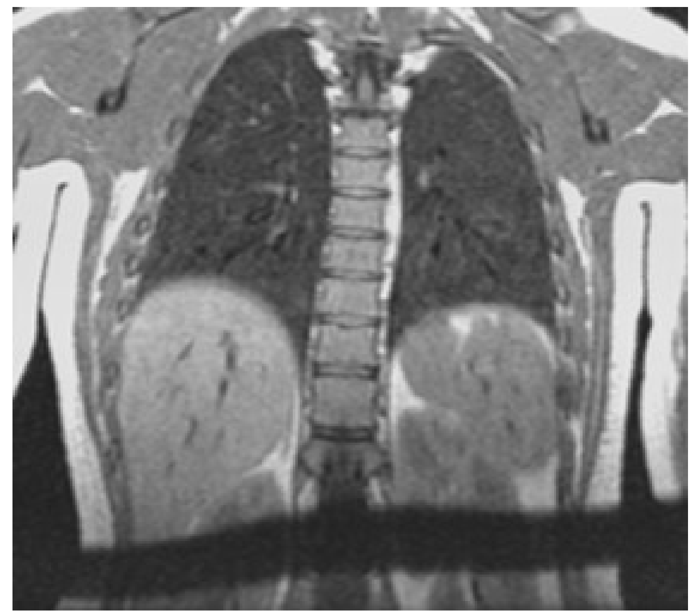

chemical shift

- proton Larmor frequency differs in different environments

- fat image and water image shifted relative to each other

  bright area:
  overlay of fat- and water protons

  dark area:
  no imaging of protons

- can be corrected with dedicated sequences
  (e.g. fat saturation)

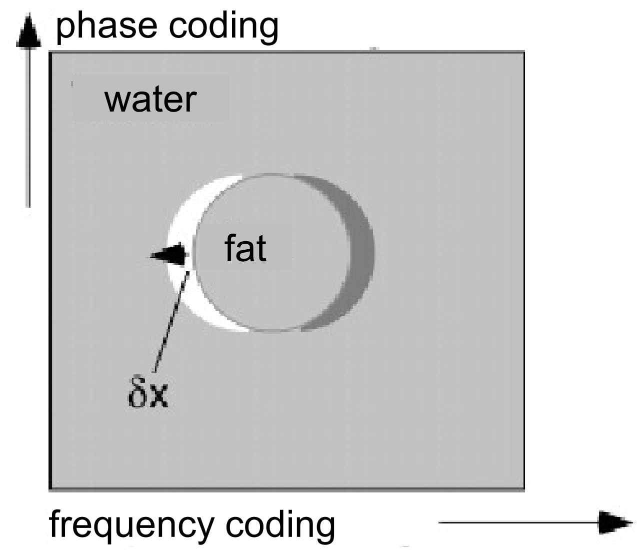

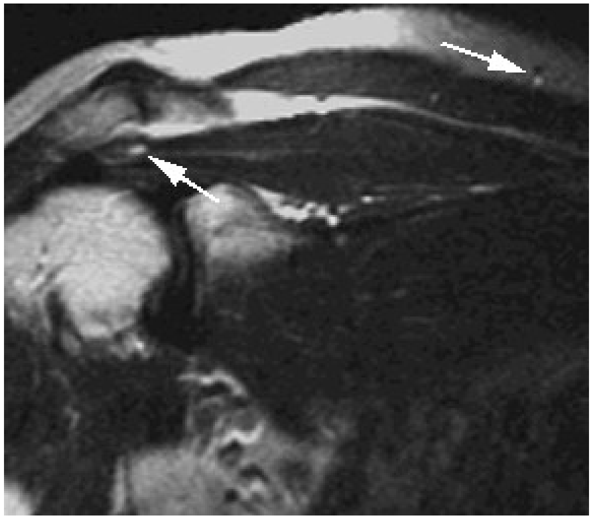

MRI-image of shoulder
without fat saturation

device-induced artifacts, insufficient sampling

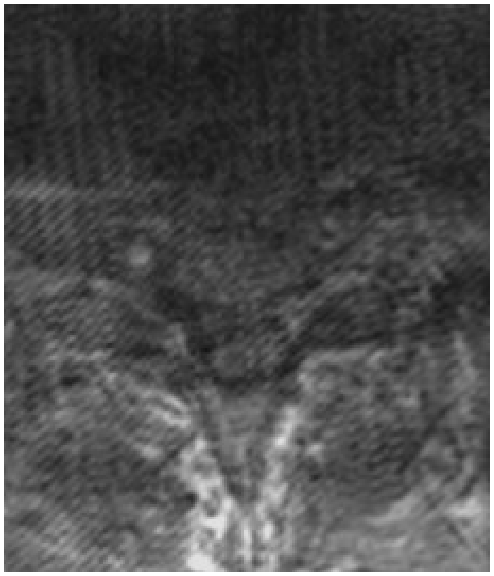

moving coil

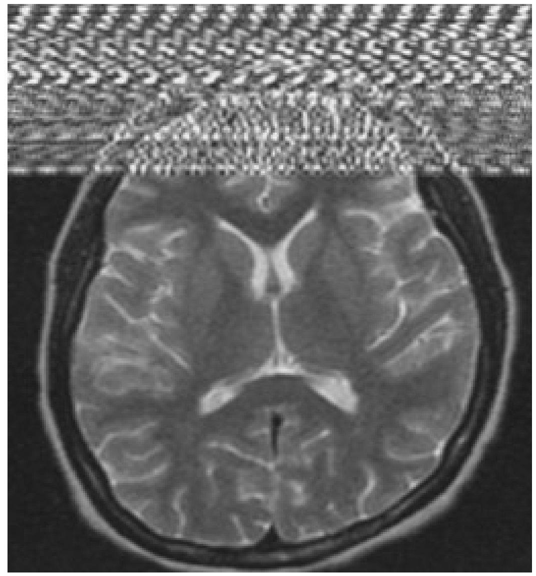

RF interference
ventilator

sampling error (aliasing)
field-of-view
too small

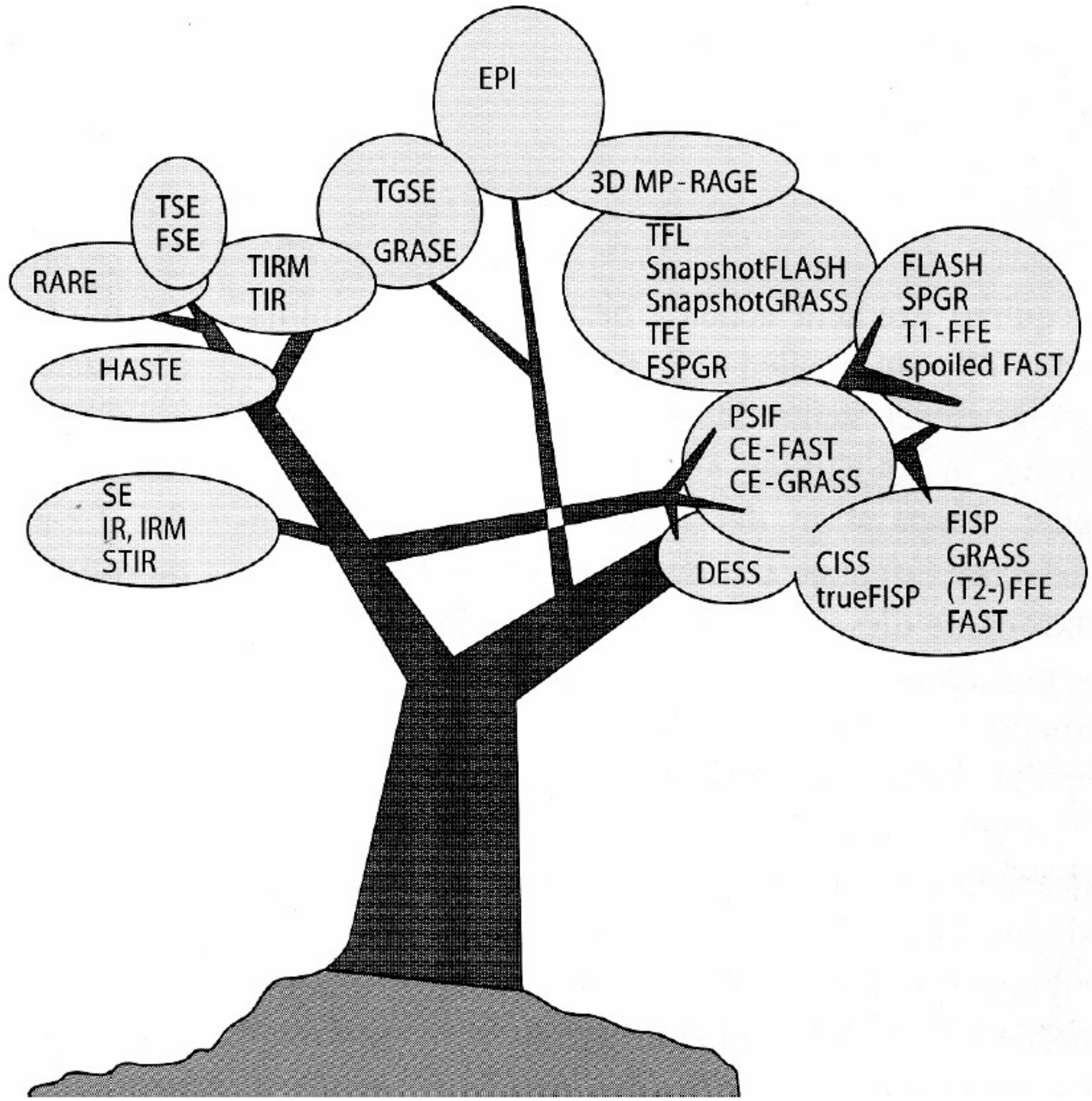
EPI
3D MP-RAGE
TGSE
GRASE
TSE
FSE
RARE
TIRM
TIR
HASTE
SE
IR, IRM
STIR
TFL
SnapshotFLASH
SnapshotGRASS
TFE
FSPGR
FLASH
SPGR
T1-FFE
spoiled FAST
PSIF
CE-FAST
CE-GRASS
DESS
CISS
trueFISP
FISP
GRASS
(T2-)FFE
FAST

k-space scanning options

conventional one echo / T_R	hybrid multiple echoes / T_R	single shot all echoes / T_R
SE GRE TurboFLAIR MP-RAGE	Turbo-SE Turbo-GSE	HASTE EPI

echo planar imaging (EPI)

- utilize gradient echoes

- after excitation (G_z): positioning in *k*-space with gradients G_x and G_y (*pos. A*)
- polarity reversal of G_x generates echo, vector moves to *pos. B* during that time
- G_y gradient shift phase to *pos. C*
- polarity reversal of G_y generates echo, vector moves to *pos. D* during that time
- etc.

- signal decays with T_2*
- requires very fast switching of G_x and G_y
- strong G_y gradient, to allow rapid sampling of row in *k*-space

- highly technically demanding (for MRI system)

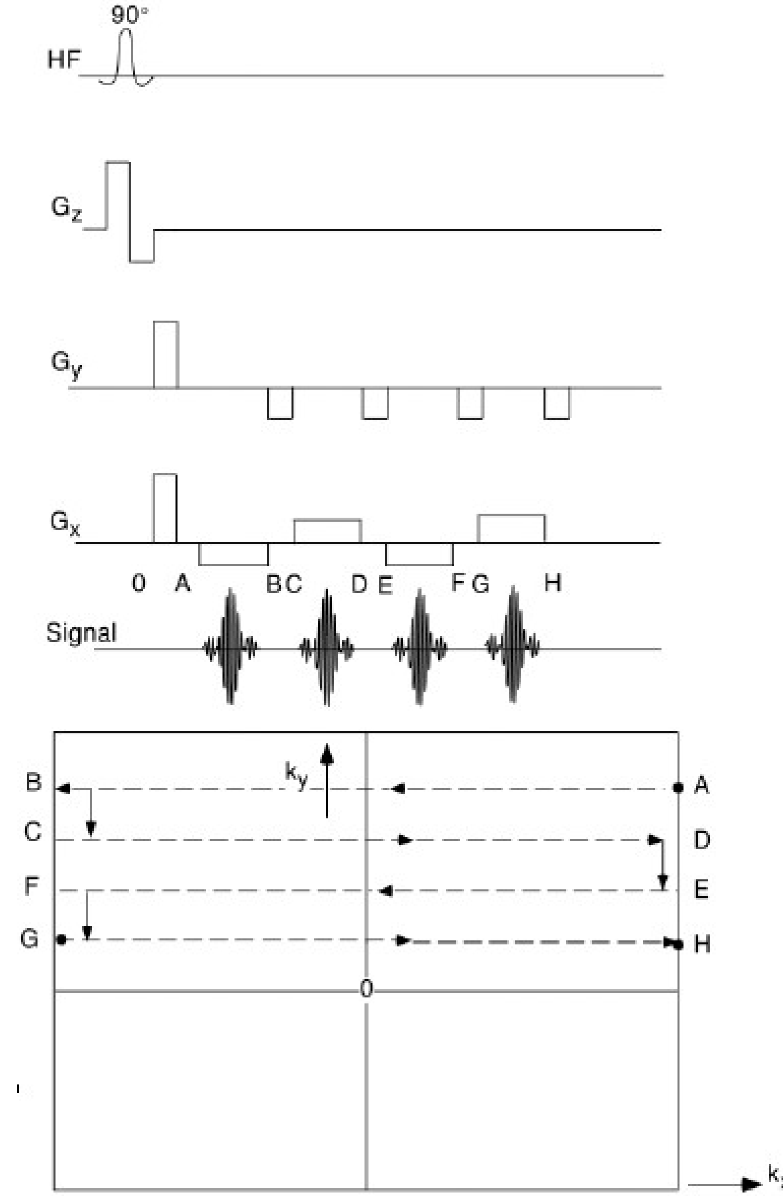

turbo spin echo (TSE)

- utilize spin echoes with 180° pulses

- after excitation (G_z, origin of coord. system): positioning (to *pos. A*) in *k*-space with gradient G_x
- mirroring with 180° pulse (*pos. B)*
- during echo: frequency coding (G_x)
- phase coding (G_y) leads to *pos. C*
- frequency coding (G_x) to *pos. D*
- echo provides next row in *k*-space
- etc.

- echo decays with T_2 (tissue-dependent !)
- max. 32 echoes after single HF excitation

- *k*-space sampling equals lowpass filtering (strong damping in k_y-direction)

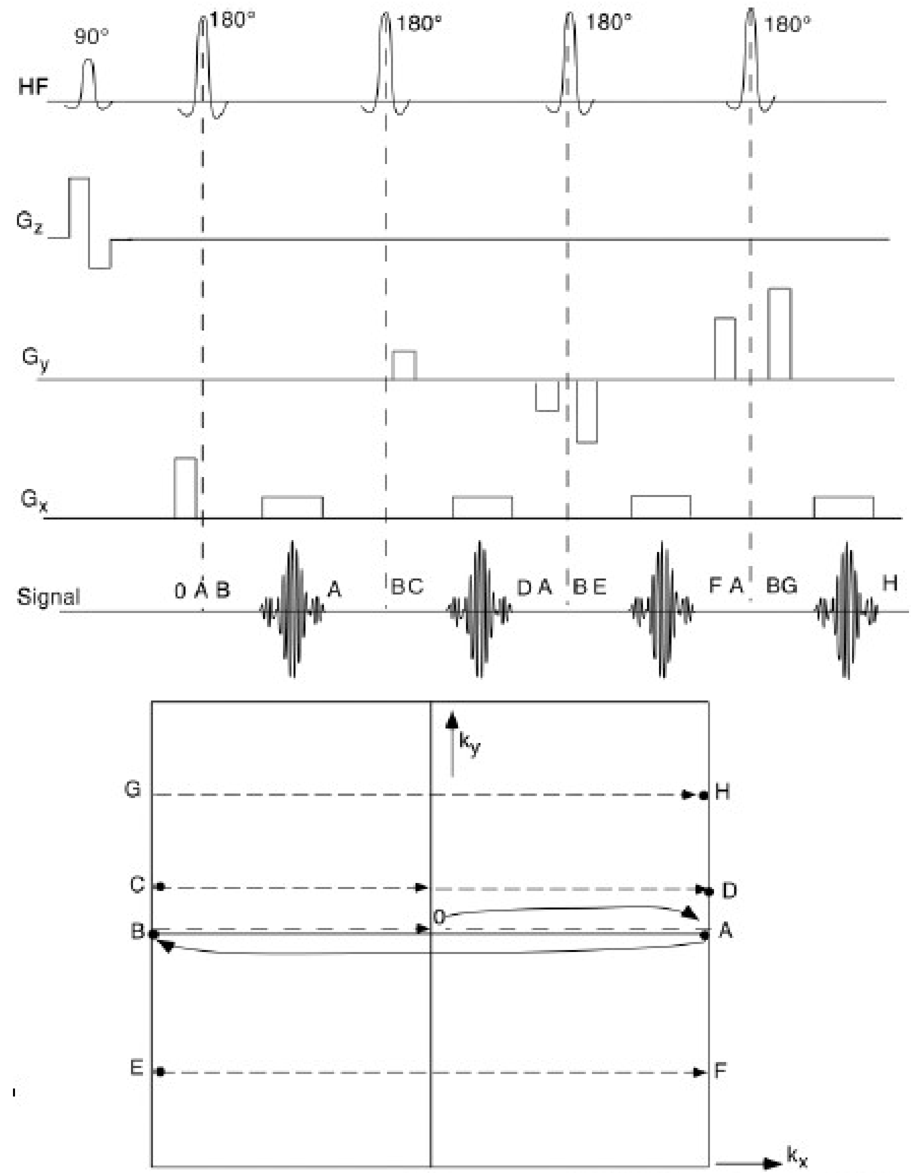

gradient and spin echo (GRASE)

- signal from EPI-sequence decays with T_2^*

- spin-rephasing with 180°-pulses $\Rightarrow$ spin echo

- GRASE: following EPI sequence generate gradient echoes with 180° pulses

- repeat until spin echo signal died out with T_2

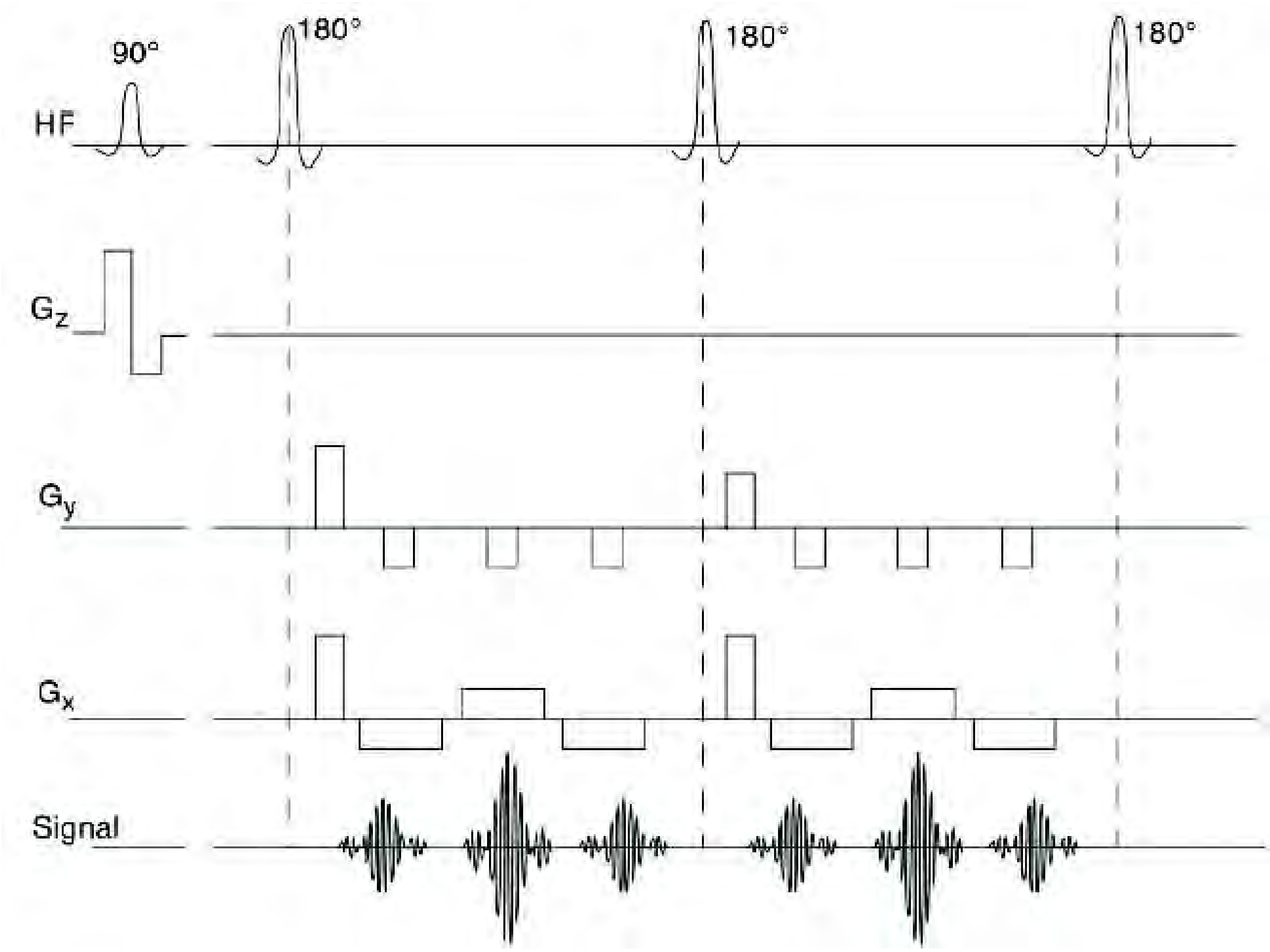

magnetic resonance imaging (MRI) *contrast agents*

- proton density can hardly be varied in tissue
- contrast agent: modify T_1 and/or T_2 with paramagnetic substances
- mostly used: Gd^{3+} (gadolinium)
- shortens T_1 time (T_1-weighted images: increased signal amplitude)
- applications: e.g. angiography
- Gd^{3+} highly toxic, requires embedding, e.g. in chelate compound:
  Gd-DTPA (Gd-**d**iethylene-**t**ri-amine-**p**enta-acetic **a**cid)

- (other, particularly body-intrinsic contrast agents: cf. fMRI)

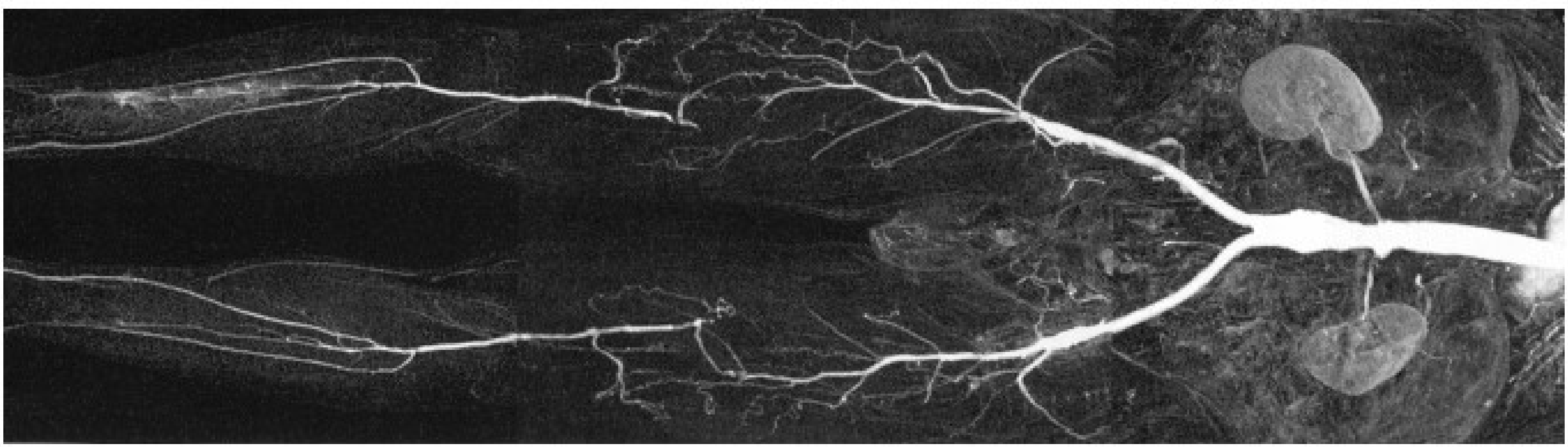

magnetic resonance imaging (MRI) *applications*

head	tumor, infarct, multiple sclerosis, epilepsy, Alzheimer‘s disease dementia, chron. headache, mental retarding
spinal cord	diseases of spinal cord, tumor, ruptured disk, bleeding, infarct, vascular malformations, trauma
ENT	tumors affecting nose, pharynx, mouth, tongue
thorax	chest wall, pleura, tumor
ophthalmology	diseases of cavity of eye, intraocular tumor
cardio-vascular	thrombosis or occlusion
locomotor system	necrosis, meniscus, cruciate ligament, cartilages, joints
gastro-enterology	tumors in liver, gall bladder, pancreas
urology	tumors in prostate
gynecology	alterations in uterus

MR-angiography (heart + lung)

infarct (heart)

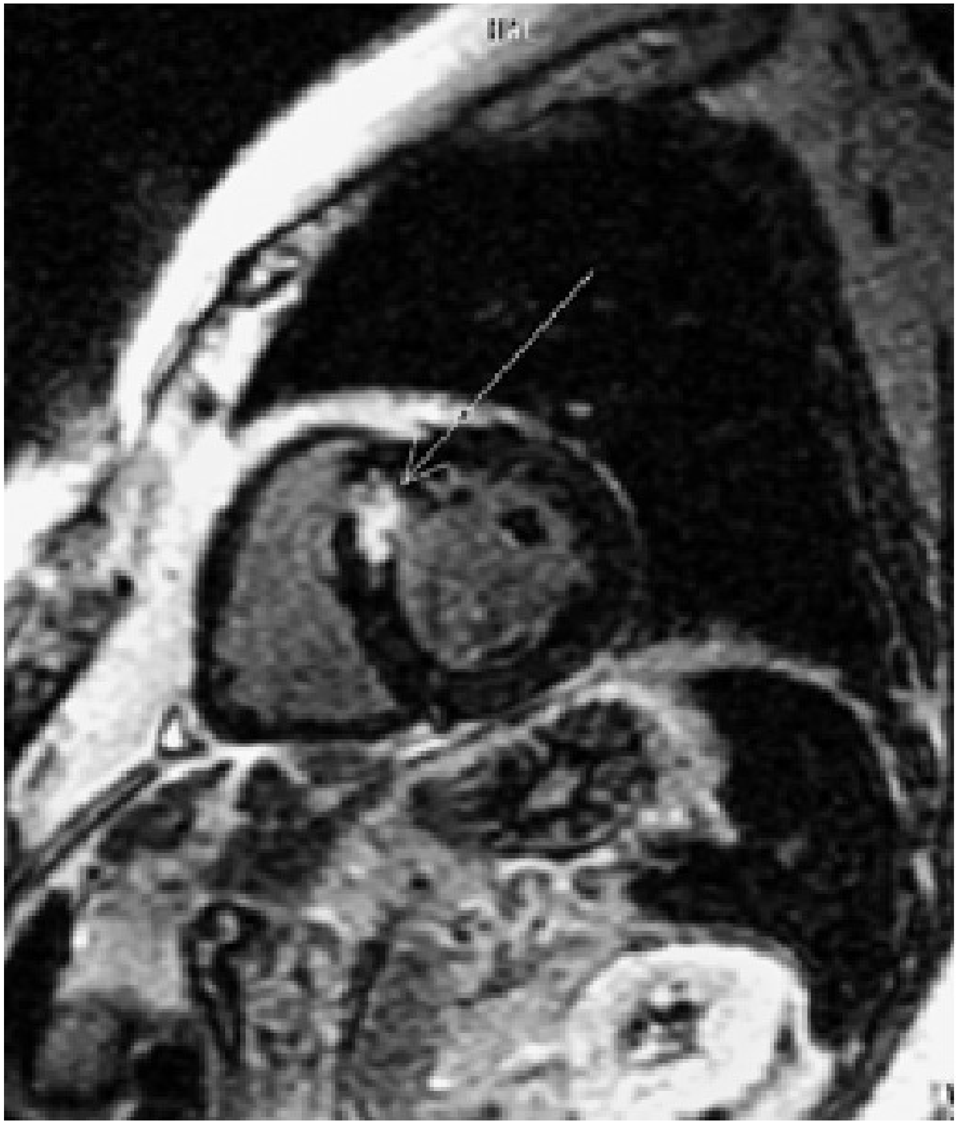

stenosis of aorta cerebri

magnetic resonance imaging (MRI)

advantages

- multi-planar slicing
- high contrast of soft tissue
- no ionizing radiation
- signal depends on large number of physical parameter

  $\Rightarrow$ high flexibility

disadvantages

- high costs

  x 10 compared to x-ray imaging, x 4 compared to CT

- availability
- contraindications

magnetic resonance imaging (MRI)

comparison to other medical imaging techniques (structure)

	x-ray	**CT**	**MRI**
presentation bones	+++	+++	+
presentation soft tissue	-/+	-	++
presentation vessels	++	++	++
presentation volumes	-	++	++
functions	-	-	++ (fMRI)
image quality	very good	good	acceptable
psychiatric burden	low	medium	high (↓)
physical burden	high	high	low
invasivity	no	no	no
exam time	10 min	25 min	25 min

fields of application of medical imaging techniques (structure)

	x-ray	CT	MRI
bones	+++	+++	+
bone marrow	-	-	++
lung	+++	+++	-
soft tissue	-/+	+++	++++
brain	-	+++	++++
spinal cord	-	(+)	++++
gastro-intestinal syst.	+++	+/++	+/-
cartilage	-	-/+	+++
vascular system	+++	++	++/+++
heart	+	+/++	++/+++
liver/spleen	-	+++	++
kidneys	+/++	+++	++